SPATIAL CONTROL OF GENE DELIVERY ON BIOENGINEERED SCAFFOLDS FOR TISSUE REGENERATION

by

Wei-Wen Hu

A dissertation submitted in partial fulfillment
of the requirements for the degree of
Doctor of Philosophy
(Biomedical Engineering)
in The University of Michigan
2009

Doctoral Committee:

Professor Paul H. Krebsbach, Chair
Professor Scott J. Hollister
Professor David H. Kohn
Associate Professor Joerg Lahann

ACKNOWLEDGEMENTS

The accomplishment of this thesis is contributed by so many people, and thus I would like to express my gratitude to everyone who has helped and support me. Without their help and encouragement, I would not be able to complete my graduate study. First of all, I would like to express my heartfelt appreciation to Prof. Paul Krebsbach for being my advisor. Thank for his willingness to offer continuous guidance, support and encouragement which are driving forces for me to complete this thesis. His vast knowledge, attitude of research, and skill of presentation are an invaluable resources to me. He is an admirable professor and will always be a role model for me.

I also would like to thank Prof. Scott Hollister for the scaffolds support and the micro-CT assistance, Prof Joerg Lahann for the help of material surface modification, and Prof. David Kohn for his valuable suggestions to improve my scientific reasoning and problem solving. I am extremely grateful for having an exceptional doctoral committee and thank for their continual support and encouragement to shape this thesis.

I extend many thanks to my colleagues, both past and current, in Krebsbach's Lab: Zhuo Wang (Joe), Junhui Song (Jun), Michael Lang, Premjit Arpornmaeklong, Luis Villa-Diaz, Shelley Brown, Erica Scheller, Ying Zhang, Michael Pressler, Wilbur Tong, Rachel Schek, Elly Liao, Darice Wong, Jessica Kemppainen, Pat Racenis, and Colleen

Flanagan. Especially, I would like to thank Joe for the collaboration of the *in vivo* study. His abundant medical knowledge and delicate skill of surgery operation greatly helped me to test the feasibility of the delivery model to the real application. Michael did me a lot of favor, both in experiments and English writing. It is impossible to complete this thesis without their help.

I also would like to express my deepest appreciation to my funding source of this thesis work, AO Foundation and NIH grants. Due to their support I can continuously my research in these interesting topics. Sincere thanks to the staffs of Department of Biologic & Materials Sciences, especially Liz for her comprehensively assistances so that I can completely focus on my projects.

Finally, I am extremely grateful for the love and encouragement of my family and friends. The support from my parents and my sister Cassie has upheld me to pursue this doctoral degree. To my dear wife I-Lin, all I can say is it would take another thesis to express my deep love for you, not only due to your understanding and unfailing support, but also the most valuable treasure of my life you gave me, our son Ting-Yu. I would like to dedicate this thesis to you.

Thank you all.

TABLE OF CONTENTS

LIST OF FIGURES

LIST OF TABLES

CHAPTER 1

INTRODUCTION

1.1 Problem Statement

The goal of tissue engineering is to repair and regenerate new tissues by mimicking natural processes. One tissue engineering strategy to regenerate tissue is to deliver cell-signaling factor directly from biomaterials. In this paradigm, fine control over the release of bioactive factors plays a critical role for tissue regeneration. In most studies to date, protein-based bioactive factor delivery has typically used an encapsulated carrier with scaffolds for controlled release [1-3]. These devices are designed to control the release rate of growth factors. However, physiologic release patterns are difficult to attain [4]. In addition, implanted growth factors may be enzymatically inactivated and unable to maintain activity during the desired therapeutic period. The high cost of milligram dosage needed is also impractical. Therefore, gene therapy may provide an alternative approach by which transduced cells function as mini reactors to produce bioactive signals *in vivo* [5]. This gene therapy approach may improve control over the timing, distribution, and the concentration of multiple regenerative factors.

Regenerative gene therapy differs from traditional gene therapy which was originally conceived as a means to correct hereditary disorders [6]. The goal of

regenerative gene therapy is to facilitate tissue regeneration by transducing cells that may provide sustained levels of biologically active molecules that can recruit or direct the differentiation of host cells at target sites [7]. Therapeutic genes may be delivered by either *ex vivo* or *in vivo* approaches to express bioactive factors. Compared to *ex vivo* gene therapy, *in vivo* gene therapy avoids the need for two surgical procedures and the complex *in vitro* cell-processing steps, such as purification, amplification, transduction, and then implantation, is also eliminated [7]. Viral vectors are frequently applied for *in vivo* gene therapy due to their excellent transduction efficiency. However, the controlled delivery of viral vectors from scaffolds is difficult because viruses are labile. In addition, viral vectors may diffuse immediately after implantation and lead to systemic infection and a serious immune response. Therefore, our goal was to develop methods to spatially control the release of adenoviral vectors from biomaterials scaffolds to regulate new tissue growth only in the target sites.

The goal of this study was to develop regenerative gene therapy methods to improve bone regeneration. Bone loss caused by trauma, neoplasia, reconstructive surgery, congenital defects or infection usually results in osseous defects that are difficult to reconstruct and regenerate [7]. Approximately 6.2 million fractures occur annually in the United States. Of these, 5-10% fail to heal properly due to non-union or delayed union [8]. Because of the complexity of size, shape, and location of skeletal defects, alternative therapies are necessary to improve therapeutic effects. For small bone defects that are not compromised by infection or radiation treatment, administrating osteoinductive proteins, such as bone morphogenetic proteins, is enough to enhance regeneration. In contrast, if

defects are large and cannot heal spontaneously (critical-sized defects), a more robust stimulus would be required. A gene therapy approach would satisfy this regeneration by delivering a gene whose expression may be sustained. Therefore, to effectively improve bone regeneration, we applied our established controlled gene delivery to facilitate bone formation in large skeletal defects, and also tested if these strategies would be effective in wounds compromised by radiotherapy (XRT).

Furthermore, the regeneration of tissue interface is still a challenge for tissue engineering. For example, the healing of osteochondral defects is always difficult because cartilage defects often penetrate to the subchondral bone. Therefore, tissue engineering should regenerate not only cartilage but also subchondral bone in wound sites [9]. Currently, the main strategy to repair tissues in interfaces is to combine multiple biomaterial scaffolds loaded with different cells to mimic tissue formation [10-14]. Although these bi-phasic scaffolds may provide suitable environments in two distinct regions, cell loading and *in vitro* cultures in bioreactors are often required. This process requires longer preparation time before implantation and also increases the risks of contamination [9]. Because bioactive factors function to guide cell differentiation, the controlled release of appropriate cues at the interface microenvironment may be able to direct multiple tissue formation at tissue interfaces. Therefore, we developed a gene therapy-based treatment to control growth factor distribution in specific sites. In this study, genes have been delivered in a controlled fashion, in which transduced and non-transduced cells were distributed in different regions with a distinct interface. This spatial control strategy could be a platform for multiple growth factor delivery.

1.2 Overall Hypothesis

The hypothesis of this thesis is that controlled gene release from biomaterial scaffolds will transduce host cells *in situ*. This delivery will not only increase cell transduction efficiency, but also spatially control bioactive factor gene distribution in scaffolds to direct tissue regeneration.

1.3 Specific Aims

Specific Aim 1

To localize adenovirus encoding the BMP-2 gene on biomaterials to improve viral transduction efficiency.

Specific Aim 2

To immobilize adenovirus on biomaterial surfaces through bioconjugation, by which virus infection is spatially controlled to transduce cells on specific sites.

Specific Aim 3

To tailor bioconjugation through scaffold surface modification with specific functional groups to control the delivery of cell-signaling factors.

1.4 Summary of Thesis Contents

Chapter 2 is a review of pertinent studies in tissue engineering, bone regeneration, regenerative gene therapy, gene delivery, and biomaterial surface modification. Chapter 3

details local gene delivery using a lyophilization technique to transduces cells in wounds sites for bone reconstruction. This research focuses on regenerating critical-sized bone defects, and also demonstrates an application of reconstructing defects compromised by radiotherapy. Chapter 4 consists of two different virus immobilization strategies in which adenovirus were either tethered on biomaterials surfaces using avidin-biotin or antibody-antigen interactions. To specifically control virus distribution, two different small chemicals were used. Biotin and digoxigenin conjugations were developed to modify viral surfaces as antigen determinants for avidin and anti-digoxigenin antibody recognition, respectively. Chapter 5 describes a surface modification method using chemical vapor deposition (CVD) to functionalize biomaterials surfaces. The modified surfaces were custom-tailored with specific functional groups for bioconjugation to control the distribution of virus immobilization. Chapter 6 is a summary of the above-mentioned chapters and a comprehensive discussion of their relationship to tissue engineering and regenerative medicine applications.

1.5 References

1. M.P. Lutolf, F.E. Weber, H.G. Schmoekel, J.C. Schense, T. Kohler, R. Muller, J.A. Hubbell, Repair of bone defects using synthetic mimetics of collagenous extracellular matrices, Nat Biotechnol 21 (5) (2003); 513-518.

2. M.H. Sheridan, L.D. Shea, M.C. Peters, D.J. Mooney, Bioabsorbable polymer scaffolds for tissue engineering capable of sustained growth factor delivery, J Control Release 64 (1-3) (2000); 91-102.

3. Y. Tabata, Tissue regeneration based on growth factor release, Tissue Eng 9 Suppl 1 (2003); S5-15.

4. T. Boontheekul, D.J. Mooney, Protein-based signaling systems in tissue engineering, Curr Opin Biotechnol 14 (5) (2003); 559-565.

5. M.D. Kofron, C.T. Laurencin, Bone tissue engineering by gene delivery, Advanced Drug Delivery Reviews 58 (4) (2006); 555-576.

6. T. Friedmann, Human gene therapy--an immature genie, but certainly out of the bottle, Nat Med 2 (2) (1996); 144-147.

7. R.T. Franceschi, Biological approaches to bone regeneration by gene therapy, J Dent Res 84 (12) (2005); 1093-1103.

8. M.P. Bostrom, K.J. Saleh, T.A. Einhorn, Osteoinductive growth factors in preclinical fracture and long bone defects models, Orthop Clin North Am 30 (4) (1999); 647-658.

9. J.F. Mano, R.L. Reis, Osteochondral defects: present situation and tissue engineering approaches, Journal of Tissue Engineering and Regenerative Medicine 1 (4) (2007); 261-273.

10. R.M. Schek, J.M. Taboas, S.J. Segvich, S.J. Hollister, P.H. Krebsbach, Engineered osteochondral grafts using biphasic composite solid free-form fabricated scaffolds, Tissue Engineering 10 (9-10) (2004); 1376-1385.

11. D. Schaefer, I. Martin, G. Jundt, J. Seidel, M. Heberer, A. Grodzinsky, I. Bergin, G. Vunjak-Novakovic, L.E. Freed, Tissue-engineered composites for the repair of large osteochondral defects, Arthritis Rheum 46 (9) (2002); 2524-2534.

12. G.G. Niederauer, M.A. Slivka, N.C. Leatherbury, D.L. Korvick, H.H. Harroff, W.C. Ehler, C.J. Dunn, K. Kieswetter, Evaluation of multiphase implants for repair of focal osteochondral defects in goats, Biomaterials 21 (24) (2000); 2561-2574.

13. B. Kreklau, M. Sittinger, M.B. Mensing, C. Voigt, G. Berger, G.R. Burmester, R. Rahmanzadeh, U. Gross, Tissue engineering of biphasic joint cartilage transplants, Biomaterials 20 (18) (1999); 1743-1749.

14. J. Gao, J.E. Dennis, L.A. Solchaga, A.S. Awadallah, V.M. Goldberg, A.I. Caplan, Tissue-engineered fabrication of an osteochondral composite graft using rat bone marrow-derived mesenchymal stem cells, Tissue Eng 7 (4) (2001); 363-371.

CHAPTER 2

REVIEW OF LITERATURE

2.1 Bone Repair and Reconstruction

The development of effective bone regeneration methods is an important clinical issue. In the United States, 2-3 % of children under 5 years of age experience some type of craniofacial defect or trauma. Reports by the US Health Cost and Utilization Project state that 12,700 cranial bone grafts are performed annually to repair craniofacial defects in children at a cost of over $549 million [1]. These craniofacial deficiencies have a devastating functional, cosmetic, and emotional impact on patients. For example, patients with cleft palates tend to have problems with mastication, articulation, and swallowing. It is estimated that more than one hundred million dollars is spent annually on these treatments [2]. Therefore, several therapies have been investigated to facilitate bone healing, so that normal form and function can be achieved while minimizing patient morbidity [3-5].

2.1.1 Conventional bone regeneration therapies

In clinical treatment, skeletal grafting therapies have been broadly applied to treat bone defects. For example, autologous bone harvested from patient or allogenic bone from cadaver banks are common tissue sources for bone repair [6]. However, there are

some difficulties yet to overcome. The iliac crest, fibula, and rib are the common donor sites from which non-vascularized bone can be harvested. When augmenting artificial implants, these bone grafts can successfully induce bone regeneration in small defects. However, non-vascularized bone grafts tend to fail in large defects, or in complex defects that are often compromised by microbiologic contamination, reduced blood supply, and radiotherapy [7, 8]. Vascularized bone grafts increase the success rate to 90 % in large defects [9, 10]. By suturing blood vessels during implantation, circulation can be immediately restored to improve the survival rates of grafts. Nevertheless, donor site morbidities such as infection, scaring, chronic pain, gait disturbances, and limb ischemia, are often impossible to overcome [11, 12]. The availability of adequate bone from donor sites is also problematic. Moreover, the availability of microvascular surgeons and the length of time necessary for surgery also increase the difficulty of this treatment.

Compared to autografts, the sources of allogenic bone are relatively sufficient. However, reduced bioactivity and mechanical strength as well as the risk of disease transmission make it inadequate for broad application in clinical situations. Synthetic graft materials have also been explored, but they are insufficient for tissue regrowth in large defects and carry the risk of initiating an inflammatory reaction [6].

2.2 Tissue Engineering for Bone Reconstruction

Transplantation is a generally accepted medical treatment to reconstitute damaged organ or tissue caused by trauma, accident, or tumor [13-15]. Although organs or tissues from patients or donors are frequently able to repair defect sites and recover function, the

limited tissue sources, repeated surgeries, as well as the risks of infection and immunogenic response suggest that this medical technique is incapable of being wildly applied [16]. To overcome these difficulties, engineering approaches have been applied in defects to facilitate tissue regeneration, which is called tissue engineering [17, 18]. The tissue engineering paradigm is to isolate appropriate cells and culture them in biodegradable scaffolds combined with appropriate bioactive factors to direct target tissue grow, and finally implant to defects sites to facilitate tissue regeneration [19]. In the coordination of bioactive factor, cells, and scaffolds, damage tissues may be repaired to recover normal function [20].

Using tissue engineering methods, different strategies have been developed to address bone regeneration difficulties by incorporating unique matrices, cells, and bioactive factors to significantly enhance the healing of bone defects [21-23]. Matrix-based therapy utilizes biocompatible scaffolds with mechanical and architectural properties that mimic the *in vivo* microenvironment to induce bone formation [24]. However, the matrix alone is typically not sufficient for bone repair. Therefore, the application of osseoconductive scaffolds is often used as an adjuvant strategy to carry cells or bioactive factors. Materials such as hydroxyapatite and tricalcium phosphate are able to enhance osteoprogenitor cells adhesion and differentiation because they are not only chemically similar to the mineral component of bone tissues, but also provide appropriate mechanical strength to support mineralized tissue growth [25, 26].

Cell-based therapy involves implanting osteogenic progenitors in target sites. Bone

marrow stromal cells (BMSCs) are most frequently applied cell source due to their ease of isolation and ability to differentiate into bone forming osteoblasts [27]. Although direct BMSC implantation in defects demonstrates some potential to facilitate bone formation, the relatively small fraction of osseous precursors limits the application of undifferentiated BMSCs in clinical research [28]. Sorting of mesenchymal stem cells (MSCs) using surface marker allows enrichment of the osseous progenitor cell population, and demonstrates promising results for bone regeneration [29]. Nevertheless, the yield of cell sorting is so low that the quantity of cells necessary for therapeutic utilization is still insufficient for clinical practice. *In vitro* cell culture used for MSCs expansion can increase cell number but often results in the loss of their differentiation potential [30].

Recent progress in embryonic stem (ES) cell research indicates that they are a promising potential cell population for tissue regeneration due to their pluripotentiality [31]. However, correctly inducing ES cells to differentiate to specific cell types without forming tumors is still a challenge for scientists [32]. Additionally, cell-based therapy needs to be combined with appropriate biomaterial scaffolds to ensure the microenvironment is suitable to implant cells with enough mechanical support. Compared to the two previously discussed strategies, the use of bioactive factors is most effective in improving regeneration. By delivering transcription or growth factors to target sites, cells can be directed to repair osseous defects. The bioactive factors can be directly delivered as recombinant protein or indirectly expressed by transduced cells.

2.2.1 Bone morphogenetic proteins for bone regeneration

To effectively repair bone defects, numerous growth factors have been applied to improve microenvironment in wound sites and facilitate bone formation. For example, transforming growth factor-β (TGF-β) [33, 34], parathyroid hormone [35, 36], fibroblast growth factor [37, 38], bone morphogenetic proteins (BMPs) [39-42], platelet-derived growth factors [43, 44], and osteoprotegerin (OPG) [45, 46] have been applied to facilitate bone repair. Although these therapeutic proteins have been shown to induce bone formation *in vivo*, BMPs are now the most frequently applied growth factors because of their excellent bone inductivity [47-49].

BMPs are multi-functional growth factors that belong to the TGF-β superfamily, excluding BMP-1 [50]. The activity of BMPs was first identified by Urist in 1965 [51]. BMP 2, 4, 6, 7, and 9 induce the differentiation of mesenchymal cells toward the osteoblastic lineage and generate bone *in vivo* [39, 52-54]. When osteoblasts undergo terminal differentiation and cellular matrix mineralization, they begin to apotosis since BMPs action is blocked [55]. BMPs also induces OPG gene transcription, and this may temper their effects on osteoclastogenesis [56].

Some studies have demonstrated that BMP expression was increased in mesenchymal and osteoprogenitor cells, fibroblasts, and proliferating chondrocytes at fracture sites [57-59]. These BMPs were also found in multinucleated osteoclast-like cells on the newly formed trabecular bone [59]. These results suggest that BMPs may cooperatively work in fracture healing and bone regeneration [60]. Because bone regeneration may be impaired if endogenous BMP levels are insufficient, recombinant

human BMPs (rhBMPs) have been applied in many preclinical studies [61-64]. BMPs can also change the phenotype of some cell types, especially fat and muscle cells, into the osteoblastic lineage [65]. For example, C2C12 is a myoblastic cell line whose phenotype is switched in response to rhBMP 2 [66].

Clinical Application of BMPs

Implantation of the osteogenic BMPs at osseous or extraosseous sites results in endochondral bone formation [65]. Several animal models have been used to evaluate the osteoinductive capacity of BMPs. The healing of long bone critical-size defects (CSD) models with BMPs has been performed with success in rats, rabbits, dogs, sheep and non-human primates [67-71]. Bone marrow stromal cells transduced by adenovirus encoding BMP-2 implanted in PLLA splints have been successful for maxillofacial bone regeneration [72] and also have been used to regenerate bone around dental implants [73]. The systemic administration of rhBMP-2 was used to enhance mesenchymal stem cell activity of osteopenic mice to improve bone formation [74]. In addition, BMPs have been used as bone graft substitutes in spinal fusion surgery. In many circumstances, the efficacy of these factors for inducing successful fusion is superior to that of autogenous bone graft [75]. These studies all suggest that BMPs are effective and safe biological signals for bone regeneration.

2.3 Regenerative Gene Therapy

Inductive bioactive factors are important to many tissue engineering strategies because the appropriate cues may not only recruit host cells to grow into scaffolds, but

also direct cells to differentiate to desired tissues [76, 77]. A key component of regenerative gene therapy is the transfer of genetic material into individuals for therapeutic purposes by altering cellular function or structure at the molecular level [78]. There are approximately 38,000 genes identified within the human genome, 5000 of which may be considered for future therapeutic use. Utilizing vectors for therapeutic purposes is a major goal of post-genomic scientists [79]. The earliest indication that gene transfer could be a treatment for clinical application was proposed in 1968, "the next step was to build a modified virus…and use the virus to transmit" [80].

2.3.1 Route of gene delivery

There are two general ways that gene therapy can be performed: (1) a direct *in vivo* method and (2) an indirect *ex vivo* method.

In the *in vivo* method, genetic material is transferred into the target site by direct injection [81, 82]. Viral vectors have higher transduction efficiencies and some vectors can target specific cell-types. However, the risk and safety concerns are the main issues for clinical caution. For example, retrovirus randomly incorporates into the host genome, which may induce insertional mutagenesis and malignant transformation [83].

Ex vivo gene therapy involves the transfer of therapeutic genes to cells *in vitro* followed by transplantation of these modified cells to target tissues. Different from the *in vivo* method, *ex vivo* therapy needs to use appropriate surrogate cells as vehicles for transportation. These cells should: (1) be readily available and relatively easily obtained;

(2) be able to survive for long periods of time *in vivo*; (3) be able to express transgenes at high levels for an extended duration; and (4) not elicit a significant host mediated immune reaction. Some advantages of the *ex vivo* approach include: the cell population can be characterized and monitored during *in vitro* infection, the virus can be excluded before implantation to avoid the deleterious properties, and the transgene can be only expressed by modified cells to avoid systemic infection. Furthermore, some viral vectors with low transduction efficiency can be used because uninfected cells can be screened out from the transplant population [83]. However, this method is very laborious and thus may not be cost effective. Because several weeks may be required for adequate cell proliferation, this treatment cannot be applied to emergency cases. The *in vitro* cell culture process also holds a risk of contamination. Furthermore, an additional surgery is necessary to transplant the transduced cells.

2.3.2 Gene delivery vehicles

To safely and effectively deliver genes for tissue regeneration, different vector systems have been developed. Adenovirus and retrovirus are the most commonly applied vectors for gene delivery because they are easy to manipulate and have high transduction efficiency. Nonviral vectors and recombinant adeno-associated virus (rAAV) vectors are relatively new delivery vehicles and carry less risk for immune response and mutation.

Non-viral Vectors

Non-viral vectors, such as naked DNA [84, 85] or DNA associated with cationic polymer and liposomes [86], are vehicles used to transport genes *in vivo* by penetrating

the cell membrane. These vectors are easy to manufacture and are generally not limited by the size of DNA fragments [87]. Liposomes are micelles composed of phospholipids that can easily merge with lipid bilayer cell membranes to deliver genes [88]. The BMP-2 gene has been encapsulated into liposomes, which was then delivered by a collagen carrier in critical-sized swine calvarial defects for bone regeneration [89]. Because the aggregation of lipoplexes may decrease structure stability, polycationic lipids have been applied to directly complex with anionic nucleotides to enhance the stability of vector particles [90]. Commercial polycantionic vectors are now available to deliver genes more effectively. For example, Lipofectamine is a liposome with polycationic lipids which can stabilize DNA within the vector. It has been used to deliver BMP-2 for improving bone formation in rabbit skull defects [91]. SuperFect is another commercial non-viral vector made by cationic dendrimers that can surround therapeutic genes to facilitate gene transfer [92]. It has been used to deliver the BMP-2 gene to enhance bone formation in rabbit cranial defects [93]. Other polycationic vectors, such as Polyethyleneimine (PEI) and Poly(ethyleneglycol)-block-catiomer (PEG-b-P[Asp-(DET)]), are also able to successfully deliver osteoinductive genes to induce bone growth in skull defects [94, 95]. Although non-viral vectors are attractive for their safety profiles and the ability to control their chemical and physical properties, their low transfer efficiency relative to viral vectors results in the need to delivery high dose of vectors [96, 97]. Consequently, the high amounts of lipid or polymer often lead to cytotoxicity [98]. In addition, the transgene expression is transient and the nonspecific cell targeting also prevents them from general clinical administration [99].

Viral Vectors

Compared to non-viral vectors, viral vectors have extremely high transduction efficiencies and can deliver the target genes into host cells with high efficiency. Some viral vectors have the potential for targeting selected cell types [100]. Therefore, they are more generally used for preclinical and clinical therapy.

Retrovirus

Retroviruses are enveloped, single-stranded RNA viruses that are broadly used for gene therapy. Because retrovirus is small, it can only incorporate 10 kb of foreign DNA. Low immunogenicity and antigeneity is the main advantage of the retrovirus, and thus they are widely used for clinical trials [101]. The main retroviral vector used for gene therapy is derived from murine leukemia virus (MLV) which was applied as the first viral vector for human gene therapy trials [102]. Retrovirus can incorporate into host genome and thus is used for long-term gene therapy for chronic or inherited diseases. However, because the viral DNA insertion is random, it may activate a cell proto-oncogene or disrupt a tumor suppressor gene [103]. To avoid the risk of mutation, retroviral vectors are suitable for *ex vivo* gene therapy [104]. The therapeutic gene overexpression may also cause toxicity [105]. In addition, retrovirus can only infect dividing cells, which limits the application for some tissues with non-dividing cells, such as nerves and muscles. This problem can be overcome by using lentivirus, a class of retrovirus that is capable of infecting non-dividing cells.

Adenovirus

Adenovirus is another well-studied viral vector for regenerative gene therapy. It is a non-enveloped, double-stranded DNA virus that has been developed as a gene delivery vector since the early 1980s [106]. Adenovirus can infect many different cell types, both dividing and non-dividing cells, with extremely high efficiency. The capacity for foreign genes is 7.5kb, and the third generation (gutless vectors) can even accommodate genes up to 35kb [105]. The genome of adenovirus can be translocated into host cell nuclei, but the viral DNA exists as an episome. Therefore, insertional mutations do not occur during adenovirus infection. Compared to retrovirus which incorporates into the host genome for long-term expression, the transgene expression mediated by adenoviral vectors is transient. This time-limited expression is appropriate for regenerative gene therapy during the therapeutic period. Because adenovirus is easy to manipulate with high titers (10^{10}-10^{12} plaque forming units per milliliter), it is the most frequently used viral vector in gene therapy for bone regeneration [107]. The immune response is the main disadvantage of adenovirus administration. A local inflammatory reaction may be induced by a T-cell mediated response against adenoviral proteins, which can cause cell lysis and thus reduce the duration of transgene expression [108].

Adeno-associated virus

Adeno-associated virus (AAV) is a non-enveloped small single stranded DNA parvovirus. The capacity of foreign DNA for AAV is only about 5kb. It was first discovered associated with adenovirus which is required as a helper virus to replicate AAV in the productive phase [109]. In the absence of helper virus, *wt*AAVs remains in latency by integrating into host cells at the AAV-S1 locus on human chromosome 19

[110]. AAV *rep* proteins are required during the integration process, however, this sequence was removed from recombinant AAV (rAAV) [111, 112]. Therefore, rAAV vectors have an extremely low frequency of integration, and also lose the specificity of chromosome 19 [113, 114]. When rAAV vectors are internalized into host cells, the single-stranded AAV genome is converted into a double-stranded form by using host cell DNA polymerases and persists as linear or circular episomes [100]. Therefore, the duration of transgene expression is highly dependent on the lifespan of the host cells [115, 116].

Recombinant AAV was first applied as a gene delivery method in 1984 [117]. It has become increasingly popular for gene therapy due to its safety profile. In the absence of coinfection with helper virus, rAAV is unable to enter in the lytic cycle in host cells. In addition, due to a lack of viral protein expression, it can avoid eliciting destructive cellular immune responses against transduced cells [100]. AAV is also well-known for its non-pathogenic properties. The small packaging capacity is the main drawback of rAAV. Another disadvantage of AAV is the expensive and complex purification process. It is also difficult to produce sufficiently high titers. To address these difficulties, numerous strategies have been developed to increase virus titer or improve infection efficiency [118-120].

Optimizing Gene Delivery Vehicles

There are several considerations for an appropriate vehicle for gene transfer. The manipulation of a virus should be easy and inexpensive. It should be produced and

purified in large amounts and at high concentration. Different sized therapeutic genes should be easily incorporated into vectors. The vector should be efficient for gene delivery and should deliver genes to both dividing and non-dividing cell types. Only the target cell population should be tranduced. Vectors should not induce inflammatory, immune response, or cytotoxicity. The transgene expressions can be sustained and controllable. To avoid insertional mutation, transgene integration into host cells should be controlled to specific chromosomal sites. Table 2.1 list the comparison advantage and disadvantage of different viral and non-viral vectors, by which an appropriate gene delivery vehicles may be determined in different clinical applications.

2.4 Gene Delivery

Traditionally, gene delivery by vector injection or inhalation, known as systemic or bolus delivery, leads to the presence of vector in the target cell population for a short time prior to clearance, but only a fraction of the vector is internalized [121, 122]. This is problematic since the target cell population must often be exposed to signaling factors throughout the entire course of tissue repair [123]. There are two delivery systems that may overcome this mass transportation limitation: polymeric release and substrate-mediated delivery [98].

Polymeric release incorporates viral vectors in the polymer matrix and controls release by polymer degradation [124]. Because the viral concentration will decrease with increasing distance, it can create a gradient of transduction and transgene expression. It can not only help localizing the infection, but also may recruit specific cells directed by

the therapeutic protein gradient. In addition, long-term release is also feasible since the viral vectors are released slowly and may be maintained for periods of continuous transduction.

Compared to polymeric release, substrate-mediated delivery immobilizes vectors on biomaterial substrates for direct exposure in a cellular environment. Because these vectors can only infect cells on the material surface, it restricts the transduction region and spatially controls the therapeutic protein expression only on the substrate. Due to the concentrated vectors on the material surface, it also reduces the required amount of virus relative to bolus delivery to achieve the same expression level [125]. This may decrease cytotoxicity and increase transduction efficiency [126, 127]. The consideration of the substrate materials is not only for cell support and vector adhesion, but also allows vectors to be internalized into the cell. Strongly immobilized vectors may limit cellular internalization, whereas weakly immobilized vectors are incapable of being retained on the substrates for presenting to cells [98]. To maintain vectors on substrates, numerous immobilization techniques may be applied, including: simple adsorption [128], enzyme incorporation [129] or covalent chemical conjugation [130]. For covalent conjugation, carbodiimide chemistry [131], Michael-type addition [132], and photo chemical grafting [133] are the most frequently used strategies.

Collagen covalently conjugated to IgG against the adenovirus hexon has been used to tether virus on surfaces. Cells are transduced by endocytosis of antibody-virus complexes and intracellular process to express target gene [134].The release of

antibody-virus complex can be controlled through the use of enzymatically cleavable and hydrolysable linkers [135, 136]. This has been applied to localize gene expression by coating a gel on porcine ventricles [134], stainless steel stents [137], and platinum microcoils [136].

An avidin-modified material with biotinylated vectors is a new approach for specific virus binding on materials. Plasmid DNA complexed with biontinylated Poly-L lysine (PLL) and Polyethyleneimine (PEI) can be immobilized to neutravidin-modified substrates [138-140]. The complex has been utilized for plasmid delivery from porous scaffolds *in vivo* [141]. Maximal binding occurs when there is a high affinity of the complex for the substrate; however, this may also reduce transfection [140].

For virus biotinylation, *N*-hydroxysuccinimide (NHS) ester reaction has been applied to graft a layer of biotin on viral capsid proteins [142]. Adenoviruses bound to streptavidin-coated microbeads have been shown to possess enhanced infectivity, particularly on poorly permissive cells. They did not diffuse from the areas initially placed and could be combined with paramagnetic cores for spatial control [143]. Streptavidin coated culture wells were also able to immobilize the biotinylated virus to enhance infection efficiency [142].

2.5 Surface Modification

Biomedical devices are mostly manufactured from polymers and metals. The current trend in biomaterial research is to develop new materials with both appropriate

mechanical properties and improved biocompatibility [144]. Nevertheless, many materials that satisfy mechanical performance are far from having acceptable biocompatibility and often lack sufficient functional groups [145]. In addition, covalent linkage of biomolecules to material surfaces requires suitable chemical groups. If materials do not bear reactive groups of appropriate types and densities, they must be introduced by either a surface functionalization step or via the deposition of a functionalized thin-film coating [146].

Treatment with high energy sources including plasma, laser, or ion beam have been used to generate functional groups on material surfaces [147-149]. Plasma exposure for surface etching is a non-specific modification for non-reactive biomaterials. Low pressure ammonia plasma treatment has been developed to create a layer of amine groups on the poly (3-hyoxybutyrate) (PHB) film [150]. This modification changed the surface from a hydrophobic to a hydrophilic nature without significant altering the morphology. Hollinger and Hu also modified Polylactic acid (PLA) films by the same process to conjugate poly (L-lysine) and Arg-Gly-Asp (RGD) peptide [151]. This surface modification was durable, however, it was only capable of being applied to 2-D films or very thin 3-D scaffolds because of the limitation of plasma penetration [152].

Surface coating is another strategy to create a layer of functionalized film on a material. Dip coating is the simplest approach but it is limited by adhesion, homogeneity, and biocompatibility due to the use of solvents and additives [144]. Chemical vapor deposition (CVD) is an improved modification. Monomers are sublimated, activated, and

then deposited to polymerize on the material surface. The CVD process shows promising features like absolute conformance to substrate topology and the ability to penetrate porous structures for coating complex geometries. Because the conversion from monomer gas to polymer film is direct, no solvents, plasticizer, catalysts, or accelerants are used, resulting in a low intrinsic cytotoxicity [144]. Polymers of poly (p-xylylene) (PPX) type provide an ideal material for CVD. PPX is equipped with different functional groups, including amine, alcohol, aldehyde, activated carboxylic acids and anhydrides[146, 153], that can be established as a layer on material surfaces. In addition, it also exhibits excellent biocompatibility properties compared to other polymer coatings and thus is a potential technique for biologic application [144].

2.6 Conclusions

Due to the limits in the source of bone for transplantation, bone regeneration by tissue engineering has been developed to help patients suffering from extensive bone loss. Bioactive factor-based therapy significantly improves bone regeneration in defects. However, steady and sustained growth factor exposure during a therapeutic period is critical to optimize tissue regeneration. Consequently, gene therapy may be an alternative approach to continuously deliver required biosignals. To effectively control cell transduction in wound sites, substrate-mediated gene delivery has been utilized to restrict transduced cell distribution only in and around scaffolds. The aforementioned studies laid the groundwork for the realization of tissue engineering. Therefore, in this thesis we investigated the feasibility of *in situ* cell transduction via spatially controlled gene delivery. By localizing or immobilizing viral vectors on specific sites of scaffolds, the

distribution of cell signaling proteins may thus be manipulated to accurately guide appropriate tissue formation.

Table 2.1. The comparison of different vectors for gene delivery

Vectors	Genome mode	Insert capacity	Mode of expression	Advantage	Disadvantage
Non-viral vectors	DS DNA	Non-limitation	Episomal	● Non-immunogenic; ● Easy to manufacture; ● No capacity limitation; ● Simple to scale up ● Broad cellular tropism; ● Easy to storage and quality control; ● Nonpathogenic	● Low transduction efficiency; ● Cytoxicity induced by vehicle materials; ● Transient expression
Retrovirus	SS RNA	10kb	Chromosomal integration	● Good transduction efficiency; ● Low immunogenicity; ● Life-long expression; ● Simple to scale up	● Insertional mutation risk; ● Only infect to dividing cells; ● Must be delivered by *ex vivo* route
Adenovirus	DS DNA	1st generation: ΔE1 7kb 2nd generation: ΔE1+ΔE2 10kb 2nd generation: ΔE1+ΔE4 10kb 3rd generation: gutless vector 35kb	Episomal	● High transduction efficiency; ● Non insertional mutation risk; ● Broad cellular tropism; ● Large capacity; ● Easy to manufacture; ● Simple to scale up	● Inflammatory induced; ● Highly immunogenic; ● Transient expression
rAAV	SS DNA	5kb	Episomal	● Good transduction efficiency; ● Moderate immunogenicity; ● Long-term expression; ● Broad cellular tropism; ● Nonpathogenic	● High cost for purification; ● Difficult to manufacture; ● Small capacity

2.7 References

1. C. Steiner, A. Elixhauser, J. Schnaier, The healthcare cost and utilization project: an overview, Eff Clin Pract 5 (3) (2002); 143-151.

2. N.J. Panetta, D.M. Gupta, B.J. Slater, M.D. Kwan, K.J. Liu, M.T. Longaker, Tissue engineering in cleft palate and other congenital malformations, Pediatr Res 63 (5) (2008); 545-551.

3. B. Nussenbaum, P.H. Krebsbach, The role of gene therapy for craniofacial and dental tissue engineering, Adv Drug Deliv Rev 58 (4) (2006); 577-591.

4. Z.S. Ai-Aql, A.S. Alagl, D.T. Graves, L.C. Gerstenfeld, T.A. Einhorn, Molecular mechanisms controlling bone formation during fracture healing and distraction osteogenesis, Journal of Dental Research 87 (2) (2008); 107-118.

5. N. Kimelman, G. Pelled, G.A. Helm, J. Huard, E.M. Schwarz, D. Gazit, Review: Gene- and stem cell-based therapeutics for bone regeneration and repair, Tissue Engineering 13 (6) (2007); 1135-1150.

6. C.G. Finkemeier, Bone-grafting and bone-graft substitutes, J Bone Joint Surg Am 84-A (3) (2002); 454-464.

7. A.K. Adamo, R.L. Szal, Timing, results, and complications of mandibular reconstructive surgery: report of 32 cases, J Oral Surg 37 (10) (1979); 755-763.

8. W. Lawson, H.F. Biller, Mandibular reconstruction: bone graft techniques, Otolaryngol Head Neck Surg 90 (5) (1982); 589-594.

9. M.L. Urken, A.G. Bridger, K.B. Zur, E.M. Genden, The scapular osteofasciocutaneous flap: a 12-year experience, Arch Otolaryngol Head Neck Surg 127 (7) (2001); 862-869.

10. M.L. Urken, D. Buchbinder, P.D. Costantino, U. Sinha, D. Okay, W. Lawson, H.F. Biller, Oromandibular reconstruction using microvascular composite flaps: report of 210 cases, Arch Otolaryngol Head Neck Surg 124 (1) (1998); 46-55.

11. E.H. Hartman, P.H. Spauwen, J.A. Jansen, Donor-site complications in vascularized bone flap surgery, J Invest Surg 15 (4) (2002); 185-197.

12. T.P. Vail, J.R. Urbaniak, Donor-site morbidity with use of vascularized autogenous fibular grafts, J Bone Joint Surg Am 78 (2) (1996); 204-211.

13. J. Nishida, T. Shimarnura, Methods of reconstruction for bone defect after tumor excision: A review of alternatives, Medical Science Monitor 14 (8) (2008); RA107-RA113.

14. C.N. Paul, Skin grafting in burns, Wounds-a Compendium of Clinical Research and Practice 20 (7) (2008); 199-202.

15. G.G. Niederauer, D.R. Lee, S. Sankaran, Bone grafting in arthroscopy and sports medicine, Sports Medicine and Arthroscopy Review 14 (3) (2006); 163-168.

16. D.J. Mooney, A.G. Mikos, Growing new organs, Sci Am 280 (4) (1999); 60-65.

17. H. Shin, S. Jo, A.G. Mikos, Biomimetic materials for tissue engineering, Biomaterials 24 (24) (2003); 4353-4364.

18. J.P. Vacanti, R. Langer, Tissue engineering: the design and fabrication of living replacement devices for surgical reconstruction and transplantation, Lancet 354 Suppl 1 (1999); SI32-34.

19. K.Y. Lee, D.J. Mooney, Hydrogels for tissue engineering, Chem Rev 101 (7) (2001); 1869-1879.

20. R. Langer, J.P. Vacanti, Tissue engineering, Science 260 (5110) (1993); 920-926.

21. P.H. Krebsbach, M.H. Mankani, K. Satomura, S.A. Kuznetsov, P.G. Robey, Repair of craniotomy defects using bone marrow stromal cells, Transplantation 66 (10) (1998); 1272-1278.

22. K. Sato, M.R. Urist, Induced regeneration of calvaria by bone morphogenetic protein (BMP) in dogs, Clin Orthop Relat Res (197) (1985); 301-311.

23. S.C.N. Chang, F.C. Wei, H.L. Chuang, Y.R. Chen, J.K. Chen, K.C. Lee, P.K.T. Chen, C.L. Tai, J.R. Lou, Ex vivo gene therapy in autologous critical-size craniofacial bone regeneration, Plastic and Reconstructive Surgery 112 (7) (2003); 1841-1850.

24. J.E. Fleming, C.N. Cornell, G.E. Muschler, Bone cells and matrices in orthopedic tissue engineering, Orthopedic Clinics of North America 31 (3) (2000); 357-+.

25. L.C. Palmer, C.J. Newcomb, S.R. Kaltz, E.D. Spoerke, S.I. Stupp, Biomimetic Systems for Hydroxyapatite Mineralization Inspired By Bone and Enamel, Chemical Reviews 108 (11) (2008); 4754-4783.

26. G.P. Liu, L. Zhao, L. Cui, W. Liu, Y.L. Cao, Tissue-engineered bone formation using human bone marrow stromal cells and novel ss-tricalcium phosphate, Biomedical Materials 2 (2) (2007); 78-86.

27. Q.X. Shang, Z. Wang, W. Liu, Y.H. Shi, L. Cui, Y.L. Cao, Tissue-engineered bone repair of sheep cranial defects with autologous bone marrow stromal cells, Journal

of Craniofacial Surgery 12 (6) (2001); 586-593.

28. J.R. Werntz, J.M. Lane, A.H. Burstein, R. Justin, R. Klein, E. Tomin, Qualitative and quantitative analysis of orthotopic bone regeneration by marrow, J Orthop Res 14 (1) (1996); 85-93.

29. R.K. Jaiswal, N. Jaiswal, S.P. Bruder, G. Mbalaviele, D.R. Marshak, M.F. Pittenger, Adult human mesenchymal stem cell differentiation to the osteogenic or adipogenic lineage is regulated by mitogen-activated protein kinase, J Biol Chem 275 (13) (2000); 9645-9652.

30. Z. Wang, J. Song, R.S. Taichman, P.H. Krebsbach, Ablation of proliferating marrow with 5-fluorouracil allows partial purification of mesenchymal stem cells, Stem Cells 24 (6) (2006); 1573-1582.

31. S. Yamanaka, J.L. Li, G. Kania, S. Elliott, R.P. Wersto, J. Van Eyk, A.M. Wobus, K.R. Boheler, Pluripotency of embryonic stem cells, Cell and Tissue Research 331 (1) (2008); 5-22.

32. D. Howard, L.D. Buttery, K.M. Shakesheff, S.J. Roberts, Tissue engineering: strategies, stem cells and scaffolds, J Anat 213 (1) (2008); 66-72.

33. M.E. Joyce, S. Jingushi, M.E. Bolander, Transforming growth factor-beta in the regulation of fracture repair, Orthop Clin North Am 21 (1) (1990); 199-209.

34. K.K. Macdonald, C.Y. Cheung, K.S. Anseth, Cellular delivery of TGF beta(1) promotes osteoinductive signalling for bone regeneration, Journal of Tissue Engineering and Regenerative Medicine 1 (4) (2007); 314-317.

35. H. Chen, E.P. Frankenburg, S.A. Goldstein, L.K. McCauley, Combination of local and systemic parathyroid hormone enhances bone regeneration, Clin Orthop Relat Res (416) (2003); 291-302.

36. G.J. Pettway, J.A. Meganck, A.J. Koh, E.T. Keller, S.A. Goldstein, L.K. McCauley, Parathyroid hormone mediates bone growth through the regulation of osteoblast proliferation and differentiation, Bone 42 (4) (2008); 806-818.

37. X. Guo, Q.X. Zheng, I. Kulbatski, Q. Yuan, S.H. Yang, Z.W. Shao, H. Wang, B.J. Xiao, Z.Q. Pan, S. Tang, Bone regeneration with active angiogenesis by basic fibroblast growth factor gene transfected mesenchymal stem cells seeded on porous beta-TCP ceramic scaffolds, Biomedical Materials 1 (3) (2006); 93-99.

38. M.S. Park, S.S. Kim, S.W. Cho, C.Y. Choi, B.S. Kim, Enhancement of the osteogenic efficacy of osteoblast transplantation by the sustained delivery of basic fibroblast growth factor, Journal of Biomedical Materials Research Part B-Applied Biomaterials 79B (2) (2006); 353-359.

39. P.H. Krebsbach, K. Gu, R.T. Franceschi, R.B. Rutherford, Gene therapy-directed osteogenesis: BMP-7-transduced human fibroblasts form bone in vivo, Hum Gene Ther 11 (8) (2000); 1201-1210.

40. K. Partridge, X.B. Yang, N.M.P. Clarke, Y. Okubo, K. Bessho, W. Sebald, S.M. Howdle, K.M. Shakesheff, R.O.C. Oreffo, Adenoviral BMP-2 gene transfer in mesenchymal stem cells: In vitro and in vivo bone formation on biodegradable polymer scaffolds, Biochemical and Biophysical Research Communications 292 (1) (2002); 144-152.

41. M. Geiger, R.H. Li, W. Friess, Collagen sponges for bone regeneration with rhBMP-2, Advanced Drug Delivery Reviews 55 (12) (2003); 1613-1629.

42. J.Y. Lee, D. Musgrave, D. Pelinkovic, K. Fukushima, J. Cummins, A. Usas, P. Robbins, F.H. Fu, J. Huard, Effect of bone morphogenetic protein-2-expressing muscle-derived cells on healing of critical-sized bone defects in mice, Journal of Bone and Joint Surgery-American Volume 83A (7) (2001); 1032-1039.

43. Q. Jin, O. Anusaksathien, S.A. Webb, M.A. Printz, W.V. Giannobile, Engineering of tooth-supporting structures by delivery of PDGF gene therapy vectors, Mol Ther 9 (4) (2004); 519-526.

44. Y.M. Lee, Y.J. Park, S.J. Lee, Y. Ku, S.B. Han, P.R. Klokkevold, C.P. Chung, The bone regenerative effect of platelet-derived growth factor-BB delivered with a chitosan/tricalcium phosphate sponge carrier, Journal of Periodontology 71 (3) (2000); 418-424.

45. P.J. Kostenuik, B. Bolon, S. Morony, M. Daris, Z. Geng, C. Carter, J. Sheng, Gene therapy with human recombinant osteoprotegerin reverses established osteopenia in ovariectomized mice, Bone 34 (4) (2004); 656-664.

46. S.Y. Yang, L. Mayton, B. Wu, J.J. Goater, E.M. Schwarz, P.H. Wooley, Adeno-associated virus-mediated osteoprotegerin gene transfer protects against particulate polyethylene-induced osteolysis in a murine model, Arthritis Rheum 46 (9) (2002); 2514-2523.

47. P.C. Bessa, M. Casal, R.L. Reis, Bone morphogenetic proteins in tissue engineering: the road from laboratory to clinic, part II (BMP delivery), Journal of Tissue Engineering and Regenerative Medicine 2 (2-3) (2008); 81-96.

48. O.P. Gautschi, S.P. Frey, R. Zellweger, Bone morphogenetic proteins in clinical applications, Anz Journal of Surgery 77 (8) (2007); 626-631.

49. T. Nakase, H. Yoshikawa, Potential roles of bone morphogenetic proteins (BMPs) in skeletal repair and regeneration, Journal of Bone and Mineral Metabolism 24 (6)

(2006); 425-433.

50. D. Chen, M. Zhao, G.R. Mundy, Bone morphogenetic proteins, Growth Factors 22 (4) (2004); 233-241.

51. M.R. Urist, Bone: formation by autoinduction, Science 150 (698) (1965); 893-899.

52. S.E. Gitelman, M. Kirk, J.Q. Ye, E.H. Filvaroff, A.J. Kahn, R. Derynck, Vgr-1/BMP-6 induces osteoblastic differentiation of pluripotential mesenchymal cells, Cell Growth Differ 6 (7) (1995); 827-836.

53. K.D. Luk, Y. Chen, K.M. Cheung, H.F. Kung, W.W. Lu, J.C. Leong, Adeno-associated virus-mediated bone morphogenetic protein-4 gene therapy for in vivo bone formation, Biochem Biophys Res Commun 308 (3) (2003); 636-645.

54. T.D. Alden, E.J. Beres, J.S. Laurent, J.A. Engh, S. Das, S.D. London, J.A. Jane, Jr., S.B. Hudson, G.A. Helm, The use of bone morphogenetic protein gene therapy in craniofacial bone repair, J Craniofac Surg 11 (1) (2000); 24-30.

55. R.M. Pereira, A.M. Delany, E. Canalis, Cortisol inhibits the differentiation and apoptosis of osteoblasts in culture, Bone 28 (5) (2001); 484-490.

56. M. Wan, X. Shi, X. Feng, X. Cao, Transcriptional mechanisms of bone morphogenetic protein-induced osteoprotegrin gene expression, J Biol Chem 276 (13) (2001); 10119-10125.

57. M.P. Bostrom, J.M. Lane, W.S. Berberian, A.A. Missri, E. Tomin, A. Weiland, S.B. Doty, D. Glaser, V.M. Rosen, Immunolocalization and expression of bone morphogenetic proteins 2 and 4 in fracture healing, J Orthop Res 13 (3) (1995); 357-367.

58. T. Nakase, S. Nomura, H. Yoshikawa, J. Hashimoto, S. Hirota, Y. Kitamura, S. Oikawa, K. Ono, K. Takaoka, Transient and localized expression of bone morphogenetic protein 4 messenger RNA during fracture healing, J Bone Miner Res 9 (5) (1994); 651-659.

59. T. Onishi, Y. Ishidou, T. Nagamine, K. Yone, T. Imamura, M. Kato, T.K. Sampath, P. ten Dijke, T. Sakou, Distinct and overlapping patterns of localization of bone morphogenetic protein (BMP) family members and a BMP type II receptor during fracture healing in rats, Bone 22 (6) (1998); 605-612.

60. J.M. Schmitt, K. Hwang, S.R. Winn, J.O. Hollinger, Bone morphogenetic proteins: an update on basic biology and clinical relevance, J Orthop Res 17 (2) (1999); 269-278.

61. S.D. Cook, G.C. Baffes, M.W. Wolfe, T.K. Sampath, D.C. Rueger, Recombinant human bone morphogenetic protein-7 induces healing in a canine long-bone segmental defect model, Clin Orthop Relat Res (301) (1994); 302-312.

62. S.D. Cook, J.E. Dalton, E.H. Tan, T.S. Whitecloud, 3rd, D.C. Rueger, In vivo evaluation of recombinant human osteogenic protein (rhOP-1) implants as a bone graft substitute for spinal fusions, Spine 19 (15) (1994); 1655-1663.

63. M. Mayer, J. Hollinger, E. Ron, J. Wozney, Maxillary alveolar cleft repair in dogs using recombinant human bone morphogenetic protein-2 and a polymer carrier, Plast Reconstr Surg 98 (2) (1996); 247-259.

64. H.D. Zegzula, D.C. Buck, J. Brekke, J.M. Wozney, J.O. Hollinger, Bone formation with use of rhBMP-2 (recombinant human bone morphogenetic protein-2), J Bone Joint Surg Am 79 (12) (1997); 1778-1790.

65. S. Ebara, K. Nakayama, Mechanism for the action of bone morphogenetic proteins and regulation of their activity, Spine 27 (16 Suppl 1) (2002); S10-15.

66. T. Katagiri, A. Yamaguchi, M. Komaki, E. Abe, N. Takahashi, T. Ikeda, V. Rosen, J.M. Wozney, A. Fujisawa-Sehara, T. Suda, Bone morphogenetic protein-2 converts the differentiation pathway of C2C12 myoblasts into the osteoblast lineage, J Cell Biol 127 (6 Pt 1) (1994); 1755-1766.

67. M. Endo, S. Kuroda, H. Kondo, Y. Maruoka, K. Ohya, S. Kasugai, Bone regeneration by modified gene-activated matrix: Effectiveness in segmental tibial defects in rats, Tissue Eng 12 (3) (2006); 489-497.

68. N. Murakami, N. Saito, H. Horiuchi, T. Okada, K. Nozaki, K. Takaoka, Repair of segmental defects in rabbit humeri with titanium fiber mesh cylinders containing recombinant human bone morphogenetic protein-2 (rhBMP-2) and a synthetic polymer, J Biomed Mater Res 62 (2) (2002); 169-174.

69. G.E. Pluhar, P.A. Manley, J.P. Heiner, R. Vanderby, Jr., H.J. Seeherman, M.D. Markel, The effect of recombinant human bone morphogenetic protein-2 on femoral reconstruction with an intercalary allograft in a dog model, J Orthop Res 19 (2) (2001); 308-317.

70. K.R. Dai, X.L. Xu, T.T. Tang, Z.A. Zhu, C.F. Yu, J.R. Lou, X.L. Zhang, Repairing of goat tibial bone defects with BMP-2 gene-modified tissue-engineered bone, Calcif Tissue Int 77 (1) (2005); 55-61.

71. M. Yamamoto, Y. Takahashi, Y. Tabata, Bone induction by controlled release of BMP-2 from a biodegradable hydrogel in various animal species - from mouse to non-human primate, Asbm6: Advanced Biomaterials Vi 288-289 (2005); 253-256.

72. S.C. Chang, H.L. Chuang, Y.R. Chen, J.K. Chen, H.Y. Chung, Y.L. Lu, H.Y. Lin, C.L. Tai, J. Lou, Ex vivo gene therapy in autologous bone marrow stromal stem cells for tissue-engineered maxillofacial bone regeneration, Gene Ther 10 (24) (2003); 2013-2019.

73. D.L. Cochran, J.M. Wozney, Biological mediators for periodontal regeneration, Periodontol 2000 19 (1999); 40-58.

74. G. Turgeman, Y. Zilberman, S. Zhou, P. Kelly, I.K. Moutsatsos, Y.P. Kharode, L.E. Borella, F.J. Bex, B.S. Komm, P.V. Bodine, D. Gazit, Systemically administered rhBMP-2 promotes MSC activity and reverses bone and cartilage loss in osteopenic mice, J Cell Biochem 86 (3) (2002); 461-474.

75. H.S. Sandhu, Bone morphogenetic proteins and spinal surgery, Spine 28 (15 Suppl) (2003); S64-73.

76. A.H. Reddi, Role of morphogenetic proteins in skeletal tissue engineering and regeneration, Nature Biotechnology 16 (3) (1998); 247-252.

77. E. Alsberg, E.E. Hill, D.J. Mooney, Craniofacial tissue engineering, Critical Reviews in Oral Biology & Medicine 12 (1) (2001); 64-75.

78. D. Wu, P. Razzano, D.A. Grande, Gene therapy and tissue engineering in repair of the musculoskeletal system, J Cell Biochem 88 (3) (2003); 467-481.

79. M.T. Lotze, T.A. Kost, Viruses as gene delivery vectors: application to gene function, target validation, and assay development, Cancer Gene Ther 9 (8) (2002); 692-699.

80. S. Rogers, P. Pfuderer, Use of viruses as carriers of added genetic information, Nature 219 (5155) (1968); 749-751.

81. R.G. Crystal, Transfer of genes to humans: early lessons and obstacles to success, Science 270 (5235) (1995); 404-410.

82. T.J. Oligino, Q. Yao, S.C. Ghivizzani, P. Robbins, Vector systems for gene transfer to joints, Clin Orthop Relat Res (379 Suppl) (2000); S17-30.

83. S.M. Selkirk, Gene therapy in clinical medicine, Postgrad Med J 80 (948) (2004); 560-570.

84. J.A. Wolff, R.W. Malone, P. Williams, W. Chong, G. Acsadi, A. Jani, P.L. Felgner, Direct gene transfer into mouse muscle in vivo, Science 247 (4949 Pt 1) (1990); 1465-1468.

85. H. Herweijer, J.A. Wolff, Progress and prospects: naked DNA gene transfer and

therapy, Gene Ther 10 (6) (2003); 453-458.

86. T. Niidome, L. Huang, Gene therapy progress and prospects: Nonviral vectors, Gene Therapy 9 (24) (2002); 1647-1652.

87. A. Pfeifer, I.M. Verma, Gene therapy: promises and problems, Annu Rev Genomics Hum Genet 2 (2001); 177-211.

88. D.D. Lasic, D. Papahadjopoulos, Liposomes revisited, Science 267 (5202) (1995); 1275-1276.

89. R. Lutz, J. Park, E. Felszeghy, J. Wiltfang, E. Nkenke, K.A. Schlegel, Bone regeneration after topical BMP-2-gene delivery in circumferential peri-implant bone defects, Clin Oral Implants Res 19 (6) (2008); 590-599.

90. T. Segura, L.D. Shea, Materials for non-viral gene delivery, Annual Review of Materials Research 31 (2001); 25-46.

91. Y.J. Seol, K.H. Kim, Y.J. Park, Y.M. Lee, Y. Ku, I.C. Rhyu, S.J. Lee, S.B. Han, C.P. Chung, Osteogenic effects of bone-morphogenetic-protein-2 plasmid gene transfer, Biotechnol Appl Biochem 49 (Pt 1) (2008); 85-96.

92. M.X. Tang, C.T. Redemann, F.C. Szoka, Jr., In vitro gene delivery by degraded polyamidoamine dendrimers, Bioconjug Chem 7 (6) (1996); 703-714.

93. I. Ono, T. Yamashita, H.Y. Jin, Y. Ito, H. Hamada, Y. Akasaka, M. Nakasu, T. Ogawa, K. Jimbow, Combination of porous hydroxyapatite and cationic liposomes as a vector for BMP-2 gene therapy, Biomaterials 25 (19) (2004); 4709-4718.

94. Y.C. Huang, C. Simmons, D. Kaigler, K.G. Rice, D.J. Mooney, Bone regeneration in a rat cranial defect with delivery of PEI-condensed plasmid DNA encoding for bone morphogenetic protein-4 (BMP-4), Gene Ther 12 (5) (2005); 418-426.

95. K. Itaka, S. Ohba, K. Miyata, H. Kawaguchi, K. Nakamura, T. Takato, U.I. Chung, K. Kataoka, Bone regeneration by regulated in vivo gene transfer using biocompatible polyplex nanomicelles, Mol Ther 15 (9) (2007); 1655-1662.

96. S. Ohashi, T. Kubo, T. Kishida, T. Ikeda, K. Takahashi, Y. Arai, R. Terauchi, H. Asada, J. Imanishi, O. Mazda, Successful genetic transduction in vivo into synovium by means of electroporation, Biochem Biophys Res Commun 293 (5) (2002); 1530-1535.

97. E. Uchida, H. Mizuguchi, A. Ishii-Watabe, T. Hayakawa, Comparison of the efficiency and safety of non-viral vector-mediated gene transfer into a wide range of human cells, Biol Pharm Bull 25 (7) (2002); 891-897.

98. Z. Bengali, L.D. Shea, Gene delivery by immobilization to cell-adhesive substrates, Mrs Bulletin 30 (9) (2005); 659-662.

99. J. Yovandich, B. O'Malley, Jr., M. Sikes, F.D. Ledley, Gene transfer to synovial cells by intra-articular administration of plasmid DNA, Hum Gene Ther 6 (5) (1995); 603-610.

100. M. Ulrich-Vinther, Gene therapy methods in bone and joint disorders. Evaluation of the adeno-associated virus vector in experimental models of articular cartilage disorders, periprosthetic osteolysis and bone healing, Acta Orthop Suppl 78 (325) (2007); 1-64.

101. N.G. Rainov, H. Ren, Clinical trials with retrovirus mediated gene therapy--what have we learned?, J Neurooncol 65 (3) (2003); 227-236.

102. R.M. Blaese, K.W. Culver, A.D. Miller, C.S. Carter, T. Fleisher, M. Clerici, G. Shearer, L. Chang, Y. Chiang, P. Tolstoshev, J.J. Greenblatt, S.A. Rosenberg, H. Klein, M. Berger, C.A. Mullen, W.J. Ramsey, L. Muul, R.A. Morgan, W.F. Anderson, T lymphocyte-directed gene therapy for ADA- SCID: initial trial results after 4 years, Science 270 (5235) (1995); 475-480.

103. D. Hannallah, B. Peterson, J.R. Lieberman, F.H. Fu, J. Huard, Gene therapy in orthopaedic surgery, Instr Course Lect 52 (2003); 753-768.

104. P.D. Robbins, H. Tahara, S.C. Ghivizzani, Viral vectors for gene therapy, Trends Biotechnol 16 (1) (1998); 35-40.

105. R. Gardlik, R. Palffy, J. Hodosy, J. Lukacs, J. Turna, P. Celec, Vectors and delivery systems in gene therapy, Med Sci Monit 11 (4) (2005); RA110-121.

106. K.L. Berkner, Development of adenovirus vectors for the expression of heterologous genes, Biotechniques 6 (7) (1988); 616-629.

107. O.M. Tepper, B.J. Mehrara, Gene therapy in plastic surgery, Plast Reconstr Surg 109 (2) (2002); 716-734.

108. Z.L. Jiang, D. Reay, F. Kreppel, A. Gambotto, E. Feingold, S. Kochanek, S.A. McCarthy, P.R. Clemens, Local high-capacity adenovirus-mediated mCTLA4Ig and mCD40Ig expression prolongs recombinant gene expression in skeletal muscle, Mol Ther 3 (6) (2001); 892-900.

109. R.W. Atchison, B.C. Casto, W.M. Hammon, Adenovirus-Associated Defective Virus Particles, Science 149 (1965); 754-756.

110. T. Ogata, T. Kozuka, T. Kanda, Identification of an insulator in AAVS1, a

preferred region for integration of adeno-associated virus DNA, J Virol 77 (16) (2003); 9000-9007.

111. S.M. Young, Jr., D.M. McCarty, N. Degtyareva, R.J. Samulski, Roles of adeno-associated virus Rep protein and human chromosome 19 in site-specific recombination, J Virol 74 (9) (2000); 3953-3966.

112. S.M. Young, Jr., W. Xiao, R.J. Samulski, Site-specific targeting of DNA plasmids to chromosome 19 using AAV cis and trans sequences, Methods Mol Biol 133 (2000); 111-126.

113. W.G. Kearns, S.A. Afione, S.B. Fulmer, M.C. Pang, D. Erikson, M. Egan, M.J. Landrum, T.R. Flotte, G.R. Cutting, Recombinant adeno-associated virus (AAV-CFTR) vectors do not integrate in a site-specific fashion in an immortalized epithelial cell line, Gene Ther 3 (9) (1996); 748-755.

114. E.A. Rutledge, D.W. Russell, Adeno-associated virus vector integration junctions, J Virol 71 (11) (1997); 8429-8436.

115. K.R. Clark, T.J. Sferra, P.R. Johnson, Recombinant adeno-associated viral vectors mediate long-term transgene expression in muscle, Hum Gene Ther 8 (6) (1997); 659-669.

116. M. Ulrich-Vinther, C. Stengaard, E.M. Schwarz, M.B. Goldring, K. Soballe, Adeno-associated vector mediated gene transfer of transforming growth factor-beta1 to normal and osteoarthritic human chondrocytes stimulates cartilage anabolism, Eur Cell Mater 10 (2005); 40-50.

117. P.L. Hermonat, N. Muzyczka, Use of adeno-associated virus as a mammalian DNA cloning vector: transduction of neomycin resistance into mammalian tissue culture cells, Proc Natl Acad Sci U S A 81 (20) (1984); 6466-6470.

118. H. Ito, J.J. Goater, P. Tiyapatanaputi, P.T. Rubery, R.J. O'Keefe, E.M. Schwarz, Light-activated gene transduction of recombinant adeno-associated virus in human mesenchymal stem cells, Gene Ther 11 (1) (2004); 34-41.

119. J. Li, R.J. Samulski, X. Xiao, Role for highly regulated rep gene expression in adeno-associated virus vector production, J Virol 71 (7) (1997); 5236-5243.

120. X. Xiao, J. Li, R.J. Samulski, Production of high-titer recombinant adeno-associated virus vectors in the absence of helper adenovirus, J Virol 72 (3) (1998); 2224-2232.

121. W.C. Tseng, F.R. Haselton, T.D. Giorgio, Transfection by cationic liposomes using simultaneous single cell measurements of plasmid delivery and transgene expression, J Biol Chem 272 (41) (1997); 25641-25647.

122. C.M. Varga, K. Hong, D.A. Lauffenburger, Quantitative analysis of synthetic gene delivery vector design properties, Mol Ther 4 (5) (2001); 438-446.

123. T. Boontheekul, D.J. Mooney, Protein-based signaling systems in tissue engineering, Curr Opin Biotechnol 14 (5) (2003); 559-565.

124. R. Langer, New methods of drug delivery, Science 249 (4976) (1990); 1527-1533.

125. H. Shen, J. Tan, W.M. Saltzman, Surface-mediated gene transfer from nanocomposites of controlled texture, Nat Mater 3 (8) (2004); 569-574.

126. D. Luo, W.M. Saltzman, Enhancement of transfection by physical concentration of DNA at the cell surface, Nat Biotechnol 18 (8) (2000); 893-895.

127. Z. Bengali, A.K. Pannier, T. Segura, B.C. Anderson, J.H. Jang, T.A. Mustoe, L.D. Shea, Gene delivery through cell culture substrate adsorbed DNA complexes, Biotechnol Bioeng 90 (3) (2005); 290-302.

128. D.A. Wang, J. Ji, Y.H. Sun, J.C. Shen, L.X. Feng, J.H. Elisseeff, In situ immobilization of proteins and RGD peptide on polyurethane surfaces via poly(ethylene oxide) coupling polymers for human endothelial cell growth, Biomacromolecules 3 (6) (2002); 1286-1295.

129. J.C. Schense, J. Bloch, P. Aebischer, J.A. Hubbell, Enzymatic incorporation of bioactive peptides into fibrin matrices enhances neurite extension, Nat Biotechnol 18 (4) (2000); 415-419.

130. E. Alsberg, K.W. Anderson, A. Albeiruti, R.T. Franceschi, D.J. Mooney, Cell-interactive alginate hydrogels for bone tissue engineering, J Dent Res 80 (11) (2001); 2025-2029.

131. M.A. Princz, H. Sheardown, Heparin-modified dendrimer cross-linked collagen matrices for the delivery of basic fibroblast growth factor (FGF-2), Journal of Biomaterials Science-Polymer Edition 19 (9) (2008); 1201-1218.

132. J. Kim, Y. Park, G. Tae, K.B. Lee, C.M. Hwang, S.J. Hwang, I.S. Kim, I. Noh, K. Sun, Characterization of low-molecular-weight hyaluronic acid-based hydrogel and differential stem cell responses in the hydrogel microenvironments, Journal of Biomedical Materials Research Part A 88A (4) (2009); 967-975.

133. T.W. Chung, Y.F. Lu, S.S. Wang, Y.S. Lin, S.H. Chu, Growth of human endothelial cells on photochemically grafted Gly-Arg-Gly-Asp (GRGD) chitosans, Biomaterials 23 (24) (2002); 4803-4809.

134. R.J. Levy, C. Song, S. Tallapragada, S. DeFelice, J.T. Hinson, N. Vyavahare, J.

Connolly, K. Ryan, Q. Li, Localized adenovirus gene delivery using antiviral IgG complexation, Gene Ther 8 (9) (2001); 659-667.

135. A. Sintov, S. Ankol, D.P. Levy, A. Rubinstein, Enzymatic cleavage of disaccharide side groups in insoluble synthetic polymers: a new method for specific delivery of drugs to the colon, Biomaterials 14 (7) (1993); 483-490.

136. J.M. Abrahams, C. Song, S. DeFelice, M.S. Grady, S.L. Diamond, R.J. Levy, Endovascular microcoil gene delivery using immobilized anti-adenovirus antibody for vector tethering, Stroke 33 (5) (2002); 1376-1382.

137. B.D. Klugherz, C. Song, S. DeFelice, X. Cui, Z. Lu, J. Connolly, J.T. Hinson, R.L. Wilensky, R.J. Levy, Gene delivery to pig coronary arteries from stents carrying antibody-tethered adenovirus, Hum Gene Ther 13 (3) (2002); 443-454.

138. T. Segura, P.H. Chung, L.D. Shea, DNA delivery from hyaluronic acid-collagen hydrogels via a substrate-mediated approach, Biomaterials 26 (13) (2005); 1575-1584.

139. T. Segura, L.D. Shea, Surface-tethered DNA complexes for enhanced gene delivery, Bioconjug Chem 13 (3) (2002); 621-629.

140. T. Segura, M.J. Volk, L.D. Shea, Substrate-mediated DNA delivery: role of the cationic polymer structure and extent of modification, J Control Release 93 (1) (2003); 69-84.

141. J.H. Jang, C.B. Rives, L.D. Shea, Plasmid delivery in vivo from porous tissue-engineering scaffolds: transgene expression and cellular transfection, Mol Ther 12 (3) (2005); 475-483.

142. D.A. Hobson, M.W. Pandori, T. Sano, In situ transduction of target cells on solid surfaces by immobilized viral vectors, BMC Biotechnol 3 (2003); 4.

143. M. Pandori, D. Hobson, T. Sano, Adenovirus-microbead conjugates possess enhanced infectivity: a new strategy for localized gene delivery, Virology 299 (2) (2002); 204-212.

144. J. Lahann, D. Klee, H. Hocker, Chemical vapour deposition polymerization of substituted [2.2]paracyclophanes, Macromolecular Rapid Communications 19 (9) (1998); 441-444.

145. K.B. Lee, D.J. Kim, Z.W. Lee, S.I. Woo, I.S. Choi, Pattern generation of biological ligands on a biodegradable poly(glycolic acid) film, Langmuir 20 (7) (2004); 2531-2535.

146. H. Nandivada, H.Y. Chen, J. Lahann, Vapor-based synthesis of poly

[(4-formyl-p-xylylene)-co-(p-xylylene)] and its use for biomimetic surface modifications, Macromolecular Rapid Communications 26 (22) (2005); 1794-1799.

147. J. Yang, J. Bei, S. Wang, Enhanced cell affinity of poly (D,L-lactide) by combining plasma treatment with collagen anchorage, Biomaterials 23 (12) (2002); 2607-2614.

148. J. Heitz, H. Niino, A. Yabe, Chemical surface modification on polytetrafluoroethylene films by vacuum ultraviolet excimer lamp irradiation in ammonia gas atmosphere, Applied Physics Letters 68 (19) (1996); 2648-2650.

149. M. Celina, H. Kudoh, T.J. Renk, K.T. Gillen, R.L. Clough, Surface modification of polymeric materials by pulsed ion beam irradiation, Radiation Physics and Chemistry 51 (2) (1998); 191-194.

150. M. Nitschke, G. Schmack, A. Janke, F. Simon, D. Pleul, C. Werner, Low pressure plasma treatment of poly(3-hydroxybutyrate): toward tailored polymer surfaces for tissue engineering scaffolds, J Biomed Mater Res 59 (4) (2002); 632-638.

151. Y. Hu, S.R. Winn, I. Krajbich, J.O. Hollinger, Porous polymer scaffolds surface-modified with arginine-glycine-aspartic acid enhance bone cell attachment and differentiation in vitro, J Biomed Mater Res A 64 (3) (2003); 583-590.

152. X. Liu, P.X. Ma, Polymeric scaffolds for bone tissue engineering, Ann Biomed Eng 32 (3) (2004); 477-486.

153. J. Lahann, R. Langer, Novel poly(p-xylylenes): Thin films with tailored chemical and optical properties, Macromolecules 35 (11) (2002); 4380-4386.

CHAPTER 3

LOCALIZED VIRAL VECTOR DELIVERY TO FACILITATE BONE REGENERATION

3.1 Introduction

Transplantation of free transfer of vascularized graft is the gold standard for bone reconstruction. However, defect size and wound complexity are often the limitations of this therapy. Thus, different auxiliary therapies are necessary to improve therapeutic outcomes for patients with large skeletal defects or anomalies. For small bone defects, administration of an osteoinductive protein, such as BMPs, is often enough to enhance osseous regeneration. However, successful treatment of large defects which cannot heal spontaneously, also known as critical-sized defects, requires a more robust stimulus for longer periods of time. In addition, bone defects created by tumor resection in the head and neck are easily contaminated with oral bacteria, and are often treated with radiotherapy. Radiation is sometimes applied before surgery to sterilize the region of malignant tumor cells and to decrease the risk of local recurrence [1, 2]. However, irradiation frequently results in hypocellularity, hypoxia, and hypovascularity, which lead to scaring and fibrosis, and complicate bone regeneration after osteotomy surgery [3-6]. Therefore, it is important to develop effective adjuvant therapies to heal large or compromised osseous wounds.

Through tissue engineering approaches, wound sites may be repaired or regenerated by mimicking natural developmental healing processes. Appropriate biological signals with the correct temporal and spatial release profile may recruit host cells to wound sites and direct new tissue development within designed biomaterial scaffolds. Recombinant growth factor treatment is broadly applied in preclinical studies. VEGF, TGF-β1, and BMPs, have been delivered to compromised defects for ameliorating osteoradionecrosis [7-11]. However, these studies did not demonstrate acceptable levels of osteogenesis to repair compromised critical-sized defects using protein therapy alone. Furthermore, milligram doses may be necessary in these protein-based therapies, which is extremely expensive and thus impractical for universal clinical application. Therefore, regenerative gene therapy may be an improved treatment to addresses these difficulties [12]. The effectiveness of BMP transduced cells has been studied for repairing critical-sized bone defects [13-16]. This *ex vivo* gene therapy also has been demonstrated to be capable of healing bone defects compromised by radiotherapy [17, 18]. While these results indicated that *ex vivo* gene therapy improves bone regeneration of radiation-induced impaired bone, this method requires the harvest of different cells from patients for *in vitro* transduction followed by *in vivo* transplantation, which is very laborious and may cause contamination during *in vitro* cell culture.

In contrast, *in vivo* gene therapy directly delivers genes in wound sites, which may be performed immediately without arduous preparations. The controlled release of viral vectors from bioengineered scaffolds may reduce the need for cell based

regenerative approaches and allow for precise spatial control of cell signaling factors. However, compared to non-viral vectors, virus is sensitive to the ambient environment.

Lyophilization is an efficient method to improve the stability of labile biopharmaceuticals. Virus bioactivity can thus be preserved for long term storage. Lyophilized virus has been coated on allografts to mediate *in vivo* gene transfer [19]. In addition, localized virus delivery can enhance transduction efficiency [20]. Therefore, we hypothesized that an appropriate lyophilization method could localize active virus on biomaterial surfaces that could not only maintain viral bioactivity but also restrict virus on material surfaces to improve cell transduction.

In this study, adenovirus encoding BMP-2 was lyophilized within gelatin sponges to be locally delivered in wound sites. By this *in vivo* gene delivery approach, we hypothesized that host cells grown on scaffolds would be transduced *in situ* to induce bone formation in critical-sized defects. In addition, we further applied this local viral delivery to address clinical difficulties. Bone defects treated with preoperative radiotherapy was repaired by implanting gelatin sponges with lyophilized AdBMP-2 to evaluate if this gene delivery may improve bone formation in defects with osteoradionecrosis. The stability of lyophilized viral vectors was also evaluated to determine the feasibility of this gene delivery method in preparing adenovirus-loaded scaffolds as pre-made constructs for surgical convenience.

3.2 Materials and Methods

3.2.1 Cell culture and virus generation

C4 fibroblast cells (ATCC, Manassas, VA) were cultured in alpha-minimal essential medium (α-MEM, Gibco, Carlsbad, CA) containing 10% fetal bovine serum (FBS, Gibco) and penicillin (100 unit/ml)-streptomycin (100 μg/ml) (Gibco). Cells were seeded at density of 20,000 cells/cm^2. An adenovirus encoding the bacterial β-galactosidase gene (AdRSVntLacZ) and nuclear localization sequence was used as a reporter gene. The virus used for *in vivo* application, AdCMV-BMP-2, was a recombinant virus with the E1 and E3 genes deleted and contained the mouse BMP-2 gene, which was constructed using Cre/lox recombination as previously described [21].

3.2.2 Assessment for *in vitro* virus infection

Fibroblasts were cultured in 48 well cell culture cluster dishes (Corning, NY) at a density of $2x10^4$ per well in 350 μl culture medium for the AdLacZ virus infection. After 2 days incubation at 37 ˚C, the cells were fixed in 1% glutaraldehyde for one half hour then were washed three times with PBS. The X-gal staining solution, 0.2% 5-bromo-4-chloro-3-indolyl-h-D-galactoside (X-gal, Invitrogen, Frederick, MD) in N,N-dimethyl formamide with 2 mM $MgCl_2$, 5 mM $K_4Fe(CN)_6$_$3H_2O$, 5 mM $K_3Fe(CN)_6$ in phosphate buffered saline (PBS) (all Sigma), was prepared and 350 μl was added for 37 ˚C incubation overnight. Because transduced cells expressed β-galactosidase to hydrolyze X-gal, blue precipitate was thus formed in cells and viral bioactivity could be determined by the stained area. The blue area was digitally captured under an SMZ-U stereoscopic zoom microscope (Nikon, Melville, NY) with a DC290 digital camera (Eastman Kodak, Rochester, NY). The blue pixels in the image were analyzed by Scion Image software

(Scion, Frederick, MD). Color images were converted to gray scale then were thresholded to mark the pixel area. Pixel number was counted to indicate the level of cell transduction.

3.2.3 Virus lyophilization formulation

Different excipients were tested using methods established for long-term adenovirus storage [22]. Two different lyophilization conditions, suspension lyophilization and surface lyophilization, were tested. For suspension lyophilization, AdLacZ was diluted to $5x10^8$ pfu/ml (pfu: plaque forming unit), and 10 µl placed in a microcentrifuge tube. For surface lyophilization, 2 µl AdLacZ was diluted to $2.5x10^9$ pfu/ml and placed on 5mm diameter hydroxyapatite (HA) disks. The sintered HA disk surfaces were smooth and dense. These dense surfaces inhibited virus and cell migration into the scaffold and thus the experimental environment was limited to the top of the disk. Both groups were incubated at -80 ˚C for two hours and then were lyophilized in a freeze dryer (Virtis, Gardiner, NY) at -78.5 ˚C and 100 mtorr for 24 hours. The lyophilized virus was reconstituted in culture medium for the suspension lyophilization group. Subsequently, $1x10^4$ fibroblasts were seeded to make a final multiplicity of infection (moi) of 500. AdLacZ lyophilized in PBS alone was treated as a negative control and non-lyophilized virus served as the positive control. After two days infection, X-gal staining was performed to evaluate preservation of virus bioactivity after lyophilization. The formula with the best performance was used for all subsequent experiments.

After the optimal formula was determined, a pattern assay was performed to determine if lyophilization could precisely localize the virus on a material surface for infection. AdLacZ (10^7 pfu/glass slide) was added by micropipette in the pattern of the letters “U” and ”M” on glass cover slips. After one day lyophilization, the slides were placed in Petri dishes and cultured with fibroblasts for two days to obtain a confluent layer of cells on the glass slide. Subsequently, the cells were stained with X-gal to determine control of virus localization.

3.2.4 The efficacy of transduction by virus localization

To determine if the virus lyophilized on biomaterial surfaces could be localized to enhance transduction, viruses were lyophilized for 24 hours and infected cells by two methods: 1) virus lyophilized in microcentrifuge tubes then reconstituted in culture medium to infect cells as a free form, or 2) virus lyophilized on hydroxyapatite (HA) disks followed by culturing cells on the surface directly. Virus without lyophilization was used as a positive control. X-gal staining after a 2 day cell infection was applied to evaluate the transduction efficiency.

In addition, a low volume infection experiment was performed to simulate the lyophilized virus infection on material surfaces. AdLacZ was diluted to $5x10^9$ or $1 x10^{10}$ pfu/ml and 2 µl was added to HA disks and lyophilized for 24 hours. C4 fibroblasts were cultured on the material surface to make the final infection 500 or 1000 moi. The same amount of virus was lyophilized and then reconstituted in culture medium to infect cells directly as free-form. Two different infection volumes were used during the infections: 1)

Regular volume: fibroblasts in 350 µl medium were added in the culture wells for two days infection. 2) Low volume: fibroblasts in 20 µl medium were added on HA disk surfaces to infect in the first 3 hours, then 330 µl medium was added in culture wells and also incubated for two days. The infected cells were stained with X-gal to determine transduction efficiency.

3.2.5 Release behavior of virus lyophilized on material surfaces

Adenovirus was lyophilized on HA disks for 24 hours and then placed with 350µl culture medium at 37 ˚C to simulate the *in vitro* infection. The medium was sampled (45µl) at different time points. Non-lyophilized virus was compared as a standard. The supernatant was treated with 5 µl of 0.5% SDS in TE buffer (10mM Tris-HCl, pH=7.5, 1mM EDTA) at room temperature for 15 minutes to lyse the viral capsid. The fluorescent dye, PicoGreen (Promega, WI), which can selectively bind viral DNA was used to quantify viral DNA. Twenty microliters of diluted lysed viral standards or samples were added to 96-well microplates. Picrogreen reagent was diluted 360-fold in TE buffer and 180 µl was added to each well. After 5 minutes dark incubation, the viral DNA-PicoGreen complex was read on a microplate spectrofluorometer (Gemini XPS, Molecular Devices, Sunnyvale, CA) with 485 nm and 538 nm wavelength setting for excitation and emission, respectively [23].

3.2.6 Preservation of viral bioactivity after long term storage

AdLacZ was lyophilized either in microcentrifuge tubes or on HA disks. Viruses in PBS without lyophilization were accompanied as negative controls. Samples were

stored at -80 ºC, -20 ºC, or 4 ºC. After 1 week, 2 weeks, 1 month, 3 months, and 6 months storage, lyophilized virus in microcentrifuge tubes was reconstituted in culture medium and then used to infect fibroblasts on HA disks. Virus lyophilized on HA disks were also placed in culture wells for cell infection. Fibroblasts were cultured at a density of $1x10^4$ cells/well and the final infection concentration was 500 moi. Fresh virus without lyophilization was compared as standard for the X-gal assay to determine the change of viral bioactivity with time.

3.2.7 Polymer matrix loaded with adenovirus for BMP-2 gene delivery

Gelfoam, a gelatin sponge (Pfizer, New York City, NY), was used as a biomaterial scaffold and BMP-2 was the target gene to deliver by adenovirus for bone regeneration. Sponges were cut to fit 8mm calvarial defects and were hydrated in PBS before adenovirus loading. For the virus lyophilization groups, 20 μl adenovirus in PBS with 1 M sucrose was loaded on to the gelatin scaffolds at final concentration of 10^8 pfu then freeze dried for 24 hours. A free AdBMP-2 group was also prepared with the same virus concentration in PBS before surgery. Virus concentration was determined by a pilot experiment to titrate virus concentrations from 10^7 to 10^9 pfu for both free and lyophilized AdBMP-2 groups. Bone growth was undetectable with 10^7 pfu. In contrast, both lyophilized virus and free form virus groups exhibited new bone formation if the virus was 10^8 pfu. In experiments when the virus concentrations were greater than 10^8 pfu, there were no differences between groups because this viral titer led to bone overgrowth. Therefore 10^8 pfu was chosen as our effective dose.

3.2.8 Animal irradiation

Fisher 344 rats (Charles River, Wilmington, MA) weighing 200 to 250 grams were used in this study. The surgical sites were irradiated as previous described [18]. Briefly, rats were anesthetized and a single 12-Gy dose was delivered to D_{max} at a source-to-skin distance of 80 cm in an 11.47-min exposure to the surgical site. The rest of the body was shielded [24]. The radiation dose was administered 2 weeks before the surgical procedure to mimic a clinical pre-surgical radiation protocol.

3.2.9 Calvarial defect model and specimen harvest

Rats were anaesthetized by ketamine and xylazine mixture (80 mg/kg ketamine, 10 mg/kg xylazine of body weight). A 3-cm linear incision was made over the calvarium and the periosteum was completely cleared from the surface of the cranium by scraping. A critical-size defect was created using an 8 mm diameter trephine burr with copious PBS irrigation. The calvarial disks were carefully removed and gelatin scaffolds were placed in the defects. The incisions were closed with 4-0 chromic gut sutures (Davis-Geck, Wayne, NJ). Five animals per each group were implanted for five weeks then scarified for histology and μ-CT analysis. All specimens were fixed in buffered zinc formalin fixative, Z-Fix for one day then stored in 70% alcohol. Care and use of the laboratory animals followed the guidelines established by the University of Michigan Committee for the Use and Care of Animals.

3.2.10 Micro-CT 3D reconstruction and bone histomorphometry

Specimens were scanned by μ-CT on a MS8-CMR-100μ-CT scanner (EVS Corp, London, ON, Canada) at 10 μm voxel resolution and 80-kV. Then these reconstructed images were analyzed by Microview v2.1.0 (GE, Waukesha, WI). Auto-thresholds of the tissue density were determined by Microview to define mineralized tissue (bone). Circular regions of 8mm diameter were cropped as the region of interest (ROI). The bone volume fraction (BVF) was evaluated by the volume ratio of the mineralized tissue in ROI.

The 3-D images were performed as isosurfaces of mineralized tissue which were defined by the threshold. The superficial views were captured as in Fig 3.5 a, and then the bone covered in defects was captured by Scion Image software (Scion, Frederick, MD). Finally, the coverage of the regenerated bone was determined as bone area fraction (BAF).

3.2.11 Histology assessment

Before histological analysis, specimens were decalcified in 10% formic acid for two days. After paraffin embedding, 5 μm sections were prepared from the middle line of defects and stained with hematoxylin and eosin (H & E). These tissue sections were visualized with an inverted microscope Eclipse TE300 (Nikon, Melville, NY). The healing effects of orthotropic bone regeneration were evaluated by examining if there were even newly osseous tissue growth, bone-defect margin osseointegration, and hematopoietic bone marrows formation in these critical-size calvarial defects.

3.3 Results

3.3.1 Lyophilization preserves virus bioactivity and localizes virus on HA material surfaces

Lyophilization of adenovirus is currently the methods of choice for long-term storage of virus stocks [22]. We therefore hypothesized that the appropriate formula could be used to retain virus on material surfaces for localized gene delivery. Three different excipient formulations were tested. An adenovirus expressing β-galactosidase (AdLacZ) as a reporter gene was used to examine virus bioactivity and infection performance. For the suspension lyophilization experiment, adenovirus lyophilized in PBS only (negative control, NC) always lost its bioactivity during lyophilization (Fig 3.1 a). An excipient containing 10 mg/ml sucrose and mannitol in PBS (Suc/Man) performed better than the negative control, but was not as robust as the two other formulations. Virus bioactivity was maintained at the highest level when mixed with 40 mg/ml sucrose and mannitol with 0.001% Span 20 in PBS (Suc/Man/Span) or in PBS with 1 M sucrose (1M-Suc). These two formulae preserved bioactivities equivalent to the positive control (PC), virus without lyophilization. In addition, virus lyophilized on material surfaces in 1M-Suc and Suc/Man/Span both enhanced virus infection performance compared to the positive control in the surface lyophilization experiments (Fig 3.1 b). These findings suggested that the appropriate formulae can concentrate and localize adenovirus on material surfaces to improve transduction efficiency. Although these two formulae can both maintain viral bioactivity and localize virus infection, we chose 1 M sucrose in PBS for our following lyophilization experiments because of its ease of preparation. In addition, sucrose is a carbohydrate molecule that contains ambient hydroxyl groups.

Hydrogen bonds formed between the material surfaces and viral capsid may facilitate virus adhesion.

After the optimal lyophilization formula was determined, AdLacZ adenovirus was lyophilized on glass cover slips in defined patterns. Fibroblasts were cultured on these cover slips for two days then stained with X-gal. The cells were examined under a phase contrast microscope before X-gal staining to confirm that they grew to confluence on the slips. We observed that cells were only infected in the pre-defined "U M" pattern. This provided strong evidence that adenovirus lyophilized on material surfaces can be precisely localized in a specific pattern and maintain its bioactivity (Fig 3.1 c).

3.3.2 Virus lyophilized on material surfaces enhances transduction efficiency

Two environments with different virus concentrations were tested to evaluate infection efficiency of adenovirus delivered on biomaterials. For both tissue culture wells and HA disks, no differences were observed between before and after lyophilization treatment if virus suspended in the free-form was used for infection (Fig 3.2 a,b). However, if virus was lyophilized on HA disks, infection efficiency was significantly improved (Fig 3.2 b). The transduced cell area of surface lyophilization was nearly double to triple that of the suspended lyophilization group. These data suggest that lyophilized virus on biomaterials can effectively decrease the concentration of virus needed for infection.

We hypothesized that lyophilized virus was localized and concentrated on the material surface and thus we designed a low volume infection to mimic this situation. The virus lyophilized on HA disks had better infection performance than the free-form group (Fig 3.2 c). This result demonstrated that lyophilization enhanced the virus infection. However, there was no significant difference between these two groups when infected by the low volume procedure (Fig 3.2 d). Moreover, virus in low volume infection always had a higher transduction efficiency than the higher volume condition.

3.3.3 Lyophilized virus can be locally delivered on material surfaces

The release of viral DNA from HA surface was determined *in vitro* (Fig 3.3). Lyophilized virus released rapidly into the culture medium. In this aqueous environment, about 60% virus was released in the first hour; however, the release was subsequently slower. Approximately 30% of the virus was maintained on the HA disk surfaces after 16 hours. Since one third of the virus could be retained on the material surface without releasing, this result is consistent with our hypothesis that lyophilized virus has a more robust infection performance due to its concentration on material surfaces.

3.3.4 Bioactivity of lyophilized virus on biomaterials can be preserved for long term storage

To determine if lyophilization may effectively extend virus survival rates on biomaterial surfaces, we lyophilized AdLacZ in 1 M sucrose and then reconstituted it in culture medium at different time points to assess the decline of viability at different temperatures. At 4˚C, virus infection was detectable for three months. In the frozen environment, -20 ˚C and -80 ˚C, virus bioactivities continuously decreased in the early

period. However, after one month storage, the activity equilibrized and was maintained up to at least 6 months.

The viral survival rates at -20˚C and -80˚C were 49% ± 2% and 65% ± 2%, respectively (Fig 3.4 a). In contrast, the control group, consisting of virus in PBS, lost its bioactivity rapidly. No active virus was detected after 2 weeks when stored at 4˚C. Even at a -80˚C storage temperature there was only 40% virus bioactivity remaining at 6 months (Fig 3.4 b).

We next evaluated viral bioactivity when AdLacZ was lyophilized on HA disk surfaces. The viability trends of surface lyophilized virus were similar to the suspension lyophilization group (Fig 3.4 c). First, the initial bioactivity was 350 % ± 10 % of the positive control. This was likely due to the localized infection effect. Similar to suspension lyophilization, surface lyophilized virus exhibited a decline in bioactivity in the first month. At 4˚C, virus was maintained for 3 months. This was in contrast to surface lyophilized constructs stored at lower temperatures. In these conditions, robust virus activity was sustained and the survival rates were 140% ± 28% and 274% ± 32% when virus were stored at -20 ˚C and -80 ˚C, respectively. The high survival rates maintained at frozen conditions suggested that virus lyophilized with biomaterials could be stable for long term storage.

3.3.5 Bone regeneration in critical-size defects is improved by localizing *in vivo* gene therapy

Because adenovirus could be localized on HA disk surfaces to enhance cell infection, we sought to determine if virus localization could be effective for clinically relevant orthotopic bone regeneration. Critical-size defects provide a convenient non-loaded model to evaluate bone regeneration strategies because the defect cannot spontaneously heal during the lifetime of the animal [25]. Micro-CT was used to quantify bone volume fraction (BVF), bone mineral density (BMD), and histomorphometric analysis which was performed to determine bone area fraction (BAF) in the defect region. Free AdBMP-2 was treated as the positive control group and lyophilized AdLacZ was the negative control.

Micro-CT 3D analysis demonstrated that the lyophilized AdLacZ group had only minimal bone growth at the edges of the defect (Fig 3.5). A BVF of 14.5% ± 4.8% and a BAF of 16.8% ± 5.4% indicated that critical-size defects may not spontaneously heal using gelatin scaffolds without osteoinductive BMPs (Fig 3.6 a,b). The newly formed bone in the free-form AdBMP-2 group was mainly distributed along the defect edge with occasional isolated bony islands localized in the center region (Fig 3.5). The BVF and BAF were 43.8% ± 13.6% and 43.1% ± 14.1%, respectively, which indicated the free virus induced modest bone regeneration (Fig 3.6 a,b). In contrast, the lyophilized AdBMP-2 group had almost double the bone growth than the free-form group in terms of both BVF and BAF (88.7% ± 23.5% and 75.4% ± 15.0%), demonstrating that transduction can be improved to induce more bone regeneration in orthotopic defects by localizing adenovirus on biomaterials (Fig 3.6 a,b). Micro-CT images of the lyophilization group also suggested that new bone was evenly distributed to cover the

defects and lead to excellent healing (Fig 3.5). Bone mineral density of lyophilized AdLacZ was only 110 ± 29 mg/cc, which is significantly lower than the other two groups (Fig 3.6 c). Interestingly, although lyophilized AdBMP-2 had significantly higher BMD than free AdBMP-2 group (250 ± 41 mg/cc vs. 178 ± 42 mg/cc), the difference was not as obvious as BVF and BAF ($p<0.05$).

By histologic analysis, only dense fibrous connective tissue with minimal osteogenesis was found in the lyophilized AdLacZ treated defects (Fig 3.7 a). Some small osseous islands were observed in the free AdBMP-2 group (Fig 3.7 b). However, extensive bone regeneration was always observed in the lyophilized AdBMP-2 group (Fig 3.7 c). Nearly all the defect space was filled with confluent bone surrounding a hematopoietic marrow. The newly formed bone was osseointegrated with the native bone and the margins were difficult to identify (Fig 3.7 c). Since the new bone was not uniformly distributed in the defects, histomorphmetry was not performed from these slides to avoid potential bias. BVF and BAF from μ-CT analysis may provide a more valid comparison to quantify the fraction of new bone formation among experimental groups. The agreement of histology and μ-CT results confirmed our hypothesis that virus lyophilization can effectively improve transduction for *in situ* regenerative gene therapy.

3.3.6 Bone regeneration in critical-size defects compromised by radiation treatment

Our previous results demonstrated that critical-sized defects were capable of being significantly repaired by AdBMP-2 lyohilized within scaffolds compared to suspended virus administration. We next tested if this local virus delivery may facilitate

bone regeneration in defects compromised by radiotherapy (XRT). Consequently, an osteoradionecrosis model was investigated to test the bone reconstruction efficiency of our novel local gene delivery method.

Adenovirus encoding BMP-2 was lyophilized within gelatin sponges before being implanted in calvarial defects compromised by preoperative radiotherapy. As previously described, free AdBMP-2 was treated as the positive control group and lyophilized AdLacZ was the negative control. The cranial specimens were harvested for μ-CT scanning to reconstruct 3-D images and processed for histologic analysis.

For the negative control group, there was almost no bone found in the defect areas except in the immediate vicinity of the surgical margins, suggesting that AdLacZ was not capable of inducing new bone formation (Fig 3.8 a). Using gelatin sponges with a free suspension of AdBMP2, few bony islands were distributed throughout the defect sites, but newly formed bone did not significantly cover the defects (Fig 3.8 b). In contrast, when AdBMP2 was delivered in a lyophilized formulation within gelatin sponges, significant regeneration spanning the entire defect was achieved (Fig 3.8 c).

Both BVF and BMD were evaluated by μ-CT scanning to quantify the newly formed bone in defects compromised by radiation therapy (Fig 3.8 d,e). Compared to the negative control group with AdLacZ treatment, suspended AdBMP2 was able to enhance the BVF from 14.2 ± 5.3% to 44.6 ± 8.5%. However, there was no significant difference in BMD between these two groups (77 ± 16 mg/cc vs. 88 ± 13 mg/cc). In contrast,

AdBMP2 lyophilized within gelatin sponges significantly improved both BVF and BMD over the AdLacZ and free AdBMP2 groups.

In order to quantify the coverage area of regenerated bone in the cranial defects, the BAF of newly formed bone was determined based on 3-D projection images captured by μ-CT (Fig 3.8 f). Compared to the free AdBMP-2 group, in which bone only covered a modest region of the defects (46.4 ± 11.3%), lyophilized AdBMP2 treatment significantly increased bone formation and most of the area of the defects was covered by mineralized tissue (68.7 ± 7.1%). These results suggested that the therapeutic effect of AdBMP2 was greatly improved when it was locally delivered within scaffolds.

3.3.7 The effects of bone regeneration in critical sized defects compromised by radiation treatment

Compared to the excellent bone repair in non radiation (No-XRT) treatment, defects treated with preoperative radiotherapy (Pre-OP) were also successfully regenerated by implanting gelatin scaffolds with lyophilized AdBMP2. Microscopic sections stained with H&E illustrated defects that were filled with newly formed bone (Fig 3.9 a). However, the bone morphology was different from the non-radiation treated group (Fig 3.7 c). The regenerative bone was admixed with soft connective tissues, forming mobile bone islands (Fig 3.9 a). The osseointegration at defect edges did not occur as completely as it did in the non-radiation treated group (Fig 3.9 b) and some of the non-resorbed gelatin structures remained in soft tissues (Fig 3.9 c). Mineralized tissues were deposited as irregular small islands without lamellar architecture, indicating that normal bone remodeling was negatively affected by radiation damage. Some

immature bone marrow structure was distributed in regenerated bone (Fig 3.9 c,d).

Bone regeneration was also compared using μ-CT analysis. From 3-D images, newly formed bone in the Pre-OP group (Fig 3.8 c) illustrated a similar coverage in defects as in the No-XRT group (Fig 3.5). However, compared to the Pre-OP group in which non-union bone gaps existed between newly formed bone and defect margins, bone was well integrated with defect edges in No-XRT group.

The quantified data demonstrated that the BVF and BAF in these two groups had no significant differences (Fig 3.10 a,b). However, the BMD of the Pre-OP group was significantly less than the No-XRT group (108±12 mg/cc vs. 250±41 mg/cc), suggesting the level of mineralization in the Pre-OP group was reduced, which may have been caused by radiation damage (Fig 3.10 c). The sagittal section images were consistent with this result, demonstrating that the radiographs of defects in the Pre-OP group were less radiopaque than in the No-XRT group (Fig 3.5, 3.9 c).

3.3.8 Lyophilized adenovirus with gelatin sponges preserves viral bioactivity

In this study, approximately 80% of adenovirus activity within lyophilized with biomaterials scaffolds was maintained for longer than 6 months. Therefore, we tested the practicality of preparing virus-scaffold complexes as pre-made constructs for potential clinical applications. AdBMP2 lyophilized in gelatin sponges were stored at -80˚C for 1 month, and were implanted in rat calvarial defects with preoperative radiotherapy (1M-PreOP). The 3-D images captured by μ-CT scanning illustrated that bone formation in the

1M-PreOP group had a similar bone defect coverage as in the Pre-OP group (Fig 3.11 a). The bone volume, area, and density assessments all demonstrated no significant differences between the Pre-OP and 1M-PreOP groups, suggesting that lyophilized AdBMP2 within gelatin sponges had similar therapeutic effects before and after 1 month storage (Fig 3.11 b-d). These results suggest that lyophilized AdBMP-2 were still localized in scaffolds without losing its infectivity after long-term storage.

3.4 Discussion

Adenoviral vectors are widely used as vehicles to deliver genetic material for *in vivo* gene therapy. However, a major drawback of adenoviral vectors is that the expression of viral protein may induce a significant immune response. Directly injecting AdBMP-2 in thigh musculature results in endochondral bone formation in athymic nude rats; however, little to no bone is regenerated in immunocompetent rats [26]. Many research groups have shown the inability of Ad-BMP2 to induce *in vivo* bone formation in immunocompetent animals [26-30]. Consequently, different approaches have been investigated to reduce the vector-induced immunogenicity. Immunosuppression drugs, such as cyclophosphamide, have been used to restrain the immune response [30], and the use of AAV, with a lower viral protein expression, may also decrease antigenicity [19]. Another strategy is to reduce vector dosage by improving transduction efficiency [31]. Adenovirus internalization into host cells can be enhanced by complexing with fibroblast growth factor-2 (FGF-2) through mouse monoclonal neutralizing anti-knob antibody (Fab'), and hence, fewer viral particles are needed for *in vivo* transduction [32]. Using a similar strategy, we hypothesized that adenovirus could be concentrated in defects by

immobilization on biomaterial scaffolds, and thus the effective vector dosage could be greatly reduced to improve efficiency for regenerative gene therapy.

Using lyophilization, adenoviral particles adhered to the material surface before implantation. In an aqueous environment, virus released rapidly in the early stages, while it slowed down and then plateaued so that almost 30% of the virus was maintained on the surface (Fig 3.3). Because only a small fraction of virus particles remained on the material surface, this suggests that the binding force generated by lyophilization in sucrose was not strong. From this *in vitro* releasing behavior we deduce that the distribution of the virus lyophilized on biomaterials should be between that of polymer release and subtract-mediate delivery.

To determine if the virus lyophilized on material surfaces could be concentrated to enhance transduction efficiency, we designed an experiment to transduce cells in low volume conditions that force viruses to remain in close proximity to the material surface. Thus the free virus group may perform similar to the lyophilization group in a limited medium environment. Because reducing the infection volume is impractical for *in vivo* delivery, we localized adenovirus on the material surface by lyophilizing with appropriate excipients to enhanced virus adhesion. In the experiment with a high volume environment, adenovirus lyophilized on HA disks improved infection efficiency. These data suggest that surface lyophilization reduced adenovirus diffusion to localize virus distribution for cell transduction.

Lyophilization had been investigated to apply rAAV encoding receptor activator of nuclear factor κB ligand (RANKL) and vascular endothelial growth factor (VEGF) on the cortical surface of femoral allografts for transplantation with 1% sorbitol-PBS [19]. *In vitro* releasing experiments resulted in a mosaic distribution of transduced cells suggesting that aqueous environment may release virus by free diffusion in the culture medium before infection. The transduction efficiency was modest; only 1-5% cells in the immediate proximity to the allografts were infected. This suggests that the rapid diffusion of lyophilized virus in the aqueous environment may decrease local virus concentration and reduce the transduction efficiency *in vivo*. By using sucrose as an excipient for lyophilization, we demonstrated that virus can be precisely localized on biomaterial surfaces to transduce cells in a specific pattern site (Fig 3.1 c). This suggests that sucrose may enhance virus adhesion on material surfaces, which may facilitate spatial control of infection. Furthermore, sucrose is a common carbohydrate in physiological environment. It should be safe and without cytotoxicity for *in vivo* implantation. Since this method result in the slower release of concentrated virus from material surfaces, virus administration may be reduced to decrease the risk of systemic infection.

To investigate if this local gene delivery would facilitate bone reconstruction, a critical-sized bone defect model was studied, in which AdBMP-2 was lyophilized in gelatin sponges to induce new bone growth. There was almost no bone formation in the negative control groups, suggesting that the gelatin sponge is not osteoconductive (Fig 3.5). New bone formation was mainly due to the osteoinductive effects of AdBMP-2 transduction. Three quantitative μ-CT methods were performed to evaluate bone

regeneration in these defects. Bone volume fraction (BVF) was mainly used to compare the absolute quantity of bone regenerated in defects, whereas the bone area fraction (BAF) demonstrated the mineralized tissue coverage in defects. For therapeutic purposes, BAF may be more reflective of the regeneration effect than BVF because more bony area covering the defects in the early stage may lead to better bone filling with time. The trends for BVF and BAF were consistent in our experiments. The extremely high correlation coefficients of all three groups ($r>0.9$) suggested that the regenerated bone was evenly distributed in the defects. Sagittal μ-CT images also illustrated that mineral tissue growth filled in defects with excellent spatial control (Fig 3.5). Compared to the surrounding bone, BMD of the newly formed bone was apparently less than that of the nearby normal compact bone which is approximately between 400 to 500 mg/cc, indicating the function of AdBMP-2 in orthotopic bone healing affects bone volume more than bone density in the time frame of this study (Fig 3.6 c). From the BVF and BAF assessments, the regenerated bone covered greater than 80% of defects by lyophilized AdBMP-2. This was much improved over the method of suspending virus in the biomaterials (Fig 3.6 a,b).

Histology images illustrated the newly formed bone in the lyophilized AdBMP-2 group was osseointegrated with the native bone margin (Fig 3.7 c). Contrasted to the free AdBMP-2 group in which abundant fibrous tissue filled in the defects (Fig 3.7 b), bone marrow was formed in defects treated with lyophilized AdBMP-2. The new bone was only distributed in defects, suggesting that bone regeneration was enhanced and excellent

spatial control was achieved. These promising results demonstrate that lyophilized AdBMP-2 can effectively facilitate critical-size defect healing.

Radiotherapy is sometimes applied prior to craniomaxillofacial surgery especially for the ablation of malignant tumors. Irradiation is likely to cause hypocellularity and hypovascularity as well as lead to cell death of both tumor and normal cells in the treated regions [4]. To repair osseous defects compromised by radiation damage, we determine the extend to which BMP-2 genes delivered through the use of biomaterial scaffolds would improve osteogenesis.

Compared to the suspended group, AdBMP-2 lyophilized within gelatin sponges demonstrated superior bone formation effects in compromised defects (Fig 3.8 b,c). Although the BVF and BAF in the suspended AdBMP-2 group were both higher than in the negative control group, there were no significant differences in BMD between these two groups (Fig 3.8 d-f). This suggested that the modest osteogenesis induced by free AdBMP-2 mainly increased bone quantity (BVF and BAF), but not bone quality (BMD). In contrast, lyophilized AdBMP-2 demonstrated BMD improvement over the other two groups, indicating this local virus delivery enhanced both bone quantity and quality in radiation compromised defects. Because sufficient mineral density is important in promising long term bone maintenance in defects, the lyophilization strategy was more appropriate for treating radiated bone defects than the conventional bolus gene delivery.

To compare the effects of osteoradionecrosis to bone regeneration, lyophilized

AdBMP-2 in gelatin sponges were implanted to calvarial defects with and without preoperative radiotherapy. The newly formed bone in the Pre-OP group had similar bone volume and coverage in defects as in the No-XRT group (Fig 3.10 a,b). However, the sagittal images from μ-CT scanning and the BMD analysis demonstrated that the mineral tissue in the Pre-OP group was less condensed than in the No-XRT group (Fig 3.5, 3.8 c, 3.10 c). This suggested that most of the osteoprogenitor cells were likely killed during radiotherapy. Due to the lack of a sufficient number of functional cells, bone development sequences were retarded, resulting in reduced calcium deposition in newly formed tissue. The histomorphologic assessments demonstrated that woven bones mainly formed in Pre-OP defects (Fig 3.9 a,c,d). In addition, the immature marrow suggested a poor environment caused by radiation, and the bone regeneration period may need to be longer to properly recover the defects (Fig 3.9 c,d).

Different methods for delivering bioactive factors, such as BMPs, to facilitate tissue regeneration in compromised defects have been studied, including direct protein delivery and indirect gene therapy. Although protein therapy has been broadly studied, its high expense and unsteady release profile make it difficult to be widely applied in general clinical treatments [8, 9]. *Ex vivo* gene therapy has been used to treat bone loss in critical-sized defects comprised by radiotherapy. However, the regenerated bone in defects was still significantly different from non-radiation treated groups [17]. In our study, we demonstrated that virus locally delivered by *in vivo* gene therapy may greatly improve bone formation, and the newly formed bone was comparable to the same level of the non-treated group, both in bone volume and coverage rates (Fig 3.10 a,b). These results

suggest that virus lyophilization with biomaterial scaffolds is a potential strategy for healing osteoradionecrosis.

To investigate if these virus-material complexes are feasible to store as pre-made constructs, we further examined their stability in different temperatures. The long term storage experiments indicate that lyophilized virus may lose bioactivity at 4 ˚C with time. However, in a frozen environment (-20 and -80 ˚C) the viability declined only slightly in the first month and then remained stable for longer than 6 months (3.4 a, c). Moisture may be the major reason of the instability for storage. The adenovirus was a solid crystal form when it was completely dried by lyophilization. However, it turned to a gel-like form when stored at 4 ˚C, suggesting that the lyophilized virus was rehydrated with moisture. The moisture content of the lyophilized cake is the most important factor for the recovery of adenovirus [33-35]. Residual water may disrupt excipient–protein interactions which stabilize conformation in the dry state and therefore interfere with the conformation protection offered by the excipient formulation [22, 36]. Since we stored our lyophilized virus in non-sealing scintillation vials, it may have allowed the surrounding moisture to affect the lyophilized virus leading to virus degradation at 4 ˚C. In contrast, rehydration can be effectively inhibited at -20 ˚C and -80 ˚C. The frozen environment should be able to effectively reduce moisture and thus avoid the further virus degradation in the following period. Therefore, the moisture could be eliminated by sealing storage bottles or using desiccant for dehydration to preserve viral bioactivity for long term storage. An appropriately dehydrated environment may even maintain viral bioactivity longer than 1 year at 4 ˚C [22]. Additionally, the *in vivo* experiment with

long-term storage demonstrated that the therapeutic effects of lyophilized AdBMP-2 were still maintained after 1 month in -80 ˚C, that virus localization and the infectivity were capable of being maintained in this lyophilization method (Fig 3.11). These promising results suggested that viral vectors encoding biofactor genes can be incorporated with biomaterial scaffolds and stored at low temperatures as pre-made constructs, making clinical application convenient for surgeons.

3.5 Conclusions

In summary, we developed an *in vivo* gene therapy platform by locally delivering the BMP-2 gene from biomaterial scaffolds. Adenovirus lyophilized on biomaterial surfaces with 1 M sucrose in PBS enhances transductaion efficiency both in *in vitro* and *in vivo* environments. Lyophilized adenoviral vectors are localized and concentrated on scaffolds to effectively reduce the concentration of virus administrated, which may thus diminish the risks of systemic infection and immune response. The local viral delivery effectively repairs defects both normal wounds and those compromised by radiation damage. Viral bioactivity is also maintained on biomaterials after long term storage. These findings would allow lyophilized adenovirus to be incorporated with biomaterials as a pre-made construct to be used as an off the shelve product at time of surgery. Compared to *ex vivo* gene therapy, lyophilized adenovirus *in situ* transduces cells in wound sites and simplifies the treatment process by avoiding repeated surgeries. Without the use of live cells, this method reduces the risk of contamination which may occur during *in vitro* cell culture. Therefore, this local viral delivery method is a potential

therapy for repairing very difficult clinical lesions like those experienced with osteoradionecrosis.

(a)

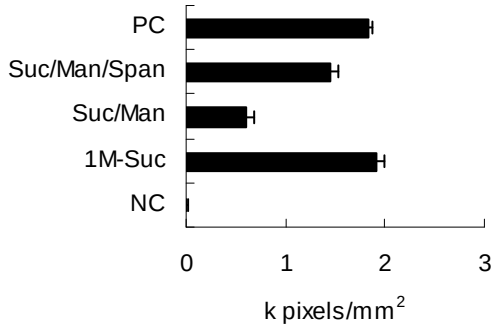

(b)

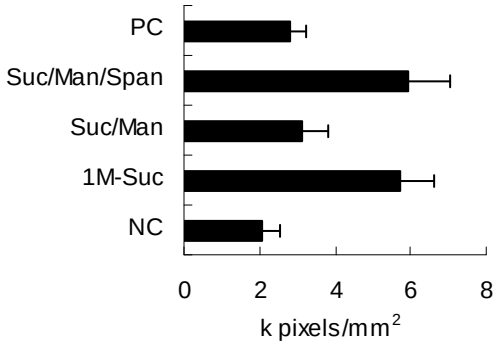

(c)

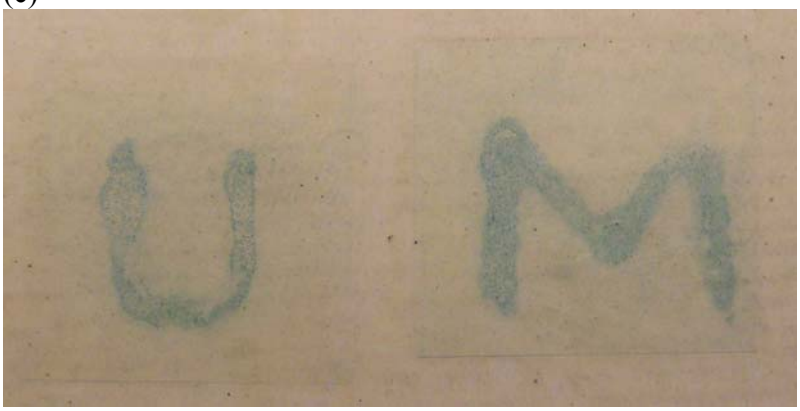

Figure 3.1. Determination of optimal excipient formulae. Lyophilization excipient formulations were compared for their ability to preserve bioactivity of lyophilized adenovirus and localize virus infection. AdLacZ was diluted in different excipient formulations for lyophilization. After infection of fibroblasts, X-gal staining was applied to determine recovery and infection efficiency. Three different excipent formulae were examined (Suc/Man/Span: 40 mg/ml sucrose, 40 mg/ml mannitol and 0.001% Span 20 in PBS; Suc/Man: 10 mg/ml sucrose and 10 mg/ml mannitol in PBS; 1M-Suc: 1M sucrose in PBS). AdlacZ lyophilized in PBS alone was treated as negative control (NC) and non-lyophilized virus served as the positive control (PC). (a) In suspension lyophilization, virus was lyophilized, then reconstitute in medium to infect cells in the free form. (b) Virus lyophilized on HA disk surfaces for cell infection. (c) AdLacZ lyophilized with 1M sucrose in PBS was added on glass cover slips in specific patterns “U” and “M”. After culturing with confluent C4 fibroblasts on the surface, X-gal staining was applied to demonstrate the transduction regions. Only cells in the pattern sites were infected, suggesting the lyophilized virus was under precisely spatial control.

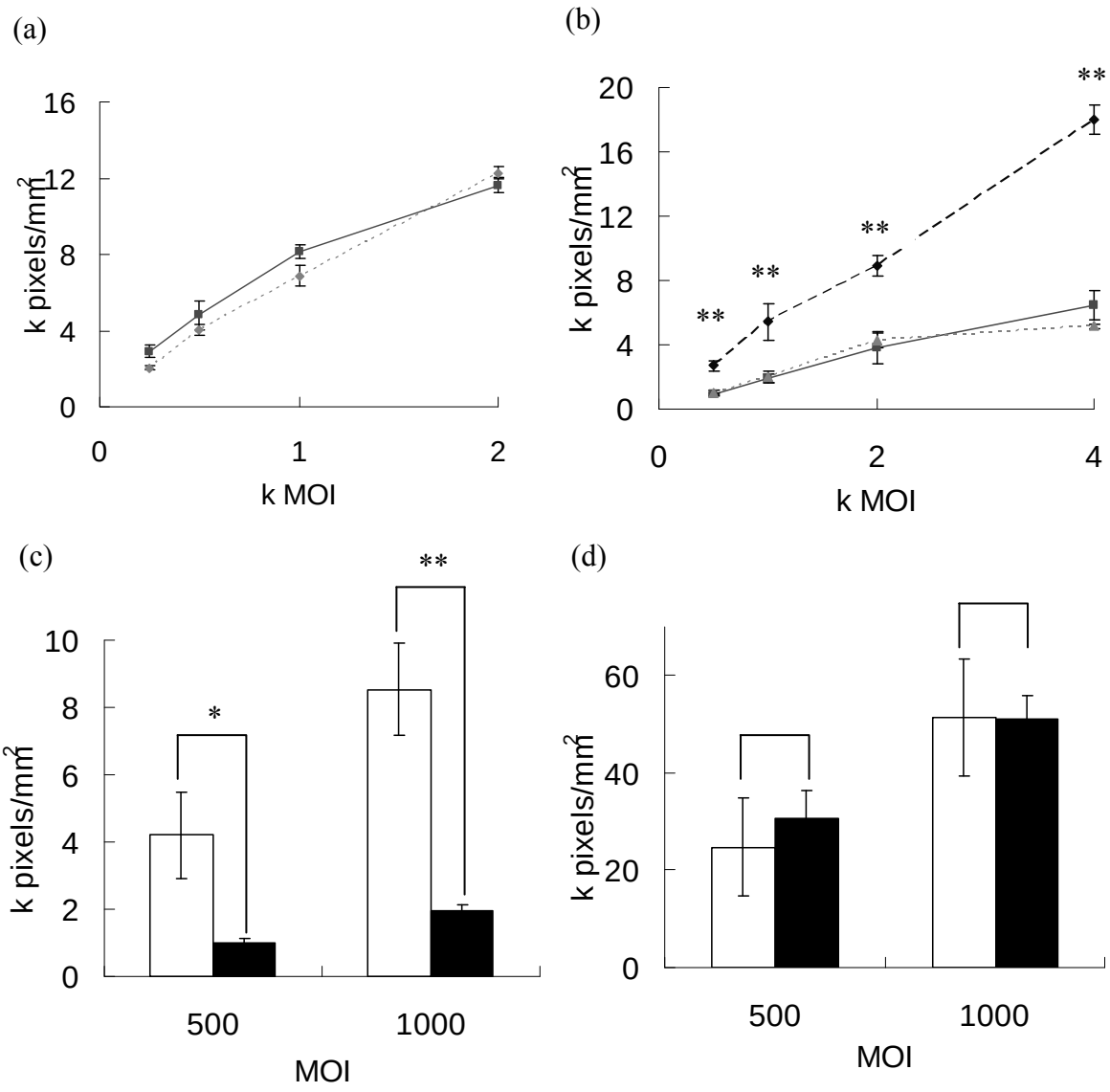

Figure 3.2. Cell transduction is improved by lyophilizing adenovirus on biomaterial surfaces. (a) AdLacZ was lyophilized then reconstituted in medium to infect C4 fibroblasts in the free form in tissue culture wells (dotted line). Different virus concentrations were test compared to AdLacZ without lyophilization (solid line). There were no differences between these two groups. (b) When culture cells on HA disks and tranduced by lyophilized (dotted line) and non-lyophilized (solid line) AdLacZ, the trends were the same as in culture wells condition. In contrast, the transduction was improved if AdLacZ was lyophilized on HA disk surface to infect cells (dash line). The improvement was almost double to triple of the free form virus in different virus concentrations. (c) AdLacZ lyophilized on HA disks (white) had higher transduction efficiency than the free form group (black) when infected in regular volume (350 µl). (d) However, low volume infection (20 µl) may forced free form virus remained to the HA disk surface (black) and thus the infection can be improved close to the surface lyophilization group (white). **: $p<0.01$

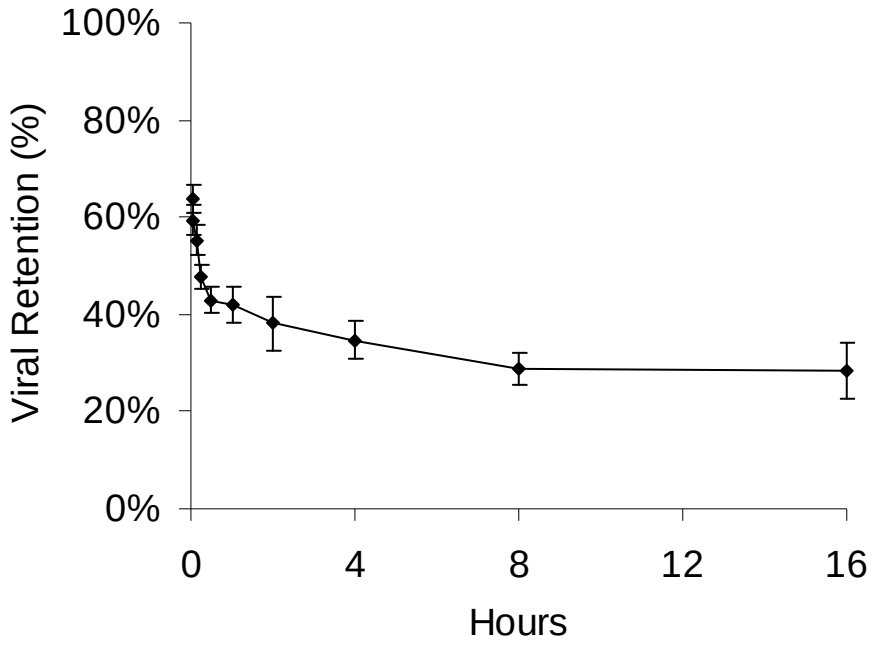

Figure 3.3. Lyophilized adenovirus released from HA disks. AdlacZ was lyophilized on HA disks then placed in culture medium to determine virus release in an aqueous environment. The virus released rapidly in the first few hours. However, the release was then slow and equilibrated and approximately 30% virus remained on HA disks after 16 hours.

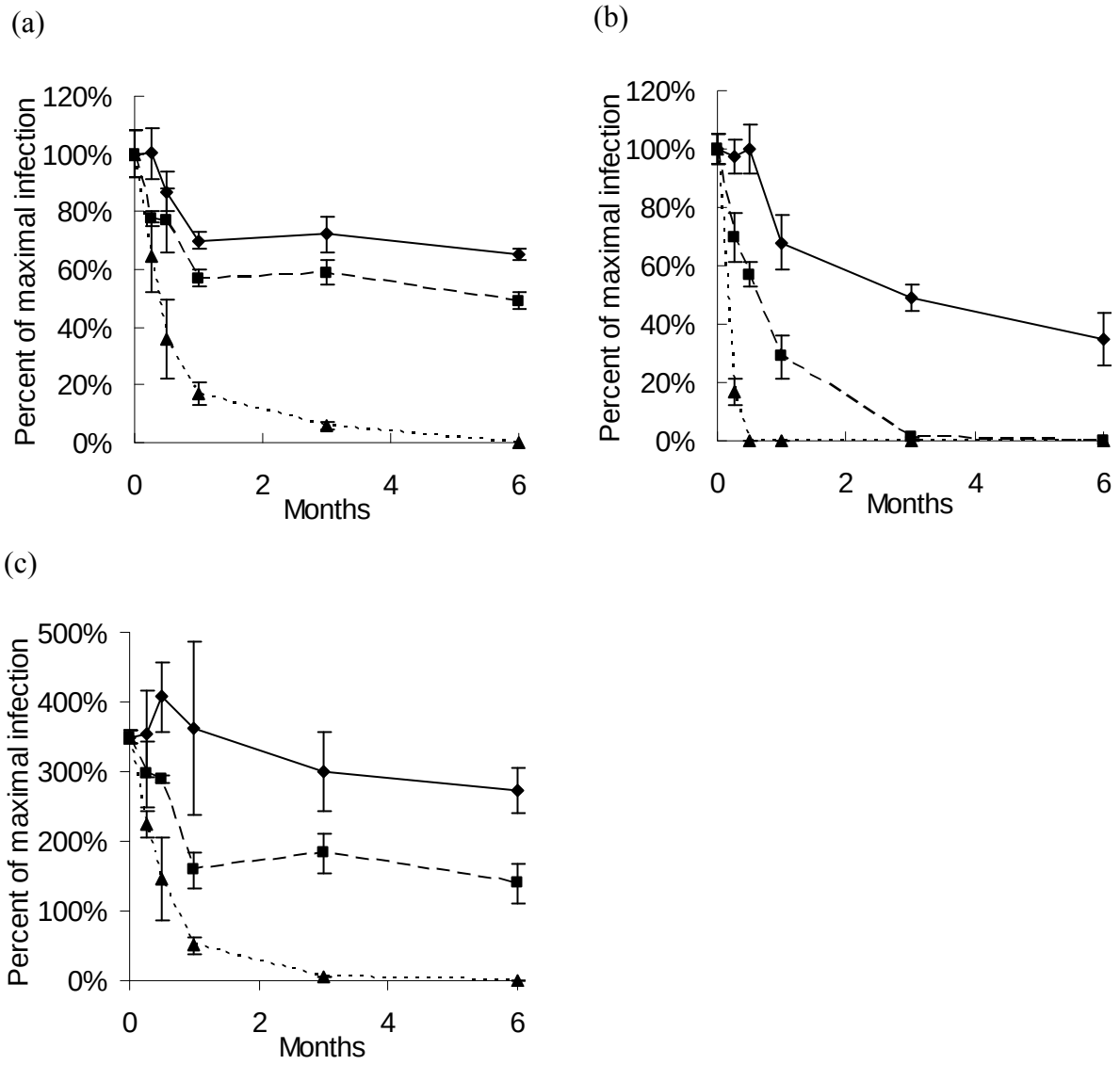

Figure 3.4. Viability of adenovirus at different temperatures. AdLacZ was stored at 4 ˚C (dotted lines), -20 ˚C (dash lines) and -80 ˚C (solid lines) for viral bioactivity analysis. (a) Suspension lyophilization of AdlacZ in 1M-Suc. (b) AdLacZ stored in PBS alone. (c) AdLacZ lyophilized on HA disks.

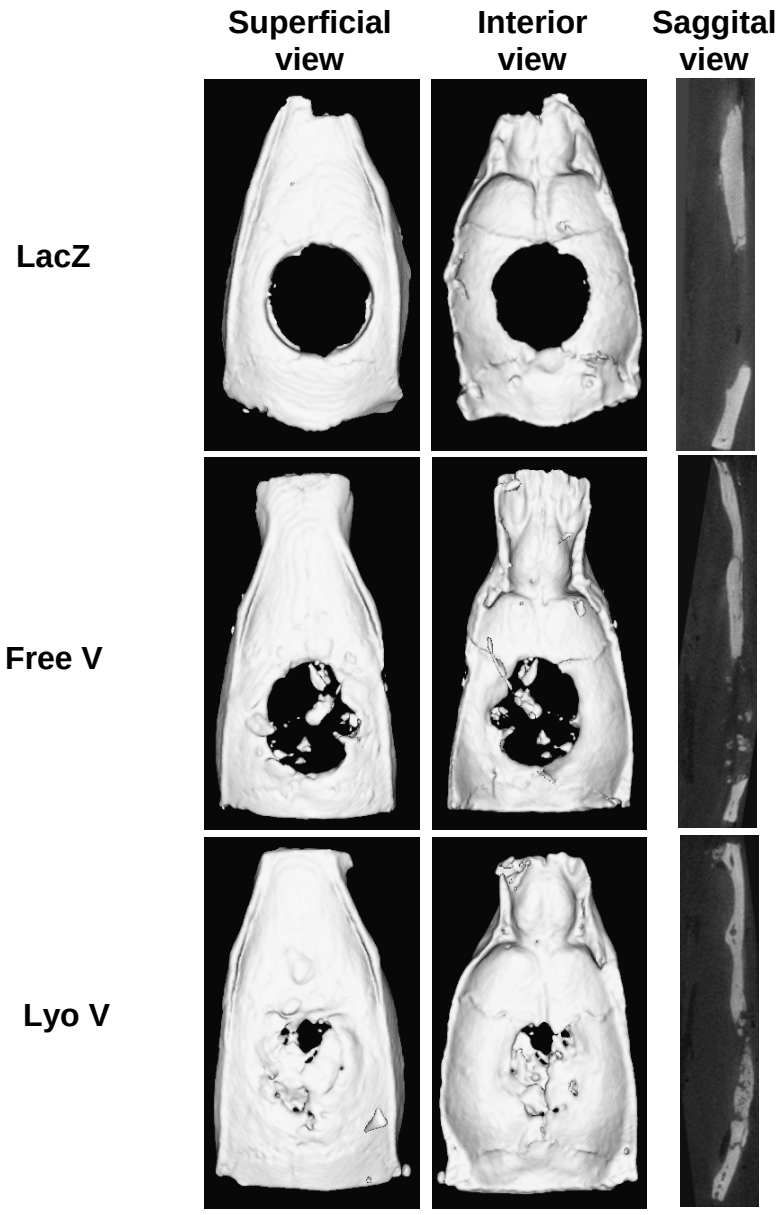

Figure 3.5. Bone regeneration in critical-size calvarial defects. Micro-CT analysis was applied to visualize bone regeneration by *in situ* gene therapy. (LacZ: AdLacZ lyophilized in gelatin sponges; Free V: AdBMP-2 suspended in gelatin sponges; Lyo V: AdBMP-2 lyophilized in gelatin sponges)

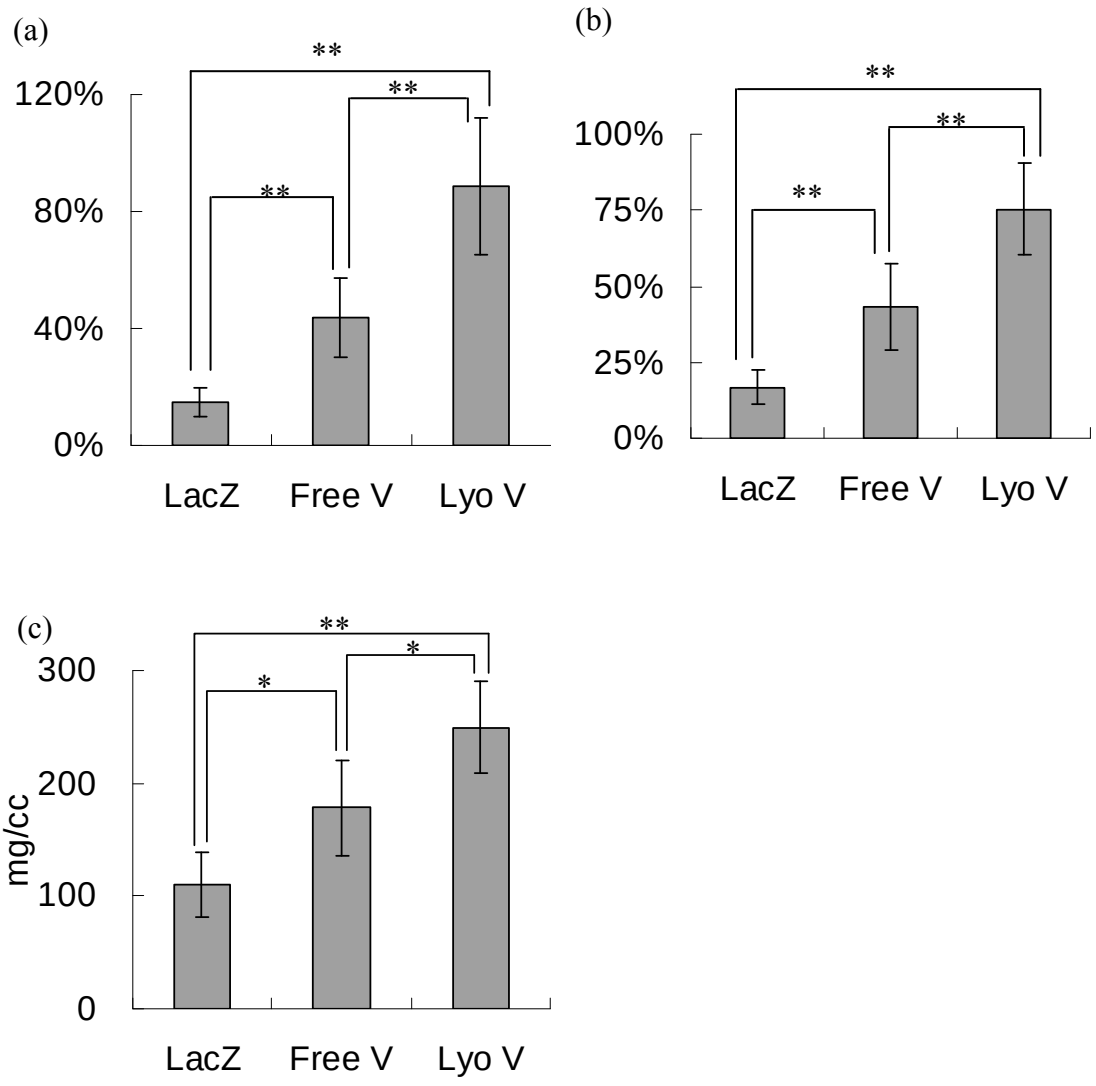

Figure 3.6. Micro-CT analysis was applied to quantify bone regeneration by *in situ* gene therapy. (LacZ: AdLacZ lyophilized in gelatin sponges; Free V: AdBMP-2 suspended in gelatin sponges; Lyo V: AdBMP-2 lyophilized in gelatin sponges) (a) Bone volume fractions (BVF) regenerated in defects (b) Bone area fraction in defects assessed from the projected area ratio of the μ-CT image (c) Bone mineral density (BMD) of new formed bone. * : $p<0.05$; **: $p<0.01$

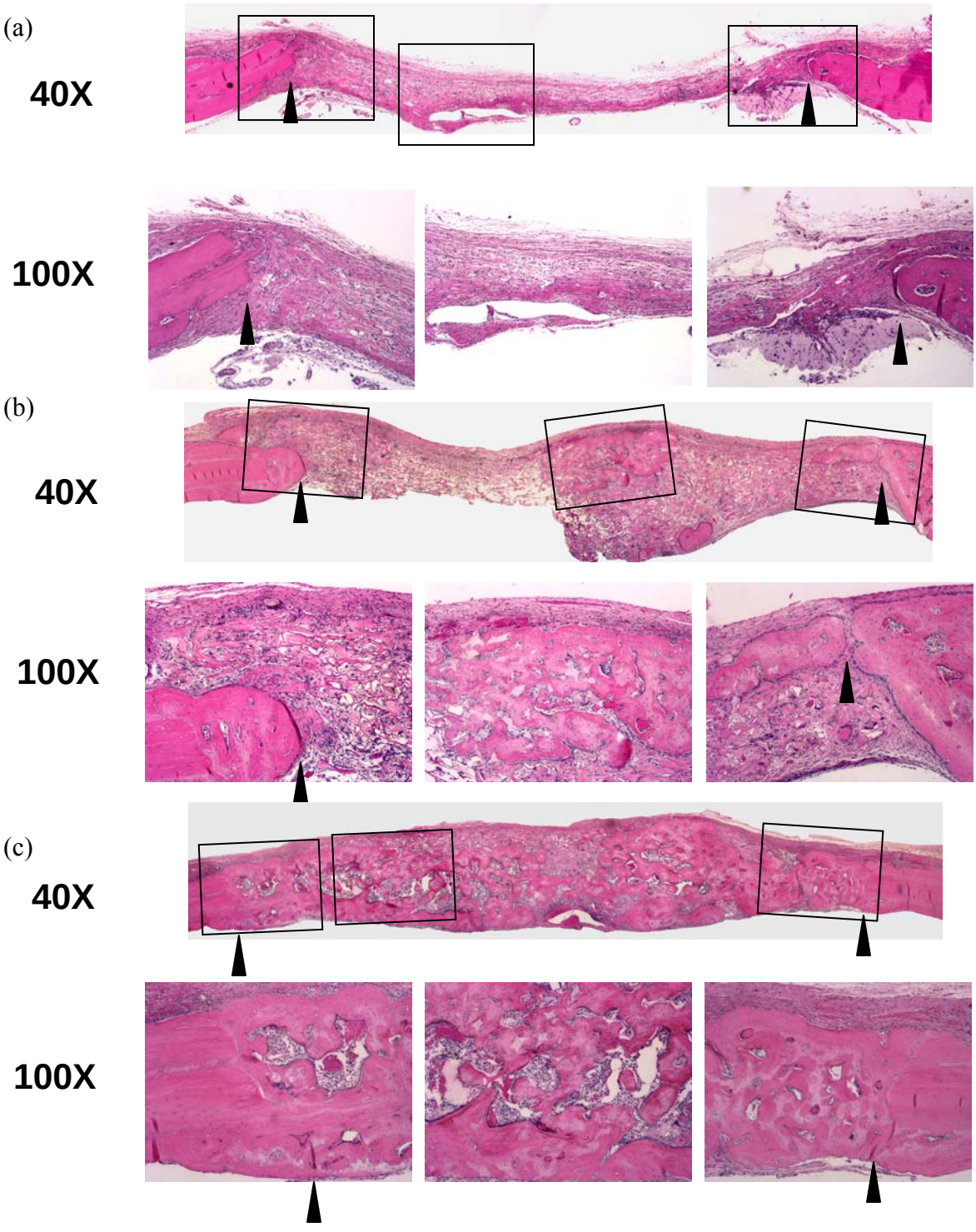

Figure 3.7. Histologic analysis of bone regeneration in critical-size defects. Sections were prepared from the middle line of defects. Black arrowheads indicated defect margins. (a) Lyophilized AdLacZ in gelatin sponges (b) Free form AdBMP-2 in gelatin sponges. (c) Lyophilized AdBMP-2 in gelatin sponges

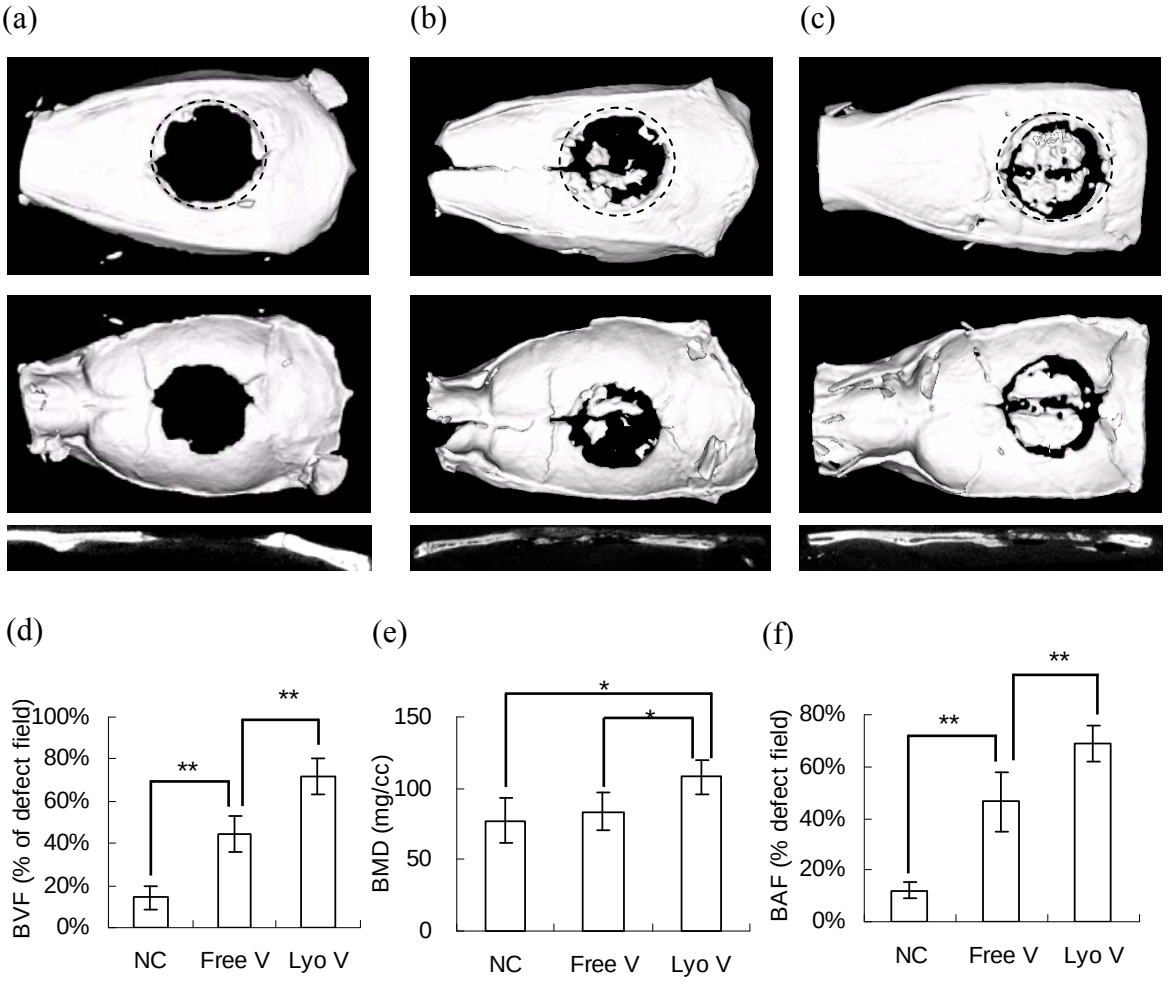

Figure 3.8. Bone formation in critical-sized calvarial defects comprised by radiation damage. μ-CT analysis was performed to visualize and to quantify bone regeneration. The 3-D images were reconstructed to illustrate the top, bottom, and sagittal section views of (a) AdLacZ lyophilized in gelatin sponges; (b) AdBMP-2 freely suspended in gelatin sponages and (c) AdBMP-2 lyophilized in gelatin sponges. Dashed lines indicate the defect margins created by osteotomy. The newly formed bone was evaluated by (d) bone volume fraction (BVF) in defects; (e) bone area fraction (BAF) in defects assessed from the projected area ratio of the μ-CT image; (f) bone mineral density (BMD) of newly formed bone. The data were compared by Student *t* test (*: $p<0.05$; **: $p<0.01$)

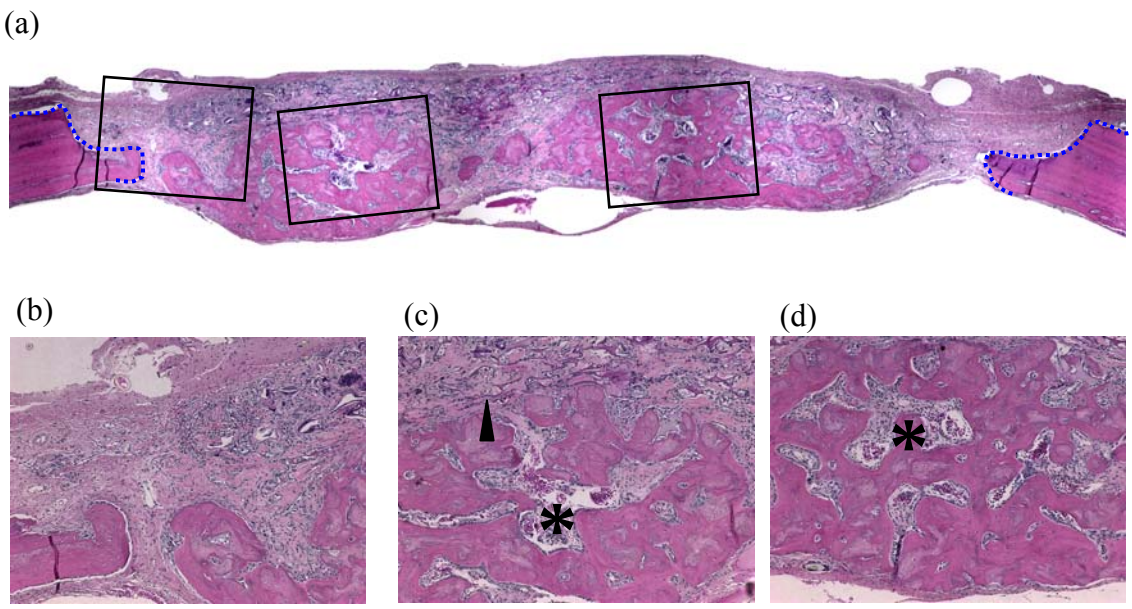

Figure 3.9. Histological analyses of critical-sized calvarial defects compromised by preoperative radiotherapy. Sections were prepared from the midline of defects. The defect margins are depicted by blue dotted lines. (Original magnitudes: (a) X40, and (b-d) X100) (Arrow head: undegraded gelatin sponges; *: bone marrow)

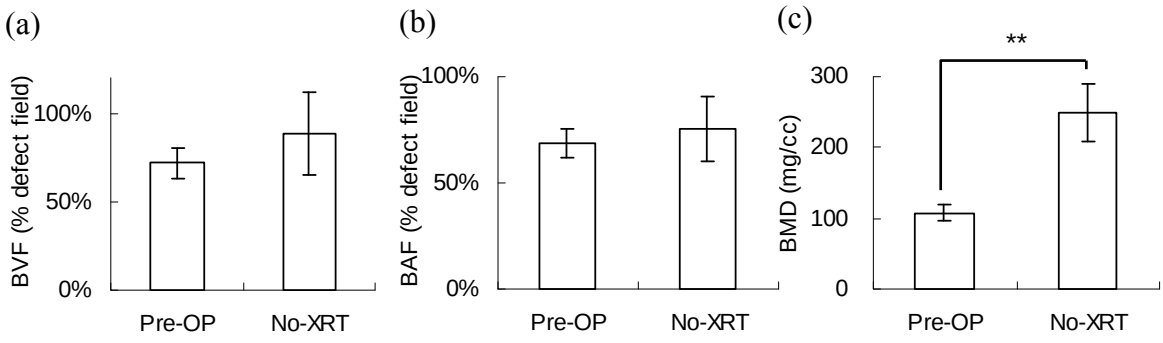

Figure 3.10. Quantification of bone formation in critical-sized calvarial defects with (Pre-OP) or without (No-XRT) radiation treatment. The new bone formations in defects were compared by μ-CT analyses: (a) BVF; (b) BAF; (c) BMD. The data were analyzed by Student *t* test (**: $p<0.01$)

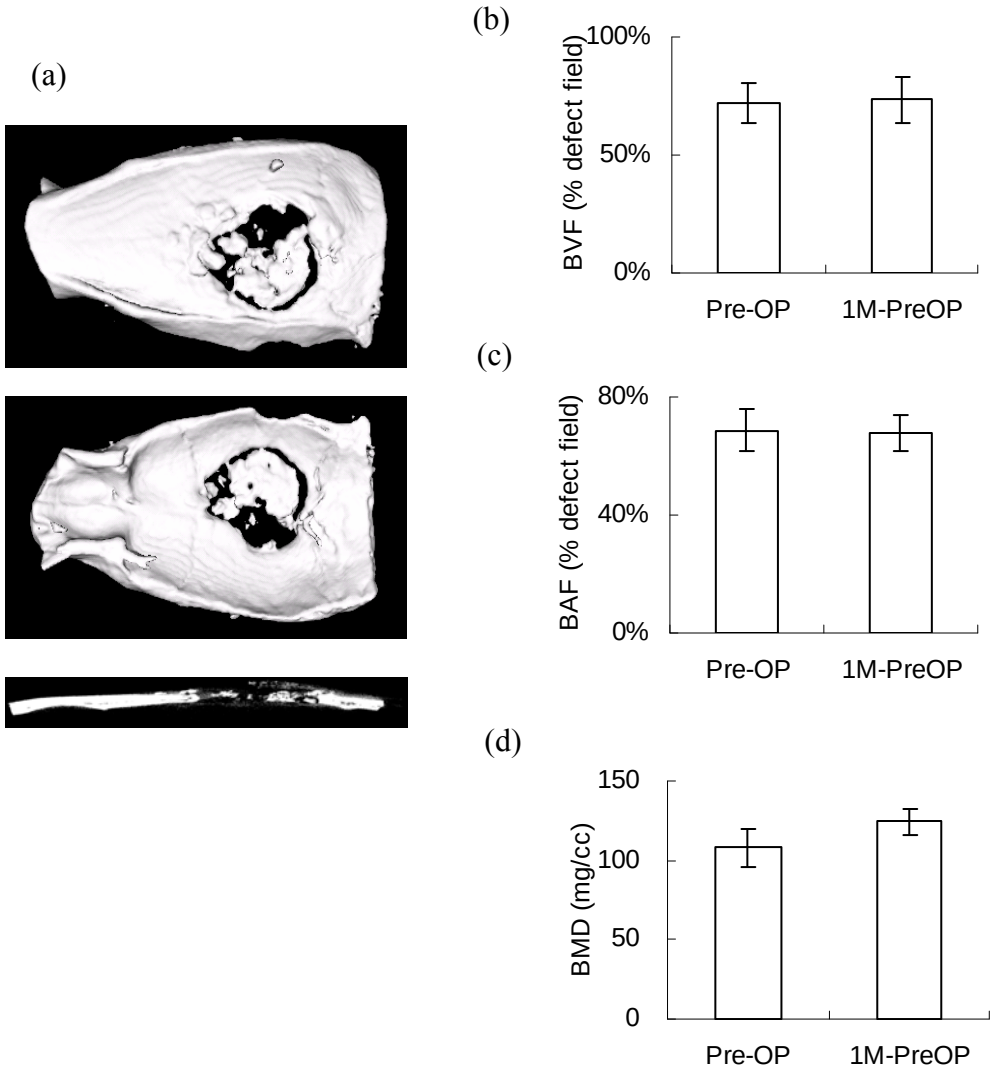

Figure 3.11. Irradiated defects healed by AdBMP-2 lyophilized in gelatin sponges stored at -80 ˚C for 1 month (1M-PreOP). (a) The 3-D images were reconstructed to illustrate the top, bottom, and sagittal section views. The bone regeneration was compared to the radiated group before storage (Pre-OP) by μ-CT analyses: (b) BVF; (c) BAF; (d) BMD. The data were analyzed by Student *t* test

3.6 References

1. W.J. Temple, C.L. Temple, K. Arthur, N.S. Schachar, A.H. Paterson, T.S. Crabtree, Prospective cohort study of neoadjuvant treatment in conservative surgery of soft tissue sarcomas, Ann Surg Oncol 4 (7) (1997); 586-590.

2. A.W. Yasko, M.E. Johnson, Recent advances in bone sarcomas, Cancer Treat Res 90 (1997); 127-147.

3. P.D. Costantino, C.D. Friedman, M.J. Steinberg, Irradiated bone and its management, Otolaryngol Clin North Am 28 (5) (1995); 1021-1038.

4. R.E. Marx, Osteoradionecrosis: a new concept of its pathophysiology, J Oral Maxillofac Surg 41 (5) (1983); 283-288.

5. M.J. Morales, R.E. Marx, C.F. Gottlieb, Effects of pre- and postoperative irradiation on the healing of bone grafts in the rabbit, J Oral Maxillofac Surg 45 (1) (1987); 34-41.

6. R.E. Marx, R.P. Johnson, Studies in the radiobiology of osteoradionecrosis and their clinical significance, Oral Surg Oral Med Oral Pathol 64 (4) (1987); 379-390.

7. D. Kaigler, Z. Wang, K. Horger, D.J. Mooney, P.H. Krebsbach, VEGF scaffolds enhance angiogenesis and bone regeneration in irradiated osseous defects, J Bone Miner Res 21 (5) (2006); 735-744.

8. K.K. Wurzler, T.L. DeWeese, W. Sebald, A.H. Reddi, Radiation-induced impairment of bone healing can be overcome by recombinant human bone morphogenetic protein-2, J Craniofac Surg 9 (2) (1998); 131-137.

9. B.K. Howard, K.R. Brown, J.L. Leach, C.H. Chang, D.I. Rosenthal, Osteoinduction using bone morphogenic protein in irradiated tissue, Arch Otolaryngol Head Neck Surg 124 (9) (1998); 985-988.

10. R.K. Khouri, D.M. Brown, B. Koudsi, E.G. Deune, L.A. Gilula, B.C. Cooley, A.H. Reddi, Repair of calvarial defects with flap tissue: role of bone morphogenetic proteins and competent responding tissues, Plast Reconstr Surg 98 (1) (1996); 103-109.

11. N.P. Ehrhart, L. Hong, A.L. Morgan, J.A. Eurell, R.D. Jamison, Effect of transforming growth factor-beta1 on bone regeneration in critical-sized bone defects after irradiation of host tissues, Am J Vet Res 66 (6) (2005); 1039-1045.

12. R.T. Franceschi, Biological approaches to bone regeneration by gene therapy, J Dent Res 84 (12) (2005); 1093-1103.

13. S.C.N. Chang, F.C. Wei, H.L. Chuang, Y.R. Chen, J.K. Chen, K.C. Lee, P.K.T. Chen, C.L. Tai, J.R. Lou, Ex vivo gene therapy in autologous critical-size craniofacial bone regeneration, Plastic and Reconstructive Surgery 112 (7) (2003); 1841-1850.

14. R. Gysin, J.E. Wergedal, M.H. Sheng, Y. Kasukawa, N. Miyakoshi, S.T. Chen, H. Peng, K.H. Lau, S. Mohan, D.J. Baylink, Ex vivo gene therapy with stromal cells transduced with a retroviral vector containing the BMP4 gene completely heals critical size calvarial defect in rats, Gene Ther 9 (15) (2002); 991-999.

15. J.T. Koh, Z. Zhao, Z. Wang, I.S. Lewis, P.H. Krebsbach, R.T. Franceschi, Combinatorial gene therapy with BMP2/7 enhances cranial bone regeneration, J Dent Res 87 (9) (2008); 845-849.

16. J.Y. Lee, D. Musgrave, D. Pelinkovic, K. Fukushima, J. Cummins, A. Usas, P. Robbins, F.H. Fu, J. Huard, Effect of bone morphogenetic protein-2-expressing muscle-derived cells on healing of critical-sized bone defects in mice, Journal of Bone and Joint Surgery-American Volume 83A (7) (2001); 1032-1039.

17. B. Nussenbaum, R.B. Rutherford, T.N. Teknos, K.J. Dornfeld, P.H. Krebsbach, Ex vivo gene therapy for skeletal regeneration in cranial defects compromised by postoperative radiotherapy, Hum Gene Ther 14 (11) (2003); 1107-1115.

18. B. Nussenbaum, R.B. Rutherford, P.H. Krebsbach, Bone regeneration in cranial defects previously treated with radiation, Laryngoscope 115 (7) (2005); 1170-1177.

19. H. Ito, M. Koefoed, P. Tiyapatanaputi, K. Gromov, J.J. Goater, J. Carmouche, X. Zhang, P.T. Rubery, J. Rabinowitz, R.J. Samulski, T. Nakamura, K. Soballe, R.J. O'Keefe, B.F. Boyce, E.M. Schwarz, Remodeling of cortical bone allografts mediated by adherent rAAV-RANKL and VEGF gene therapy, Nat Med 11 (3) (2005); 291-297.

20. M. Pandori, D. Hobson, T. Sano, Adenovirus-microbead conjugates possess enhanced infectivity: a new strategy for localized gene delivery, Virology 299 (2) (2002); 204-212.

21. S. Yang, D. Wei, D. Wang, M. Phimphilai, P.H. Krebsbach, R.T. Franceschi, In vitro and in vivo synergistic interactions between the Runx2/Cbfa1 transcription factor and bone morphogenetic protein-2 in stimulating osteoblast differentiation, J Bone Miner Res 18 (4) (2003); 705-715.

22. M.A. Croyle, X. Cheng, J.M. Wilson, Development of formulations that enhance physical stability of viral vectors for gene therapy, Gene Ther 8 (17) (2001); 1281-1290.

23. P. Murakami, M.T. McCaman, Quantitation of adenovirus DNA and virus particles with the PicoGreen fluorescent Dye, Anal Biochem 274 (2) (1999); 283-288.

24. M.T. Fields, A. Eisbruch, D. Normolle, A. Orfali, M.A. Davis, A.T. Pu, T.S. Lawrence, Radiosensitization produced in vivo by once- vs. twice-weekly 2'2'-difluoro-2'-deoxycytidine (gemcitabine), Int J Radiat Oncol Biol Phys 47 (3) (2000); 785-791.

25. J.P. Schmitz, J.O. Hollinger, The critical size defect as an experimental model for craniomandibulofacial nonunions, Clin Orthop Relat Res (205) (1986); 299-308.

26. T.D. Alden, D.D. Pittman, G.R. Hankins, E.J. Beres, J.A. Engh, S. Das, S.B. Hudson, K.M. Kerns, D.F. Kallmes, G.A. Helm, In vivo endochondral bone formation using a bone morphogenetic protein 2 adenoviral vector, Hum Gene Ther 10 (13) (1999); 2245-2253.

27. T.D. Alden, E.J. Beres, J.S. Laurent, J.A. Engh, S. Das, S.D. London, J.A. Jane, Jr., S.B. Hudson, G.A. Helm, The use of bone morphogenetic protein gene therapy in craniofacial bone repair, J Craniofac Surg 11 (1) (2000); 24-30.

28. T.D. Alden, D.D. Pittman, E.J. Beres, G.R. Hankins, D.F. Kallmes, B.M. Wisotsky, K.M. Kerns, G.A. Helm, Percutaneous spinal fusion using bone morphogenetic protein-2 gene therapy, J Neurosurg 90 (1 Suppl) (1999); 109-114.

29. W.H. Lindsey, Osseous tissue engineering with gene therapy for facial bone reconstruction, Laryngoscope 111 (7) (2001); 1128-1136.

30. Y. Okubo, K. Bessho, K. Fujimura, T. Iizuka, S.I. Miyatake, Osteoinduction by bone morphogenetic protein-2 via adenoviral vector under transient immunosuppression, Biochem Biophys Res Commun 267 (1) (2000); 382-387.

31. B.L. Davidson, J.M. Hilfinger, S.J. Beer, Extended release of adenovirus from polymer microspheres: potential use in gene therapy for brain tumors, Adv Drug Deliv Rev 27 (1) (1997); 59-66.

32. R.E. Schreiber, K. Blease, A. Ambrosio, E. Amburn, B. Sosnowski, T.K. Sampath, Bone induction by AdBMP-2/collagen implants, J Bone Joint Surg Am 87 (5) (2005); 1059-1068.

33. M.J. Pikal, K. Dellerman, M.L. Roy, Formulation and stability of freeze-dried proteins: effects of moisture and oxygen on the stability of freeze-dried formulations of human growth hormone, Dev Biol Stand 74 (1992); 21-37; discussion 37-28.

34. J.K. Towns, Moisture content in proteins: its effects and measurement, J Chromatogr A 705 (1) (1995); 115-127.

35. S. Jiang, S.L. Nail, Effect of process conditions on recovery of protein activity after freezing and freeze-drying, Eur J Pharm Biopharm 45 (3) (1998); 249-257.

36. T.I. Pristoupil, M. Kramlova, H. Fortova, S. Ulrych, Haemoglobin lyophilized with sucrose: the effect of residual moisture on storage, Haematologia (Budap) 18 (1) (1985); 45-52.

CHAPTER 4

DEVELOPMENT OF ADENOVIRUS IMMOBILIZATION STRATEGIES FOR *IN SITU* GENE THERAPY

4.1 Introduction

From our previous study, we demonstrated that lyophilized viral vectors within scaffolds improved transduction efficiency, and thus the concentration of virus administrated may be reduced [1]. However, because the lyophilized virus only coats the materials, they may be rapidly released from surfaces, and thus spatial control is limited. Viral vector immobilization on biomaterial scaffolds has been applied to control *in situ* gene delivery in a method in which the risks of virus dispersion was reduced during *in vivo* application [2-4]. Therefore, in this study we exploited this strategy to gain robust control of cell transduction from chitosan as a test material for the long term goal of regenerative gene therapy.

Chitosan is a biodegradable polysaccharide derived from crustacean shells [5]. The non-toxic and tissue compatible properties of chitosan support its use as a biomaterial for pharmaceutical and drug delivery research [6, 7]. In addition, chitosan has a hydrophilic surface that may promote cell adhesion, proliferation, and differentiation, and thus is broadly used as a tissue engineering scaffold material [8, 9]. Furthermore, chitosan is synthesized by chitin deacetylation with ambient amines, and can be easily

modified for conjugation [10]. Therefore, we used chitosan as a carrier with its active functional groups to immobilize adenovirus on its surface and investigated its potential to effectively deliver bioactive virus.

In order to specifically control virus immobilization, bioconjugation was utilized to bind viral particles to biomaterials surfaces. Because covalent bonds generate an irreversible interaction, the binding forces involved in directly conjugating a virus to a biomaterial surface may be too strong to allow an efficient release of virus for cell internalization. Therefore, bioconjugation mediated by non-covalent bonding is hypothesized be a more effective method of immobilizing viral particles on material surfaces for *in situ* transduction. In this study, we applied two specific interactions, biotin-avidin and antibody-antigen, to control virus immobilization.

The biotin-avidin interaction is known to be the strongest non-covalent bond, and this system has been used for biotechnology applications [11]. The molecules are commercially available and can be conjugated with different materials. For example, chitosan has been successfully biotinylated for enzyme immobilization as bioprobes [12], and adenovirus biotinylation has been applied to cell targeting and virus purification methods [13]. Because this system is broadly applied in different application with good specificity, we predict that it would be appropriate to bind virus on biomaterials to control gene delivery.

The antibody-antigen interaction is another frequently used method for controlled release. Virus has been immobilized by antibodies to localize gene expression on substrates, by which anti-virus antibodies tether viral particles to a scaffold, yet the viruses remain capable of being internalized by adherent cells [2, 3, 14]. This approach has been shown to be successful in delivering adenovirus to cells without diffusing from scaffolds [4, 15-17]. However, because an antibody is specific to an antigen, different viral vectors would need to be captured by different antibodies. They are incapable of spatially controlling multiple viral vector delivery to specific sites within a scaffold because anti-virus antibodies cannot distinguish between viral vectors with different transgenes. The application of pairing different viral vector strains with their specific antibodies may circumvent this difficulty. However, the administration of different vectors may lead to inconsistencies in the length of time in which transgenes are expressed. For example, the use of retrovirus would likely provide continuous expression during the lifetime of a cell, whereas adenovirus would only offer transient gene expression. In addition, different viral vectors may have interactions with each other, such as adeno-associated viral vectors being rescued to proliferate in host cells if they are co-infected with adenovirus. These risks make the co-administration of different types of viral vectors impractical. Therefore, we sought to tag the capsid proteins of adenovirus with different antigenic determinants that are capable of being distinguished by different antibodies.

Digoxigenin (DIG) is a steroid extracted from the plants *Digitalis purpurea* and *D. lanata* [18]. It is commonly used for labeling DNA probes for *in situ* hybridization. *N*-

hydroxysuccinimido-DIG (DIG-NHS) is a commerically available chemical disigned for conjugation to amine groups, by which DIG can be easily grafted to proteins. For example, red blood cells have been modified by DIG conjugation for *in vivo* aging studies [19]. Because DIG is a small chemical, we hypothesized that it would be able to tag the surface of a adenovirus without affecting viral infectivity.

Consequently, two virus immobilization approaches were developed in this study. For the biotin-avidin conjugation, we compared two different avidin immobilization strategies on material surfaces. Avidin was either directly conjugated to chitosan (virus-biotin-avidin-material, VBAM) or indirectly docked on biotinylated chitosan surfaces (virus-biotin-avidin-biotin-material, VBABM) to tether biotinylated adenovirus. By a range of experimental analyses, we determined an effective and universal viral delivery model for *in situ* transduction. For the antibody-antigen conjugation, anti-DIG and anti-adenovirus antibodies were conjugated on chitosan surfaces and a wax masking technique was applied to control the antibody conjugation area. DIG-modified and non-modified adenoviruses were immobilized on two different antibody conjugated areas in one scaffold. We hypothesized that cells could be transduced *in situ* on specific sites of the biomaterial and thus develop a defined interface between the two cell signaling factors.

4.2 Materials and Methods

4.2.1 Adenovirus modification by biotin and digoxigenin

Adenovirus was biotinylated by Sulfosuccinimidyl-6-[biotinamido] hexanoate (SulfoNHS-LC-biotin) (Pierce, Rockford, IL) which was dissolved in PBS before being reacted with adenovirus. The NHS functional groups can react with amines on viral surface proteins to form stable amide bonds. The conjugation reaction was performed at 4˚C for 2 hours, and then quenched by an equal volume 1 M glycin (Sigma-Aldrich) in PBS. Ultrafiltration was applied using centricon filters (50 kDa MWCO) (Millipore, Billerica, MA) to remove unreacted biotin.

Digoxigenin-3-O-methylcarbonyl-ε-aminocaproic acid-N-hydroxysuccinimide ester (DIG-NHS, Roche, Indianapolis, IN) was purchased from Roche for viral surface modification. After dissolving in PBS, the DIG-NHS was incubated with adenovirus for conjugation at 4˚C for 2 hours, and non-reacting, excess DIG-NHS was removed with a desalt spin column (Pierce). These modified viruses were sterilized by being passed through a 0.2 μm syringe filter (Nalgene).

4.2.2 The level of virus modification

To determine an appropriate concentration of SulfoNHS-LC-biotin for virus biotinylation, sandwich enzyme-linked immunosorbent assay (ELISA) was used to detect biotin on viral surfaces. Goat anti-adenovirus IgG (Abcam, Cambridge, MA) was coated on 96-well plates (Corning) to capature biotinylated virus. Avidin conjugated alkaline phosphatase (avidin-AP, MP biomedicals, Aurora, OH) was used to label the biotin on the plate. The same procedures were applied for digoxigenin modification, in which anti-DIG IgG-AP (Roach) was used to label DIG conjugated on viral surfaces.

The number of biotin molecules per adenovirus was quantified by a 2-(4'-hydroxyazobenzene) benzoic acid (HABA, Pierce) assay: 6 μmole HABA was added to 5 mg avidin in 10 ml PBS to prepare the HABA/avidin solution. The solution (0.9 ml) was transferred by pipette into a 1ml cuvette to read spectrophotometrically at OD_{500nm} (Beckman Coulter, Fullerton, CA). Biotinylated virus (0.1 ml) was then added and mixed in the cuvette to read OD_{500nm}. HABA had an absorption wavelength of 500 nm when added to avidin. However, this absorption decreased proportionally when biotin was added. This occurred because the biotin displaced the HABA dye due to its higher affinity for avidin. Therefore, the degree of biotinylation was calculated using the following formula:

$$\frac{biotin}{viral\_particles} = \frac{\frac{\Delta OD_{500nm}}{34000} \times 10}{mmoles\_viral\_particles/ml}$$

ΔOD_{500nm}=OD_{500nm} of HABA/avidin x 0.9 –OD_{500nm} of HABA/avidin/biotintinylated virus

4.2.3 Modified virus infectivity evaluation

To determine the extent to which biotin or digoxigenin modification affected the bioactivity of adenovirus, *in vitro* cell infection experiments were performed to determine modified virus infectivity. Fibroblasts were cultured at a density of $5x10^4$ cells/well in 24-well culture plates for one day. Subsequently, AdLacZ with or without modification in different concentrations were added to the culture wells for 48 hr infection. The

transduction efficiencies of each group were determined by the expression of β-galactosidase, which was detected using a sandwich ELISA kit (Roach).

4.2.4 Chitosan film preparation

Chitosan with molecular weight from 100 kDa to 300 kDa (Acros, Geel, Belgium) was dissolved in 0.5 M acetic acid for a final concentration of 1.5%. After melting at 60 ˚C overnight, the chitosan solution was filtered through a 0.8 μm membrane. The chitosan solution (1 ml/well) was placed into 24-well culture plates that were then incubated at 80 ˚C overnight to evaporate the acetic acid solvent. Coated wells were neutralized in 0.3 M NaOH for 30 minutes and were then washed with PBS.

4.2.5 Avidin, biotin and antibody conjugation on chitosan surfaces

Avidin Conjugation

To conjugate avidin on chitosan in the VBAM system, avidin (Pierce) in PBS was placed in chitosan-coated wells (0.25 ml/well). Glutaraldehyde (Acros), the homobifunctional crosslinker for bioconjugation, was also diluted in PBS then added 0.25 ml/well. After 2 hours the wells were washed with PBS to remove non-reactive reagent. 2 M glycine in PBS was used to quench non reactive crosslinker on the plate for 30 min. Finally, the plates were washed with 70% ethanol for sterilization.

In other experiments, avidin was indirectly docked on a biotinylated surface before immobilizing biotinylated molecules in the VBABM method. Avidin was dissolved in PBS and placed 0.25 ml/well for 2 hours incubation at room temperature and then washed with PBS to remove excess avidin.

The surface avidin was quantified by a biotin conjugated alkaline phosphatase (biotin-AP) assay: After blocking with 1% BSA-PBS, biotin-AP (Pierce) was diluted in PBS (12 ng/ml) and added to the plates (0.25 ml/well) for 1 hour, and was developed by PNPP substrate.

Avidin has a maximum absorption at a wavelength of 230 nm, which was determined by a scanning spectrum. Therefore, a UV spectrometer (Biotek, Winooski, VT) was used to measure the total amount of avidin conjugation. After avidin conjugated with glutaraldehyde on the material surface, 150 µl supernatant was transferred to UV-penetrateable 96-microwell plates (Corning). Standard avidin solutions with different concentrations were used for comparison. The immobilized avidin was determined by subtracting the supernatant avidin values from the total amount of avidin present before the reaction.

Biotin Conjugation

(+)-Biotinyl-3,6,9-trioxaundecanediamine (Amine-PEO_3-Biotin, Pierce) was dissolved in PBS and placed in chitosan-coated wells 0.25 ml/well. Glutaraldehyde was also diluted in PBS and then added 0.25 ml/well. After 2 hours incubation at room temperature, the wells were washed with PBS to remove non-reactive regent. Quenching with a glycine solution and sterilizing by 70% ethanol were performed as previously described.

Surface biotin was quantified by avidin-AP. After blocking with 1% BSA-PBS, avidin-AP was diluted in PBS (0.112 μg/ml) and added 0.25 ml/well to incubate for 1 hour, and was then detected by substrate PNPP, as previously described.

Antibody Conjugation

Chitosan was modified using *N*-(γ-maleimidobutyryloxy) sulfosuccinimide ester (Sulfo-GMBS, Pierce) to functionalize a layer of maleimide, which could react with sulfhydryl groups. After dissolving in PBS, Sulfo-GMBS (0.5 mg/well) was added at room temperature for 2 hours and then removed with several PBS washes. Simultaneously, 12.5 nmole *Tris* (2-carboxyethyl) phosphine hydrochloride (TCEP-HCl, Pierce) was dissolved in PBS with 10 mM ethylenediaminetetraacetic acid (EDTA, Sigma-Aldrich) and reacted with 1 mg goat anti-adenovirus or sheep anti-DIG IgG (AbD Serotec, Kidlington, Oxford, UK). With the TCEP treatment, the labile disulfides between heavy chains in the hinge region of IgG molecules were selectively reduced to get two half-IgG fragments with sulfhydryls. Such partial reduction of IgG disulfides usually results in sulfhydryl group attachment points that will not sterically hinder antigen binding. After one hour incubation at room temperature, the TCEP was removed using desalt spin columns. The antibody (20 μg/well) was then added on Sulfo-GMBS treated chitosan surfaces at room temperature for overnight incubation. Finally, the unbound antibody was washed out and the wells were sterilized with 70% ethanol.

4.2.6 Virus immobilization and sandwich ELISA assay

The biotinylated AdLacZ virus was immobilized on the material surface by two strategies, the VBAM system (virus-biotin-avidin-material), and the VBABM system (virus-biotin-avidin-biotin-material), which are schematically depicted in Fig. 4.8. After avidin immobilization, biotinylated virus was incubated on the chitosan surfaces for 2 hours at 4 ^{o}C, and was then washed with PBS to remove unbound virus.

DIG-modified AdLacZ (DIG-AdLacZ) was diluted in 0.5% gelatin (w/v in PBS) at different virus concentrations and was then placed on anti-DIG IgG conjugated chitosan surfaces at 4˚C for 2 hours. To determine the virus immobilization efficiency on chitosan, an indirect sandwich ELISA assay was performed: 100 µl supernatant with unbound DIG-AdLacZ was added to goat anti-adenovirus antibody coated 96-microwell plates. These viruses were detected by rabbit anti-adenovirus IgG (Abcam), and labeled by anti-rabbit IgG antibody conjugated alkaline phosphatase (Abcam).

To investigate the stability of immobilized adenovirus on biomaterial surfaces, a time course experiment was performed to determine adenovirus release. After immobilizing 1 x 10^{9} viral particles on chitosan surfaces, 1 ml PBS was added on each surface at 37 ˚C. These samples were collected at different time points and quantified by sandwich ELISA.

4.2.7 Immobilized virus distribution examined by scanning electron microscopy

Adenovirus immobilized on chitosan surfaces were washed with PBS to remove unbound viral particles, and fixed by 10% glutaraldehyde in PBS for 1 hour.

Subsequently, these samples were postfixed by 1% osmium tetroxide (Acros) for 1 hour. After two washes with distilled water, the samples were incubated at -80 ˚C for 2 hours and then lyophilized in a freeze dryer at -78.51 ˚C and 100 mTorr for 24 hours. Samples were coated with gold (SPI, West Chester, PA) and examined by scanning electron microscopy (Nova Dual Beam FIB/SEM, FEI, Hillsboro, OR).

4.2.8 *In vitro* cell infection to determine viral activity

Fibroblasts were infected with a range of AdLacZ concentrations (0 to $1.6x10^9$ pfu/well) and were cultured for 48 hours. The transduction efficiencies of each group were determined by the expression of β-galactosidase, which was detected using a sandwich ELISA kit, as previously described. The data were normalized to the amount of surface viral particles. Additionally, transduced cells were illustrated by staining with X-gal.

Adenovirus encoded blue fluorescent protein (AdBFP) and green fluorescent protein (AdGFP) were prepared by the Vector Core at the University of Michigan. The AdBFP was modified with DIG (DIG-AdBFP) and AdGFP was not modified. Both viruses were diluted in 0.5% gelatin (w/v in PBS) to a final concentration of $1x10^8$ pfu and were incubated together at 4 ^oC for immobilization. The unbound virus was removed by PBS washes and fibroblasts were cultured on the modified surface for 2 days. A red fluorescent dye that stains for nucleic acid (SYTO 62, Invitrogen, Carlsbad, CA) was used to illustrate cell distribution.

4.2.9 Heterogeneity evaluation by Sips isotherm adsorption model

Sips isotherm adsorption is a modified model from the Langmuir isotherm adsorption model $I = \frac{I^{sat}(bC)^a}{1+(bC)^a}$

where I is the intensity of adsorption that can be the optical density of the substrate PNPP (OD_{405nm}) in this study, I^{sat} is the intensity during saturation, C is the concentration of biotinylated molecules, b is the affinity of biotinylated molecules toward avidin, and a is the heterogeneity index, which is the exponent of the equation. By logarithmic expression, the equation can be expressed as:

$$\ln\left(\frac{I}{I^{sat}-I}\right) = a\ln b + a\ln C$$

The heterogeneity index, a, and the affinity factor, b, can be determined by plotting $\ln I/(I^{sat}-I)$ to $\ln C$. The slope of the least-squares regression line would be a and the intercept would be $a\ln b$.

Most often, the association constant between proteins and ligands follows a Gaussian distribution. Heterogeneity is used to describe the deviation of the association constant distribution when the protein is immobilized on a solid substrate. Because the associate and dissociate behavior between immobilized proteins and their ligands deviates from when they are in solution, this deviation is always accompanied by a higher heterogeneity. The non-uniform binding affinity distribution can be evaluated by the heterogeneity index, a, which should be between 0 and 1. When $a = 1$, the affinity of an immobilized protein to ligands is the same as it is in solution, and a lower value a indicates an increasing heterogeneity. Therefore, by a heterogeneity index comparison,

we could evaluate the level of immobilized protein affected by the conjugation reaction. Lower affinity constants and heterogeneity indexes indicate that immobilization introduces heterogeneity into the binding behavior and thus diminishes ligand binding activity [20].

4.2.10 The influence of the DIG on ATPase

As an initial test to investigate if DIG conjugated on a virus surface would be safe for *in vivo* application, an adenosine 5'-triphosphatase (ATPase) activity assay was performed to evaluate the ATPase inhibition of the DIG modified virus. ATPase activity was determined using a Quamtichrom ATPase/GTPase assay kit (Bioassay, Hayward, CA). DIG modified AdLacZ was diluted to different concentrations and 5 μl/well was placed in 96-well microplates with equal volumes of ATPase (Sigma-Aldrich) for 15 min at room temperature. Subsequently, 10 μl 4mM adenosine 5'-triphosphate (ATP, Sigma-Aldrich) was added and the plate was incubated at room temperature for 30 min. Finally, 200 μl kit reagent was added per well and incubated for 30 min before reading the OD_{620nm}. The same process was also performed for three different ATPase inhibitors ouabain, digoxigenin, and digoxin (Sigma-Aldrich). These inhibitors were used as positive control groups to compare the inhibitory effects to DIG-modified adenovirus.

4.2.11 Wax masking

Polyester wax (EMS, Hatfield, PA, USA) was melted at 40 ^{o}C and then added (200 μl/well) to cover the right side of each culture well. After the wax solidified, anti-

DIG IgG was conjugated on exposed chitosan surfaces. Finally, the wax was removed by incubation in absolute ethanol at 37 ^{o}C for 1 hr.

4.3 Results

4.3.1 Adenovirus biotinylation does not alter viral bioactivity

To maximize the level of biotinylation of adenovirus, a sandwich ELISA was used to quantify adenoviral surface biotinylation by SulfoNHS-LC-Biotin. Viral biotinylation was saturated when the concentration of SulfoNHS-LC-Biotin exceeded 0.5 mg per 10^{12} viral particles (Fig. 4.1 a). The HABA assay of biotinylated virus demonstrated that there were 6209 ± 505 biotin molecules per viral particle. This high level of biotinylation suggests that virus can be robustly immobilized on chitosan. The viral infection efficiencies of adenovirus before and after biotinylation were also compared by infecting fibroblasts. Beta-galactosidase expression by infected cells was quantified by ELISA (Fig. 4.1 b). The protein expression of biotinylated AdLacZ was between 80-90% in the non-modified virus group, suggesting that virus infectivity was preserved after biotinylation.

4.3.2 Avidin/biotin crosslinked by homobifunctional crosslinker have different binding effects

Two different strategies for avidin immobilization to chitosan, VBAM and VBABM, were developed to tether viruses for *in situ* gene therapy. To optimize the crosslinker concentration of these two immobilization strategies, avidin and biotin were conjugated to chitosan surfaces with different concentrations of the homobifunctional

glutaraldehyde crosslinker. These conjugates were analyzed using biotin-AP and avidin-AP, respectively (Fig. 4.2 a,b). The avidin and biotin conjugation profiles differed significantly. Avidin conjugation increased with glutaraldehyde concentration and was saturated at 0.75% glutaraldehyde, however, a sharp decline in conjugation occurred with glutaraldehyde levels greater than 7.5% (Fig. 4.2 a). Biotin conjugation followed a different trend than avidin. The surface biotin, when in a system with increasing crosslinker, eventually reached a plateau at about 7.5 % glutaraldehyde (Fig. 4.2 b). However, there was no decrease in conjugation at the highest concentration of crosslinker as was observed with avidin conjugation. Despite finding that 0.75% and 7.5% glutaraldehyde have the best conjugation rates for avidin and biotin, respectively, these high levels of glutaraldehyde may be harmful to cells. Therefore, to avoid potential cytotoxicity, 0.25% glutaraldehyde was applied for the following experiments because this level was effective for crosslinking and yet was non-toxic to cells in culture (data not shown).

Because high crosslinker concentrations led to a decrease in direct avidin conjugation, there may have been other factors affecting the crosslinking between avidin and material surfaces. To investigate this possibility, avidin was conjugated to chitosan with different concentrations, ranging from 1 to 250 μg/well. Two experiments were performed to determine the amount of immobilized avidin molecules and the biotin binding sites, respectively. The avidin in the supernatant after the conjugation reaction was detected by UV spectrometry to indirectly quantify the immobilized avidin

molecules on the material surface (Fig. 4.3 a). At the same time, the effective surface biotin binding sites on chitosan were directly determined with biotin-AP (Fig. 4.3 b).

From the UV detection assay, the immobilized avidin molecules on the chitosan surface increased with increasing concentrations of avidin. The conjugation efficiency was about 6.8% (Fig. 4.3 a). In contrast, when directly detecting surface binding sites on chitosan, high avidin concentrations increased biotin-AP immobilization, however, this trend plateaued with avidin concentrations greater than 30 μg/well (Fig. 4.3 b).

4.3.3 Comparison of VBAM and VBABM immobilization strategies

To demonstrate differences in biotin immobilization efficiency between the VBAM and VBABM systems, biotin-AP and biotinylated adenovirus were compared (Fig. 4.4 a,b). Biotin-AP is a small protein whereas biotinylated adenovirus is a large complex, and thus they can be used to compare different immobilization effects for small and large biotinylated molecules. The surface immobilized avidin (30 μg/well) was used in both groups according to the saturation concentration from the prior titration experiment.

Results of the biotin-AP assay demonstrated that immobilization in both systems increased with biotin-AP concentrations (Fig. 4.4 a). To investigate the affinities of surface avidin to biotinylated molecules in these two systems, we referred to the Sips isotherm adsorption model because it is an association-dissociation assessment for antibody-antigen that is similar to biotin-avidin interaction [20, 21]. The binding data was

fitted into the Sips isotherm adsorption equation and the fitting parameters are summarized in Table 4.1. The heterogeneity index, *a,* of VBABM was 1.000, suggesting that the interaction between immobilized avidin and biotin-AP was homogeneous. That is, the affinity of surface avidin for biotin-AP was similar to the affinity of avidin for biotin in solution. In contrast, the directly bound avidin in the VBAM system exhibited some heterogeneity (a = 0.894). The loading capacity in the VBABM system was also higher than in the VBAM system. The saturation intensities of bound alkaline phosphatase were 4.2 and 3.0 for VBABM and VBAM, respectively. Therefore, the lower heterogeneity index suggests that surface immobilization of the VBAM system induced heterogeneity between biotin-AP and avidin, whereas the VBABM system did not. This also suggests a diminished binding activity of the VBAM system.

For biotinylated virus immobilization, the trends of heterogeneity were more pronounced than those of biotin-AP for both the VBAM and VBABM methods (Fig. 4.4 b). The heterogeneity index of the VBAM system (a = 0.540) was less than the VBABM system (a = 0.832). The saturation intensity of VBAM (I^{sat} = 0.33) was also lower than VBABM (I^{sat} = 0.56). Moreover, the binding affinity of VBABM was almost double that of VBAM (0.269 ml/10^9VP vs. 0.135 ml/10^9VP) (Table 4.1). The lower heterogeneity indexes of both the VBAM and VBABM systems indicate that large biotinylated molecules, such as adenoviruses, may be more sensitive to steric hindrance than smaller molecules. This phenomenon of higher heterogeneity would affect the interaction between ligand (biotin) and receptor (avidin), and thus the adsorption behavior would diverge from their homogeneous interaction in solution form.

4.3.4 Immobilized virus distribution was examined by scanning electron microscopy

Scanning electron microscopy examination was performed to illustrate the surface virus distribution. In the VBAM system, virus clusters were found in low magnification (Fig. 4.5 a). These clusters were formed by uniform size particles which were more obvious in high magnification. Compared to the typical sizes of adenovirus (70 to 90 nm), these particles, with diameter between 70-80 nm, suggest that they are adenoviruses immobilized on chitosan surfaces [22].

Similarly, the VBABM system had viral particles the same size as those in the VBAM system. However, the distribution was different (Fig. 4.5 b). Evenly distributed particles without clusters were observed in this group. Moreover, the number of adenoviral particles bound in the VBABM group per unit area was obviously higher than in the VBAM group. These results suggest that biotinylated adenovirus can be more effectively immobilized by the VBABM method due to surface avidin alignment.

4.3.5 The VBABM system has an improved cell transduction efficiency over the VBAM system

AdLacZ was used to transduce fibroblasts for comparing viral infection efficiencies of two immobilization strategies. The cells were infected and incubated for two days, followed by an ELISA assay to quantify β-galactosidase expression levels (Fig. 4.6 a). The adherent cells infected with free virus (Free V) had the lowest transduction rate. This rate was improved when cells were infected with virus in a suspended solution

(Free V & Cells) because the virus likely contacted cells in a homogeneous medium rather than in a potentially heterogeneous liquid-solid environment. Virus immobilized by the VBAM system was not superior because it had a similar infection profile to the Free V group. However, the VBABM group exhibited a significantly higher transduction efficiency. Moreover, the β-galactosidase activity at saturation in the VBABM group was 3 μg/well, compared to 2 μg/well in the Free V and VBAM group and 2.5 μg/well in the Free V & Cell group. These findings suggest that biotin on biomaterial surfaces can increase the effective binding sites for biotinylated virus immobilization and thus enhance the transduction efficiency. The X-gal staining also illustrated that cells cultured on plates could be infected by VBAM and VBABM systems and the β-galactosidase expression levels were consistent to their ELISA results (Fig. 4.7).

The levels of virus in the VBAM and VBABM systems were likely underestimated because immobilized virus was not totally bound on the chitosan surfaces. Excess virus was removed by PBS washes prior to cell infection. The true amounts of immobilized virus were indirectly detected by quantifying unbound virus using a sandwich ELISA assay. In the VBABM group, 95%-100% of adenovirus can be immobilized on surfaces when there are less than $1x10^8$ viral particles per well. Higher virus concentration caused the immobilization rate to decline due to limited substrate area. In contrast, VBAM had only a 40%-60% immobilization rate in the same concentration. Therefore, we normalized the cell transduction results to the immobilized virus levels. This normalization demonstrated better performances in both VBAM and VBABM systems. The result of the VBAM group was similar to the Free V & Cell group, while

the VBABM group had a much better performance than the other three groups (Fig. 4.6 b). Beta-galactosidase expression of VBABM was saturated when there were 4 x 10^7 pfu AdLacZ, which was almost 6, 10, and 50 times that of the VBAM, Free V & Cell, and Free V groups, respectively, when using the same virus concentrations.

4.3.6 Adenoviral infectivity is preserved after DIG-NHS modification

The level of DIG modification was determined by a sandwich ELISA (Fig. 4.9 a). The amount of digoxigenin on viral surfaces increased with increasing concentrations of DIG-NHS. The level of DIG modification was saturated when the number of DIG-NHS molecules exceeded 0.075 nmole per 10^9 viral particles. We therefore used this concentration for the remainder of our experiments.

Fibroblasts were infected with AdLacZ before and after DIG modification to determine if DIG modification affected virus infectivity. After two days infection, the transduced cells were examined by a β-galactosidase ELISA assay (Fig 4.9 b). This experiment demonstrated that the β-galactosidase expression of these two groups was similar and without significant differences in the range of virus concentrations studied. These findings indicated that the DIG modification was a mild chemical reaction that did not adversely affect adenovirus infectivity.

4.3.7 Digoxigenin conjugated on viral surface reduces its inhibition of ATPase

Digoxigenin is derived from digitalis which is also well-known as a cardiac glycoside. Cardiac glycosides have inotropic effects on heart muscles, that can be cardiotoxic following *in vivo* administration [23]. To investigate the potential risk raised

by DIG modification, the toxicity of the modified virus was evaluated. The inotropic mechanism of cardiac glycosides is mediated through the blocking of Na^+/K^+ transporting ATPase transmembrane pump activity in the sarcolemma [24]. Therefore, an ATPase inhibition assay was performed to assess the extent of blockage caused by cardiac glycosides and the DIG-modified virus [25]. Three different cardiac glycosides: ouabain, digoxigenin, and digoxin, served as positive control groups in this inhibition assay. The levels of phosphate ion release significantly decreased with increasing cardiac glycoside concentration, suggesting these inhibitors blocked ATPase activity (Fig 4.10 a).

Concentrations of DIG-AdLacZ, ranging from 0 to 2 x 10^{10} viral particles, were also examined in this assay. The equivalent numbers of DIG molecules conjugated to the viral surfaces were converted by the assumption that the conjugation rate was perfect. For example, because the modification of DIG-NHS resulted in a concentration of 0.075 nmole per 10^9 viral particles, the equivalent concentration of DIG conjugated to 2 x 10^{10} viral particles in a 5 μl volume would be 300 μM. The levels of phosphate ion released in the DIG-AdLacZ group was significantly higher than the other three cardiac glycoside groups, suggesting that the ATPase supported ATP hydrolysis without interference (Fig 4.10 a).

The inhibition results were based on the ratio of reducing phosphate ion release to the ideal amount which should be released without inhibitors (Fig 4.10 b). Ouabain, digoxigenin, and digoxin significantly inhibited the ATPase activity. Even at the lowest concentration, 0.2 μM, they had inhibition effects of 18 %, 8 %, and 11 %, respectively.

In contrast, DIG-modified adenovirus displayed essentially no inhibition except at the highest concentration of DIG-AdLacZ (300 μM, *i.e.* 2 x 10^{10} viral particles), where inhibition was only about 10% of maximum. These data suggest that DIG molecules conjugated to viral surfaces significantly reduced their reactivity to ATPase by about 1,500-fold (Fig 4.10 b).

4.3.8 DIG-modified viruses are effectively and stably immobilized by anti-DIG IgG conjugation to biomaterial surfaces

The efficiency of DIG-AdLacZ immobilized by anti-DIG IgG conjugated to chitosan surfaces was determined by indirectly detecting unbound virus in supernatants after conjugation. The immobilized DIG-AdLacZ on chitosan surfaces increased with increasing DIG-AdLacZ concentrations (Fig 4.11 a). This amount of immobilized DIG-AdLacZ was compared to the amount of DIG-AdLacZ unbound in solution to determine the conjugation rates (Fig 4.11 b). The conjugation rates were perfect in the low concentrations and began to decline when the DIG-AdLacZ concentration was 10^9 viral particles per well. These data suggest that adenovirus with digoxigenin modification can be effectively bound to chitosan surfaces.

The immobilized DIG-AdLacZ viral particles were examined by SEM to determine the distribution patterns on the material surface. The adenovirus was found to be evenly bound to conjugated antibodies on chitosan surfaces (Fig 4.11 c). The stability of adenovirus with and without DIG modification was compared by incubation in PBS at 37˚C. Sandwich ELISA results demonstrated that the viral retention rates on chitosan

surfaces were similar in these two groups, suggesting the adenovirus immobilization mediated by DIG did not affect the stability (Fig 4.11 d). In addition, more than 80% of the viral particles, both with and without DIG modification, bound to the surfaces for 1 week. Approximately 70% of viral particles were present for 2 weeks. These results indicated that virus with and without DIG modification, could be stably tethered by antibodies conjugated on biomaterial surfaces.

4.3.9 Wax masking spatially controls antibody conjugation for adenovirus immobilization

Since DIG modified virus were stably bound to anti-DIG IgG, we further investigated the feasibility of cell transduction controlled via antibody conjugation patterns. Low melting point polyester wax (mp=37^{o} C) is an inert polymer that dissolves in ethanol and can thus serve as an excellent material for physical masking. After antibody was conjugated to the non-masked region of chitosan, the surface wax was removed with ethanol washes at 40^{o} C. Secondary antibody conjugated FITC was used to label the area of antibody immobilization (Fig 4.12 a). Only exposed chitosan surfaces were identified by green fluorescence, indicating that antibody conjugation was spatially controlled.

To investigate the extent to which this antibody immobilization strategy could be applied to spatially control cell transduction directly from the surface of biomaterials, anti-DIG IgG was conjugated to chitosan surfaces in which defined areas were controlled by wax masking. After removing the wax, DIG-AdLacZ was immobilized on chitosan

surfaces and fibroblasts were cultured on the material for 2 days. The transduced cells were identified as blue after X-gal staining. Non-transduced cells were only identified after counter staining with crystal violet (Fig 4.12 b). These data demonstrated that fibroblasts proliferated to confluence on chitosan surfaces, and the infected cells were restricted to the non-masked area. This suggested that adenovirus modified by DIG could be immobilized in discrete sites on biomaterials and could still be released for *in situ* cell transduction.

4.3.10 Anti-DIG IgG specifically immobilizes DIG-modified adenovirus on material surfaces

In this study, adenovirus was modified by DIG to distinguish it from non-modified adenovirus for antibody binding. To investigate the extent to which this modification could control virus immobilization at specific sites, two different antibodies, anti-adenovirus IgG and anti-DIG IgG, were separately conjugated on chitosan surfaces to demonstrate the specificity of antibodies to adenovirus with or without DIG modification.

On chitosan surfaces conjugated with anti-DIG IgG, DIG-modified adenovirus was dose-dependently immobilized on the biomaterial. The bound DIG-modified adenovirus increased with increasing virus concentration and was saturated when the virus concentration exceeded 3.2×10^{10} viral particles/well. This was likely due to the limited area of the biomaterial surface. In contrast, for non-modified adenovirus, there was only minor physical adsorption at the same concentrations, suggesting that only

adenovirus modified by DIG could be recognized and tethered on conjugated anti-DIG IgG (Fig 4.13 a).

When these two adenoviruses were individually placed on anti-adenovirus IgG conjugated surfaces, the ELISA results demonstrated that the binding affinities of these two groups were almost identical. They all increased with virus concentration and were saturated when the virus concentration was greater than $3.2x10^{10}$ viral particles per well (Fig 4.13 b). This indicated that virus modified by DIG preserved the epitopes that were recognized by anti-adenovirus IgG for immobilization.

4.3.11 Dual viral vector delivery spatially controls cell transduction with different genes

Because the anti-DIG IgG conjugated surfaces only bound DIG-modified adenovirus, while anti-adenovirus IgG could immobilize adenovirus with or without modification, we further investigated the possibility of utilizing these properties to spatially control different bioactive factor expression on material surfaces (Fig 4.14 a). In this experiment, wax masking was applied to restrict the conjugation of anti-adenovirus IgG to only the non-masked area, and anti-DIG IgG was conjugated after removing the wax mask (Fig 4.14 b). The virus-immobilized surfaces were seeded with fibroblasts to demonstrate the distribution of cell transduction. After 2 days in culture, the cells were stained with SYTO 62 and observed under a fluorescent microscope with a TRITC filter. The red fluorescence observed throughout the entire material surface demonstrated that the cells grew to confluence (Fig 4.14 c). Using a FITC and DAPI filter, green and blue

fluorescence were identified as expressed from cells transduced by AdGFP and DIG-AdBFP, respectively (Fig 4.14 c). The BFP expression was distributed throughout the material surface because DIG-AdBFP could be bound to both anti-DIG and anti-adenovirus IgG. In contrast, the GFP expression was restricted to the left side of the surface because anti-adenovirus IgG was only conjugated to the non-masked area. There were no cells that expressed both blue and green fluorescence, suggesting that co-infection did not occur on the modified material surface. These results demonstrated that two different transgenes could be spatially controlled by the dual viral vector immobilization method to generate a defined interface between the cell signaling viruses.

4.4 Discussion

Virus deliveries have a profound influence on the outcomes of regenerative gene therapy. Compared to bolus delivery which requires high viral titers and provides little control over virus diffusion, spatially controlled viral infection restricts viral transduction to only the target sites and limit systemic infection. In addition, virus local deliveries improves transduction efficiency, and thus the viral dosage may be reduced [1, 26, 27]. In this study, virus immobilization was performed by bioconjugation through specific interactions, biotin-avidin and antibody-antigen, which may tightly tether virus on material surfaces [11].

Some studies indicate that the cell transduction of biotinylated adenovirus bound on avidin coated plates for *in situ* transduction was modest in comparison to free infection delivery [28]. This may be due to steric hindrance of active binding sites which

can be inactivated when they are close to the solid support surface [29]. In addition, the microenvironment of the surface and the potential conformational changes of immobilized proteins can lead to heterogeneous binding affinity and association/dissociation kinetics to their complementary ligands [30-32]. Therefore, determining how to reduce the heterogeneity of the binding force and how to preserve protein function are important issues for protein surface immobilization.

To reduce heterogeneity, oriented immobilization is a potential strategy because it can reduce the blockage of binding sites. For example, to orient IgG on support surfaces for immunosorption, the Fc regions are used for immobilization on solid supports by either conjugating with its carbohydrate residues or by mediating protein A/G conjugation [33-35]. These strategies allow the Fab regions to be exposed and thus avoid steric hindrance due to random conjugation, suggesting that oriented immobilization reduces heterogeneity and enhances receptor-ligand adsorption. By a similar hypothesis, we assumed that biotinylated virus immobilized on material surfaces may be oriented in the VBABM system because the immobilized avidin may be aligned by the surface conjugated biotin (Fig. 4.8 b). This differs from the randomly distributed avidin in the VBAM system due to non-specific conjugation (Fig. 4.8 a). The schemes did not reflect the real scales because the virus was much larger than biotin and avidin.

In this study, biotinylated reagent was used to modify viral capsid proteins. Compared to another published study, which genetically fused a biotin acceptor peptide (BAP) to a virus and then biotinylates the virus later, this chemical modification is easier

and can be applied more generally in different viral vectors [13]. The infectivity of biotinylated adenovirus can be maintained at 80%-90%, suggesting that SulfoNHS-LC-Biotin is mild and appropriate for adenovirus modification (Fig. 4.1 b).

Conjugation with various crosslinker concentrations demonstrated different profiles of these two methods (Fig. 4.2 a,b). In the VBAM system, avidin was directly linked to the surface by glutaraldehyde, a homobifunctional crosslinker that randomly conjugates with amines to form Schiff bonds [36]. This conjugation not only links avidin to chitosan, but also to different avidins. Higher concentrations of glutaraldehyde can increase the crosslinking and thus immobilize more avidin on the material surface (Fig. 4.2 a). Saturation occurs due to the default area of chitosan coated on the wells. The amount of avidin may be increased with layering, but the total binding sites for biotin should be consistent. However, a concentration of crosslinker molecules that is too high may cause avidin conjugation to be distributed unevenly on the material surface. The increasing roughness may cause steric hindrance and thus decrease biotin immobilization. The multilayer property of the VBAM system was demonstrated by using different avidin concentrations to compare the relationship between surface avidin (UV detection) and potential binding sites (biotin-AP assay) (Fig. 4.3 a,b). The binding sites were increased with avidin concentration, and were saturated when avidin was greater than 30 μg/well. In contrast, immobilized avidin kept rising even when the avidin concentration was more then 30 μg/well. These results suggest that immobilization increases with increasing avidin concentrations during conjugation because of inter-avidin crosslinking, whereas the binding sites were limited due to the default area of the coated chitosan. Conversely,

in the VBABM system, because the Amine-PEO_3-Biotin has only one reactive end for conjugation, multilayer formation such as in the VBAM system may not occur in this condition (Fig. 4.2 b).

Because avidin conjugation is not specific, some biotin binding sites on avidin may be inactivated. In addition, if the binding regions are close to the solid phase material or hindered by other avidin molecules, the affinity could be reduced because of steric blockage effects. To evaluate the effects of steric hindrance on affinities for different sized biotinylated molecules, biotin-AP and biotin-AdLacZ were immobilized by surface avidin through the VBAM or VBABM methods. Binding affinity assessment can be achieved by the heterogeneity index evaluation from Sips isotherm adsorption model [20, 21]. The saturation intensities for both biotin-AP and biotin-AdLacZ indicated that the VBABM system had higher adsorption levels than VBAM (Fig. 4.4 a,b). Judging by Sips isotherm equations, VBABM expressed nearly homogeneous adsorption to biotin-AP. Even for large biotinylated molecules like the biotinylated-AdLacZ, the heterogeneity index of VBABM was closer to 1 than in the VBAM system (Table 4.1). This suggests that oriented avidin can enhance biotinylated molecule immobilization and reduce heterogeneity.

Scanning electron microscopy illustrated that adenovirus was immobilized on material surfaces in both VBAM and VBABM groups. There were many aggregates of the adenovirus shown in the VBAM group, which is likely due to the unevenly distributed biotin binding sites (Fig. 4.5 a). In the VBAM method, random avidin

conjugation may cause different avidin molecules to connect to each other. This inter-avidin crosslinking could lead to avidin being immobilized on the chitosan surface as clusters. In contrast, the VBABM system likely avoids this drawback, and consequently evenly distributes adenovirus on chitosan surfaces (Fig. 4.5 b).

In assessing *in vitro* cell transduction, the virus immobilized by the VBAM method demonstrated modest infection efficiency, when compared to the excellent transduction in the VBABM method. To fairly evaluate virus dosage in the VBAM and VBABM groups, suspended viral particles after conjugation were detected for normalization. The infection of VBAM was comparable to the Free V & Cell group and was better than the Free V group after normalization (Fig. 4.6 b). Interestingly, VBAM still had a lower transduction efficiency than VBABM, even with the same number of immobilized viral particles. This may be due to the virus biotinylation reagent, SulfoNHS-LC-biotin, which has a spacer between biotin and a viral protein. Because avidin immobilized by random conjugation may increase surface roughness and result in unevenly distributed binding sites, the spacer may be entangled when biotin is bound to the surface. This may inhibit a viral particle from being internalized into cells and thus reduce infection. Therefore, the oriented biotin immobilization in the VBABM strategy not only increases effective binding sites for biotinylated virus immobilization but also improves virus infection efficiency.

Virus immobilization by antibodies conjugated to biomaterial surfaces represents an effective strategy for binding viral vectors to scaffold surfaces. By covalently linking

anti-virus IgG on biomaterials, viral vectors can be stably tethered for site-specific delivery. This strategy has been applied for the immobilization of viruses on biomaterials to deliver genes in micro-coils, stents, and intra-aortic implants [4, 15-17]. While this method was applied to effectively control single gene delivery from scaffolds, this strategy would be incapable of transferring multiple genes in defined regions of scaffolds because anti-virus antibodies cannot distinguish viral vectors with different transgenes. Therefore, we sought to tag an antigenic determinant on viral surfaces so that the modified virus could be bound by antibodies against this antigen. Small chemicals were used for tagging because they proved effective in modifying viral surfaces, and because they could easily be conjugated without inhibiting virus infectivity [37]. For example, biotinylation has been applied to modify adenoviral surfaces that tether viral vectors to avidin immobilized surfaces [28, 37]. Using a similar strategy, we developed a new method for modifying viral surfaces by DIG conjugation.

In our study, DIG-NHS effectively modified adenovirus surfaces and we were able to maintain the virus titer after this reaction (Fig 4.9 b). These findings demonstrated that the grafting modification was a mild chemical reaction that preserved viral integrity. In addition, DIG should not inhibit the recognition of coxsackie-adenovirus receptors (CAR) on host cells for internalization due to its small size. The conjugation of DIG-NHS to amine groups on viral capsid proteins forms amide bonds, which is a covalent bond and thus DIG can be stably maintained on viral surfaces. The MW of DIG-NHS is only 659 Da, which is extremely small compared to adenovirus (MW=180 x 10^6 Da). Also, the entry of adenovirus into the host cell is initiated by the knob domain of the fiber

protein binding to the cell receptor. The molecular weight of fiber protein is 62 kDa, which is approximately 100 times larger than DIG-NHS. Due to the small size of the conjugated DIG, the infectivity of modified virus can be preserved after reaction.

Patient safety is an important concern in regenerative gene therapy. Although digoxigenin is broadly applied as a tag for labeling in different *in vitro* analyses, it is rarely used for *in vivo* studies because of its potential for cardiotoxicity. This cardiotoxicity is caused by ATPase inhibition [23, 24]. Therefore, as an initial measure of safety, an ATPase inhibition assay was performed in which DIG-modified adenovirus was compared with digoxigenin and two other common cardiac glycosides, digoxin and ouabain. Assuming the DIG-NHS molecules perfectly grafted on viral surfaces, the ATPase inhibition assay demonstrated that the DIG-modified virus was 1500 times less active than the three positive control groups (Fig 4.10 b). This may be caused, in part, by the overestimation of DIG molecules on the viral surfaces, resulting from an imperfect conjugation rate of DIG-NHS. In addition, the interactions between grafted DIG and ATPase may be inactivated because of an increase in steric hindrance. Because adenovirus is a very large molecule, DIG covalently linked on adenoviral surface may be too large to engage its ATPase binding sites. ATPase is located on the transmembrane Na^+/K^+ pump and steric hindrance would likely be even more significant *in vivo*, suggesting that inhibition should be even less than that observed in our experimental tests. Furthermore, it would be difficult for the bound DIG-modified adenovirus to affect cardiac muscle function via bloodstream transportation. Although extensive *in vivo*

analyses would need to be performed prior to use in humans, the experiments described here suggest that this method may be safe and without serious cardiac implications.

The functionalization of chitosan surfaces was achieved by treating the material with Sulfo-GMBS. These thiol-reactive surfaces conjugated with the sulfhydryls of half-IgG derived from reducing disulfide bonds in the antibody hinge region. By this method, IgG was conjugated to the material surface by the specific sulfhydryl groups of Fc. Therefore, this treatment forced Fab to face out from the biomaterial surface to reduce steric hindrance. The DIG-modified adenovirus immobilizations were dependent on the titer of viral vectors, suggesting that the disulfide reduction of IgG was mild, and that IgG maintained its ability to bind adenovirus (Fig 4.11 a). In addition, the conjugated anti-DIG half-IgG perfectly immobilized DIG-modified adenovirus at concentrations as high as $1x10^9$ viral particles per well (Fig 4.11 b). Higher virus concentrations caused the immobilization rate to decline due to the limited substrate area, but over 50% of the virus was still captured on the surface when virus concentration was less than 10^{11} viral particles per well. This suggests that DIG-modified adenovirus can be effectively tethered by surface anti-DIG IgG.

The DIG-modified adenovirus maintained a similar stability pattern as non-modified virus (Fig 4.11 d). At last 75% of both of these two adenoviral vectors were bound on the biomaterial for 2 weeks. In this study, although we did not investigate the temporal relationship of immobilized virus uptake by adhered cells, some other research has labeled antibody and virus by fluorescent dyes to determine the virus internalization

by cells with time [2]. These studies demonstrated that the uptake of antibody-adenovirus complex was rapid and that most of them were in host cells in first 2 hrs. Both antibody and adenovirus was internalized into cells, suggesting that vector-antibody entry occurs in cells in contact with the antibody-virus complex and that these cells can take up the complex intact with cytoplasmic processing. Therefore, our stability experiment results indicated that virus remains stable on material surfaces and only cells that adhered on scaffolds would be infected. This assured that conjugated antibody may control gene delivery on specific sites to avoid spreading from target sites and eliciting unwanted systemic infection.

To further investigate the potential of this model for *in situ* cell transduction, a low melting point wax technique was applied to spatially control anti-DIG IgG conjugation on chitosan surfaces. Secondary antibody and X-gal staining results illustrated that viruses immobilized by conjugated antibodies specifically transduced cells on the target sites (Fig 4.12 a,b). These results demonstrated that DIG modification is feasible for mediating adenoviral vector immobilization and for *in situ* cell transduction on biomaterial surfaces. Therefore, this method should be able to successfully deliver virus to specific sites on biomaterial scaffolds with the goal of generating specific interfaces between cell signaling vectors and eventually used to engineer multi-tissue interfaces.

Due to the difficulty in distinguishing viral vectors with different transgenes, we developed a viral surface modification method to differentiate multiple viral vectors.

Both adenovirus with and without DIG modification were immobilized on anti-adenovirus IgG conjugated surfaces, suggesting that DIG grafts were small enough that the epitopes maintained their antigenic properties after modification (Fig 4.13 b). Likewise, anti-DIG IgG specifically captured DIG-modified adenovirus on the surface of the biomaterial (Fig 4.13 a). Therefore, a dual adenovirus immobilization model was developed in our study to coordinately combine different bioactive factors (Fig 4.14 a). In this model, one adenovirus was immobilized on the entire scaffold, and another virus was restricted to specific regions controlled by wax masking (Fig 4.14 b). Cells expressing green or blue fluorescent proteins were both expressed in the non-masked area because anti-adenovirus IgG binds to both AdGFP and DIG-AdBFP. In contrast, the masked area that was conjugated by anti-DIG IgG contained only cells expressing BFP, suggesting that DIG modification can be used for specific virus immobilization (Fig 4.14 c). These results demonstrate that this dual adenoviral vector immobilization method can spatially control the distribution of cell signaling viruses on biomaterials and may be further developed to engineer multi-tissue interfaces *in vivo*.

4.5 Conclusions

Two new methods were developed to immobilize adenovirus on biomaterial surfaces for *in situ* gene therapy. Amine groups on chitosan surfaces were used for bioconjugation to bind virus via avidin-biotin and antibody-antigen interactions. Viral surfaces were covalently modified by biotin or digoxigenin while the infectivity was preserved. Compared to randomly conjugating avidin to biomterials, indirectly docking avidin on biotinylated materials orients biotin binding sites to increase the binding

efficiency. This virus-biotin-avidin-biotin-material (VBABM) model evenly tethered adenovirus on a chitosan surface, and improved cell transduction. Excessive viral titer, which may induce cytotoxicity and unwanted systemic infection, may thus be avoided in this system. This model of viral delivery could be adapted for use with not only a variety of biomaterials but also different types of viral vectors.

The DIG modification was developed to tag on virus surfaces as an antigenic determinant for multiple virus immobilizations. In addition, the DIG modified virus was effectively and stably immobilized on biomaterial surfaces, whereas these bound viral vectors could still be released to infect adherent cells. A wax masking technique facilitated the patterning of two different IgG conjugations on the biomaterial surfaces. By immobilizing adenovirus with and without DIG modification, cells were transduced *in situ* so that one transgene was expressed on the entire scaffold surface, while another existed only in defined regions. This dual adenoviral vector delivery system proves potential for engineering tissue interfaces by regulating multiple bioactive factor expression with spatial control. Thus, these two novel virus immobilization strategies should be beneficial for *in vivo* regenerative gene therapy.

Table 4.1. Fitting parameters for the Sips isotherm adsorption model

	Biotin-AP		***Biotinylated AdLacZ***	
	VBAM	VBABM	VBAM	VBABM
Saturation Intensity I^{sat}	3.0	4.2	0.33	0.56
Heterogeneity Index ***a***	0.894	1.000	0.540	0.832
Binding Affinity ***b***	14.1(ml/pg)	15.9(ml/pg)	0.135(ml/10^9 VP)	0.269(ml/10^9 VP)

VP: Viral particles

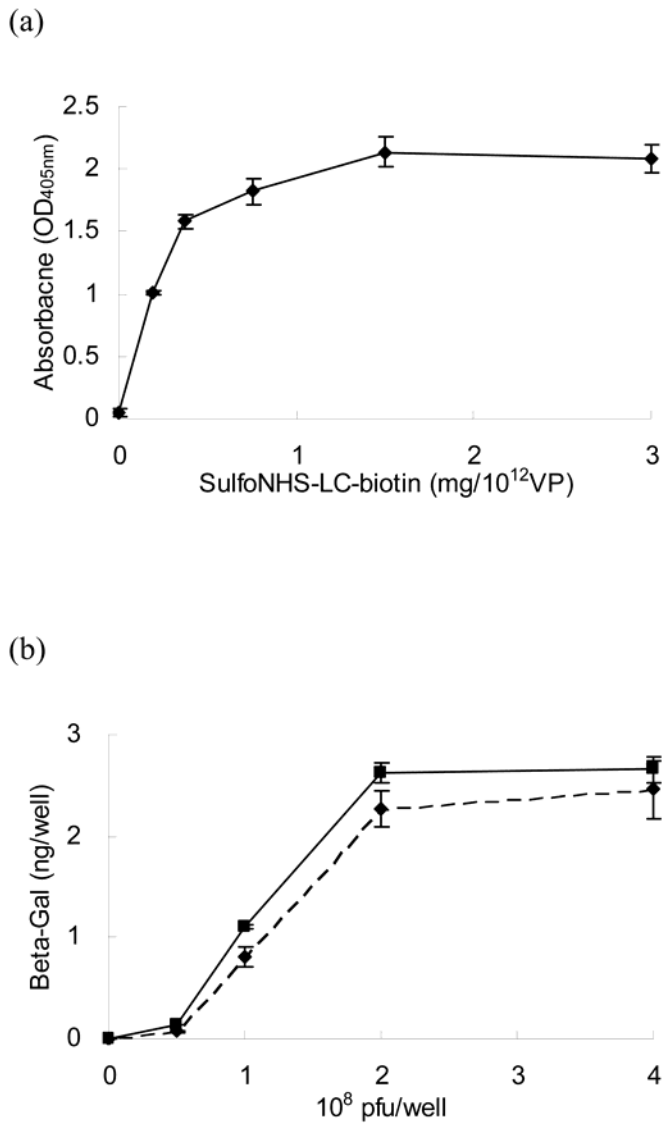

Figure 4.1. Adenovirus encoding LacZ can be biotinylated by SulfoNHS-LC-biotin. (a) Biotinylated virus was immobilized on ELISA plates to detect and quantify biotin on viral surfaces by avidin-AP. The data suggest that biotinylation is dose dependent and saturated when SulfoNHS-LC-biotin is greater than 0.5 mg per 10^{12} viral particles. (b) The β-galactosidase expression from cells infected by AdLacZ before (solid line) and after (dashed line) biotinylation were compared by sandwich ELISA. The results demonstrate that AdLacZ can maintain infection efficiency between 80-90% after biotinylation. The data were compared by Student *t* test, and there were no significant differences between these two groups in all concentrations. (n=3) (VP: viral particles)

(a)

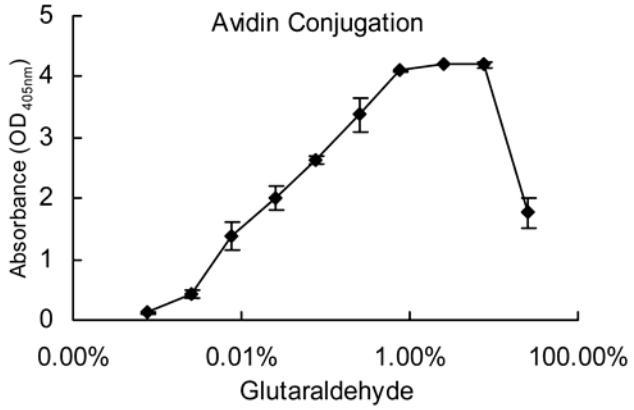

(b)

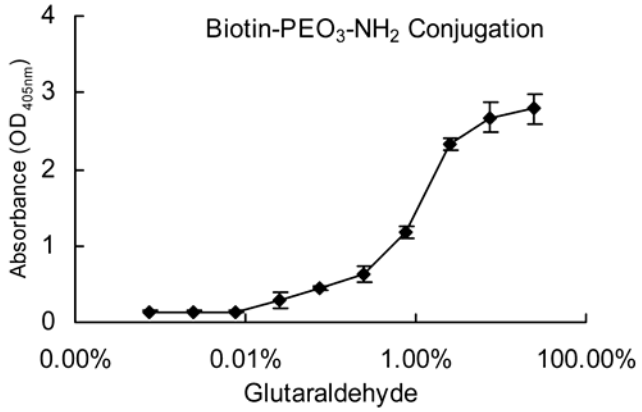

Figure 4.2. The conjugation profiles of homobifunctional crosslinker in the VBAM and VBABM systems are different. (a) In the VBAM system, avidin immobilized on chitosan increased with increasing concentrations of the crosslinker. However, extremely high crosslinker concentrations led to a decrease in surface immobilization. (b) Because biotin conjugation by Amine-PEO_3-Biotin can avoid self-crosslinking due to a single reactive amine group, the conjugation remained strong at saturation levels even in high crosslinker concentrations. (n=3)

(a)

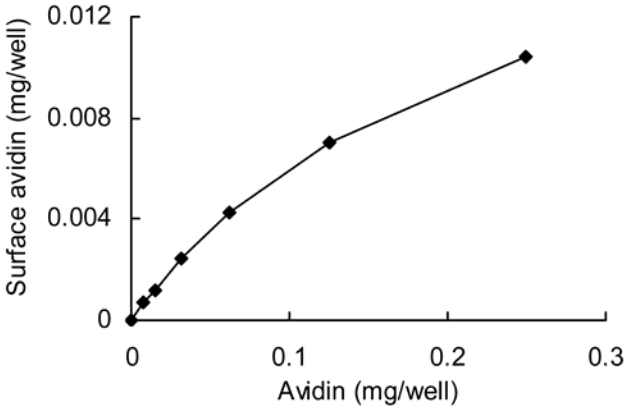

(b)

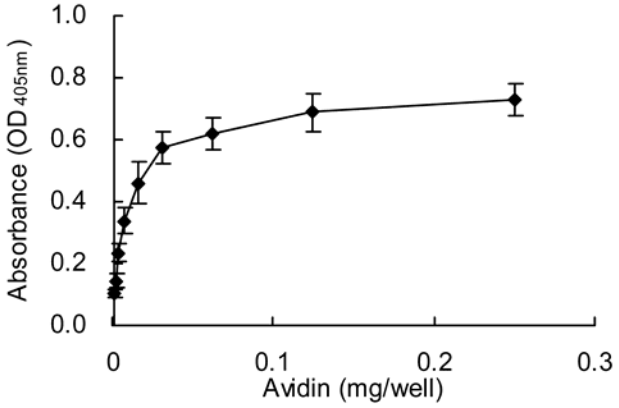

Figure 4.3. Avidin is conjugated on chiotsan as a multilayer. (a) Immobilized avidin molecules were evaluated by indirectly detecting unbound avidin suspended after conjugation. Immobilized avidin increased with increasing avidin concentration. (b) In contrast, biotin-AP analysis suggested that the surface binding sites reached a plateau when avidin concentrations were greater than 0.03 mg/well, which is due to limited chitosan surfaces. The inconsistent trends suggested that a multilayer of avidin formed on the chitosan surface. (n=3)

(a)

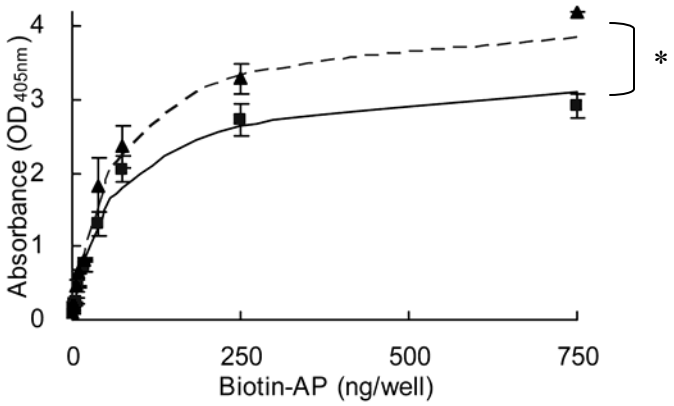

(b)

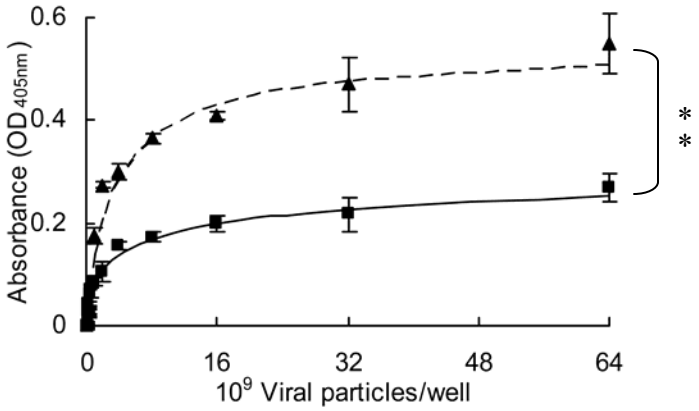

Figure 4.4. Biotinylated molecule immobilization of the VBABM system is greater than that of the VBAM system. Two different biotinylated molecules, (a) biotin-AP and (b) biotinylated AdLacZ, were applied and the binding capacities were compared. The dashed and solid lines represent the Sips model fits of the data of VBABM (triangle) and VBAM (square) systems, respectively. The data were compared by Student *t* test (n=3, *: $p<0.05$, **: $p<0.01$)

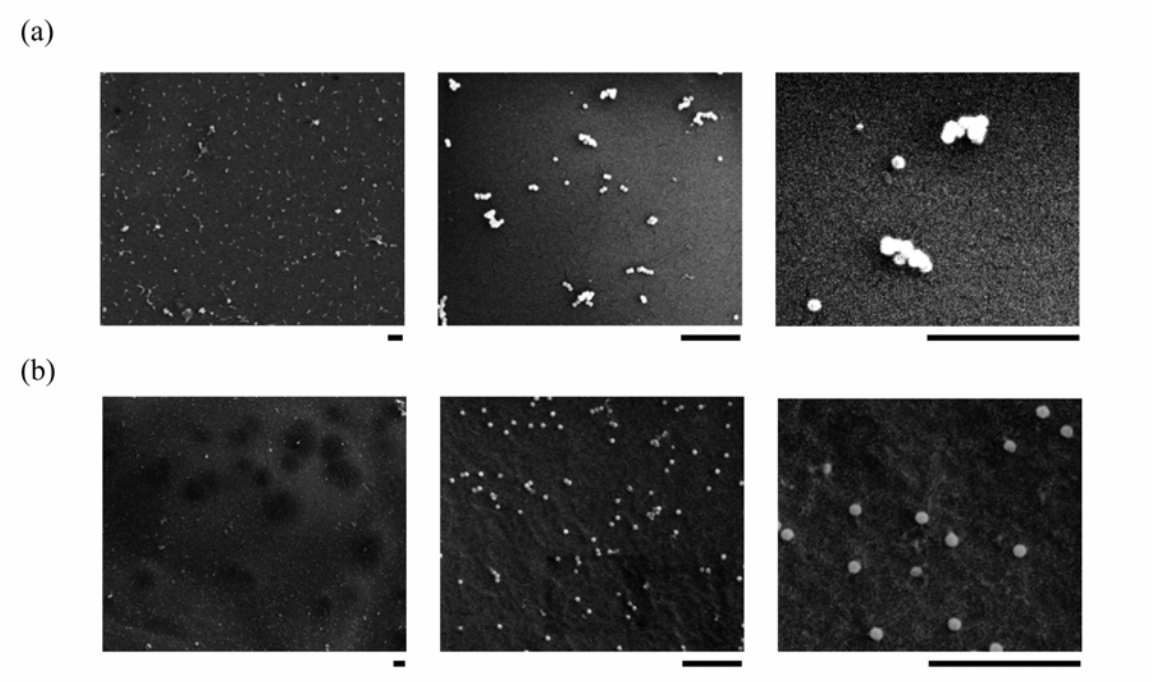

Figure 4.5. Scanning electron microscopy images illustrate virus immobilization in both the VBAM and VBABM systems. Adenovirus immobilized on chitosan surfaces was demonstrated by SEM examination. The chitosan surface images of (a) VBAM and (b) VBABM groups are shown with different magnifications. Viral particles tended to form aggregates or clusters in the VBAM system, whereas the VBABM system led to evenly distributed viral particles. The scale bars under each picture are 1 μm.

(a)

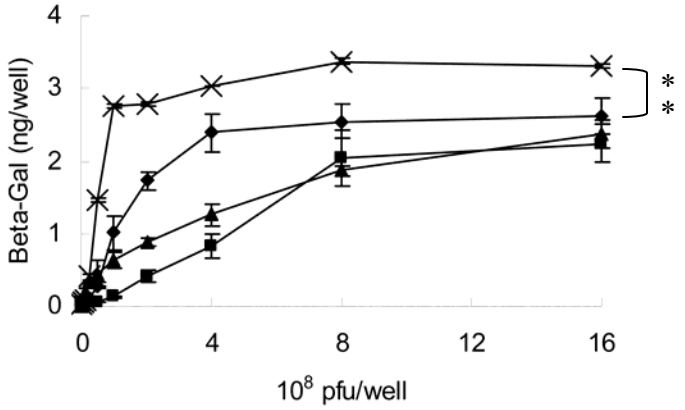

(b)

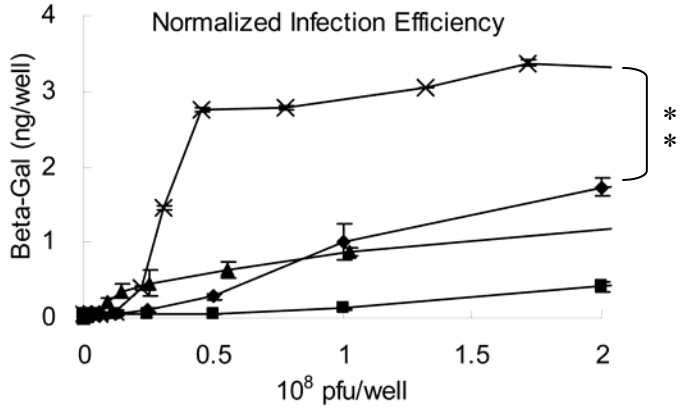

Figure 4.6. *In vitro* cell transduction demonstrates the infection efficiency of the immobilized virus. (a) Virus was immobilized by the VBAM (triangle) or VBABM (cross) methods on 24-well culture plates and then cultured with $2x10^5$ cells/well. There were two control groups using suspended virus infection: 1) cells were plated for 24 hr prior to infection in solution (Free V, square) and 2) cells and virus were mixed together before the cells were plated (Free V& Cell, diamond). (b) The viral particles on chitosan surfaces were indirectly estimated by detecting unbound virus after immobilization. This reflects the real surface virus number and normalizes the virus infection result. The data between VBAM and VBABM were compared by Student *t* test (n=4, **: $p<0.01$)

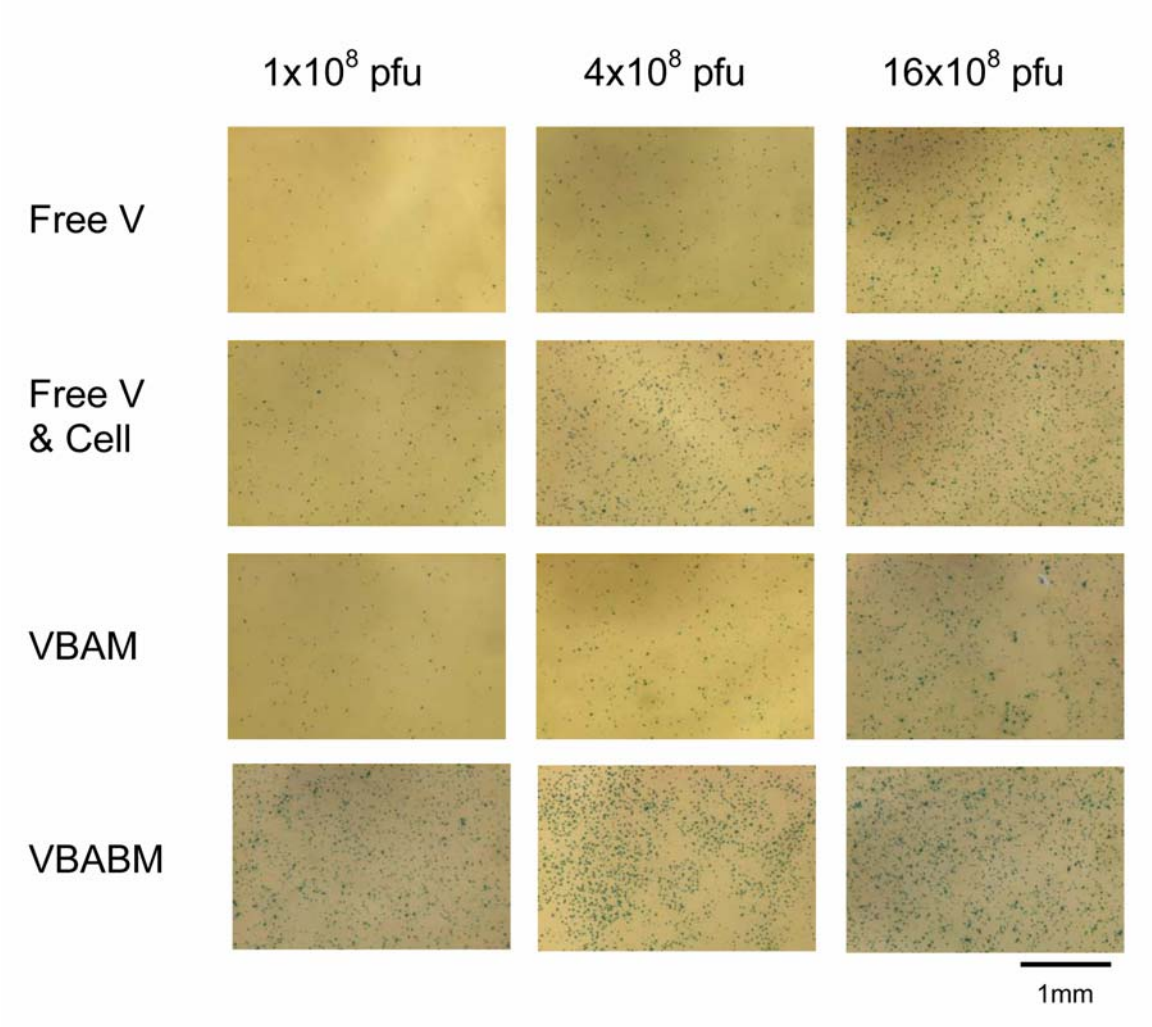

Figure 4.7. X-gal staining demonstrates β-galactosidase activity in infected cells using the four infection models and a range of viral particles ($1x10^8$ to $16x10^8$ pfu). Darkly blue stained cells represent β-gal expression in transduced cells. The VBABM system performed much better than the other groups and had maximal activity with as little as $1x10^8$ pfu.

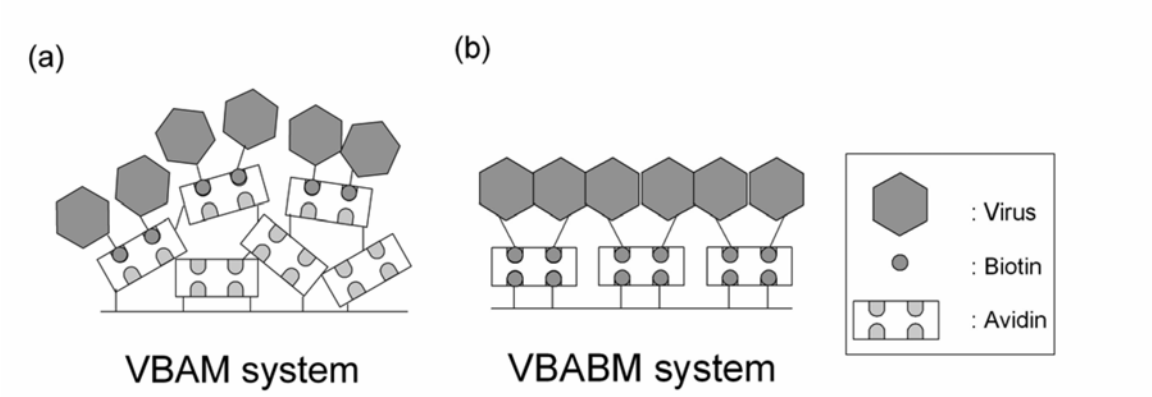

Figure 4.8. Schematic models of the two virus immobilization systems developed in this study. (a) virus-biotin-avidin-material (VBAM) system and (b) virus-biotin-avidin-biotin-material (VBABM) system.

(a)

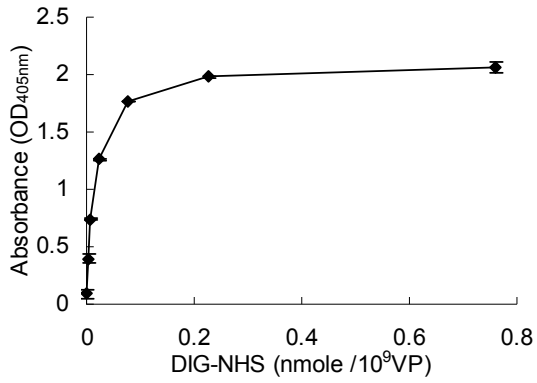

(b)

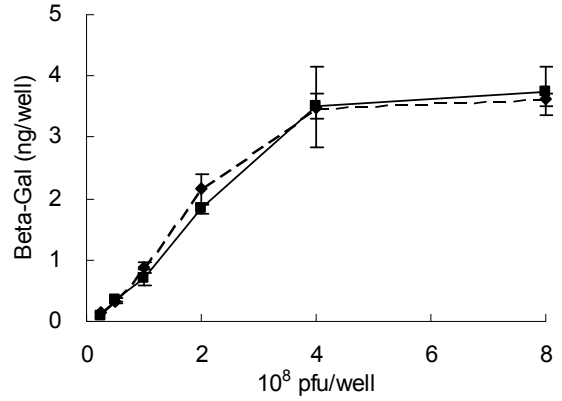

Figure 4.9. Adenovirus modified by DIG-NHS maintains its infectivity. (a) DIG-NHS treated AdLacZ was captured on ELISA plates to detect and quantify DIG molecules on viral surfaces with anti-DIG Ab-AP. The data suggest that the DIG modification was dose dependent and saturated when there were more than 0.075 nmole DIG-NHS per 10^9 viral particles. (b) The β-galactosidase expression from cells infected with AdLacZ with (solid line) and without (dashed line) DIG modification were compared by sandwich ELISA. The results demonstrate that there were no significant differences between these two groups with different virus concentrations, suggesting that this modification was mild, and that viral infectivity could be maintained. The data were compared by Student *t* test, and there were no significant differences between these two groups in all concentrations. (n=3) (VP: viral particles)

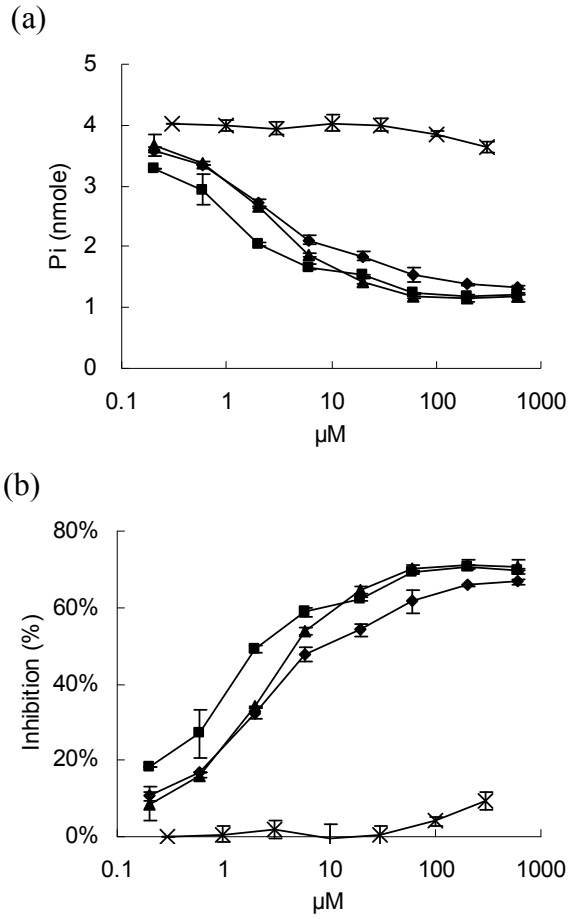

Figure 4.10. An ATPase inhibition assay was performed to investigate the potential toxicity caused by DIG modification. ATPase was reacted with different concentrations of DIG-AdLacZ (cross), and the enzymatic activities of ATPase were determined by the freeing of phosphate ions released from ATP. Three different cardiac glycosides, ouabain (square), digoxigenin (triangle), and digoxin (diamond), were compared as positive controls. (a) The phosphate ion concentrations decreased with increasing inhibitors because the enzymatic activity of ATPase was blocked. DIG-AdLacZ only slightly reduced phosphate release. (b) Three cardiac glycoside molecules demonstrated a dose dependent inhibition of ATPase activity, while an equivalent dose of DIG-AdLacZ exhibited nearly undetectable levels. (n=3)

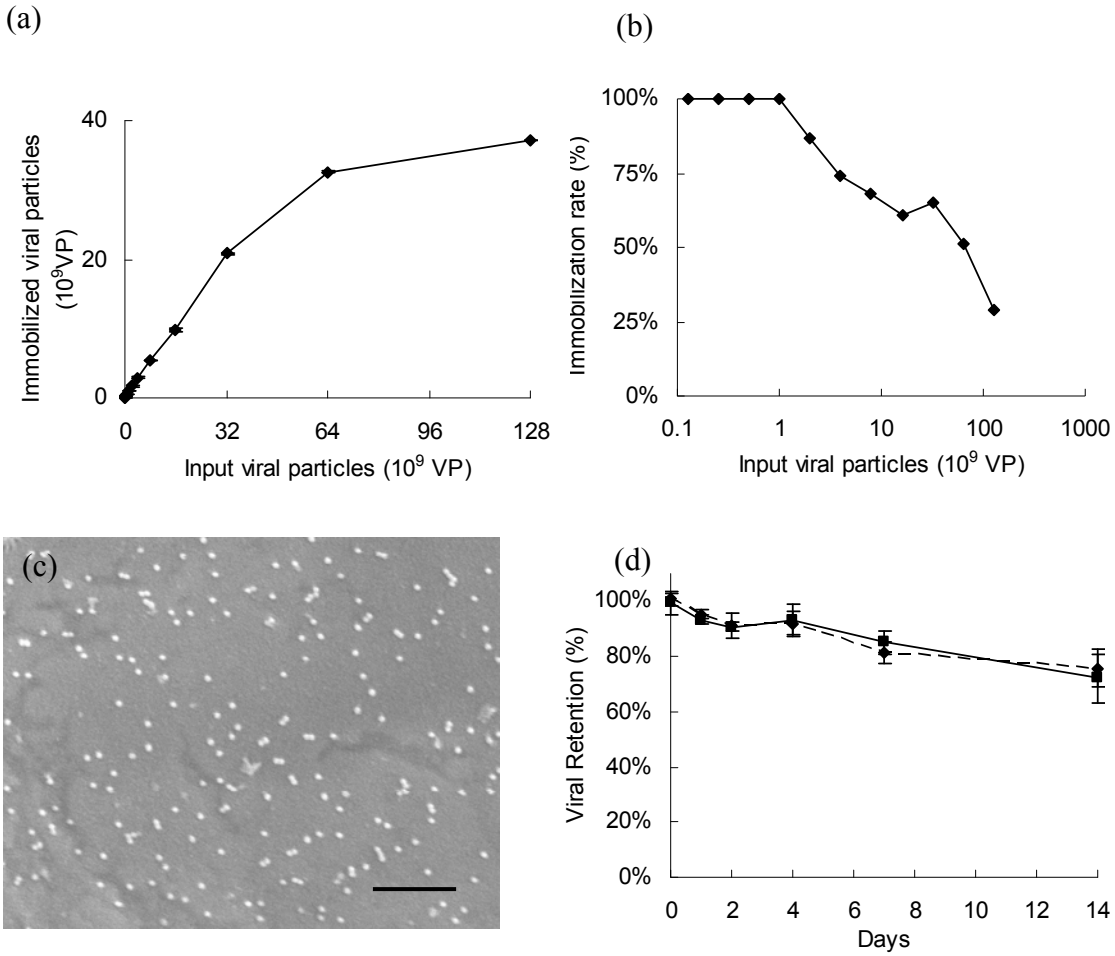

Figure 4.11. The binding capacity of conjugated anti-DIG IgG on chitosan and the virus immobilization stability were determined by an indirect sandwich ELISA assay. (a) The DIG-AdLacZ immobilized on chitosan was proportional to the concentration of incubated DIG-AdLacZ. (b) The immobilization rate of DIG-modified adenovirus was 100% when the concentration was equal to or less than 10^9 viral particles per well. Higher virus concentrations led to lower immobilization rates due to a limited substrate area. (c) The distribution of immobilized DIG-AdLacZ on anti-DIG conjugated chitosan surfaces was illustrated by SEM examination. The scale bar in the picture is 1 μm. (d) Adenovirus with and without DIG modification were placed on anti-DIG IgG (solid line) and anti-adenovirus IgG (dashed line) conjugated surfaces, respectively. The released viral particles were detected at different time points to determine retention rates. The data were compared by Student *t* test and there were no significant differences between these two groups. More than 75% of the virus could be stably maintained for two weeks. (n=3)

(a)

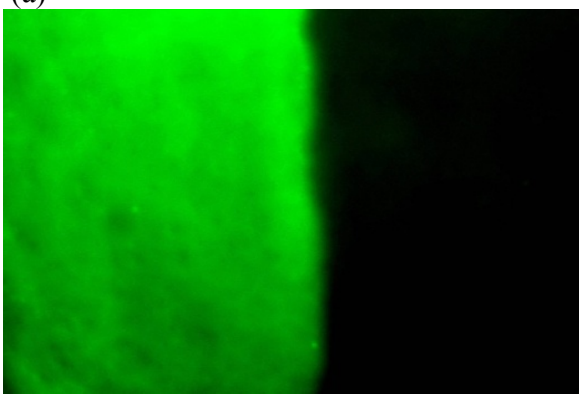

(b)

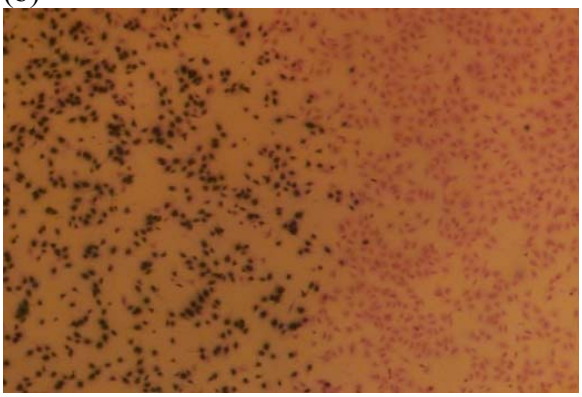

Figure 4.12. Anti-DIG IgG immobilization was spatially controlled by a low melting point wax masking technique. (a) Anti-sheep IgG antibody conjugated FITC was used to label the surface antibody. Only the exposed area without wax protection illustrated green fluorescent expression. (b) HGF cells were cultured on chitosan surfaces for 2 days. The transduced cells turned blue after X-gal staining. Cells grew to confluence on the material surfaces; however, cell transduction was restricted to the non-masked area. These findings are consistent with the results of the fluorescent labeling.

(a)

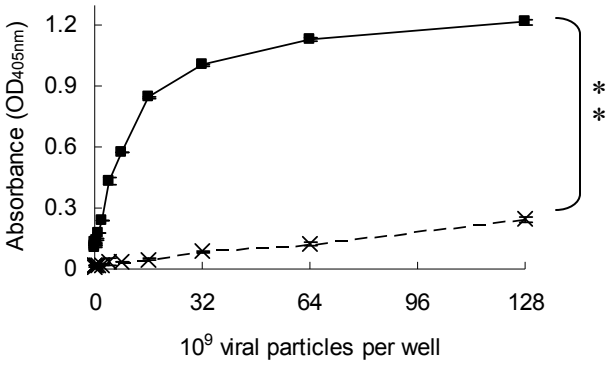

(b)

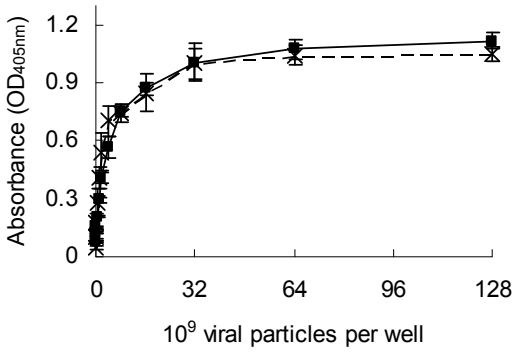

Figure 4.13. Adenoviruses, with (solid line) or without (dashed line), DIG modification were placed on antibody conjugated chitosan surfaces to investigate the specificity of the conjugated antibody to adenovirus. (a) On anti-DIG IgG conjugated chitosan surfaces, DIG-modified virus was immobilized by surface antibodies in a dose dependent manner, whereas there was only a slight adsorption of non-modified adenovirus due to nonspecific binding. (b) On anti-adenovirus IgG conjugated chitosan, both adenovirus with and without DIG modification were bound to the surfaces with a similar affinity. The data were compared by Student *t* test. (n=3, **: $p<0.01$)

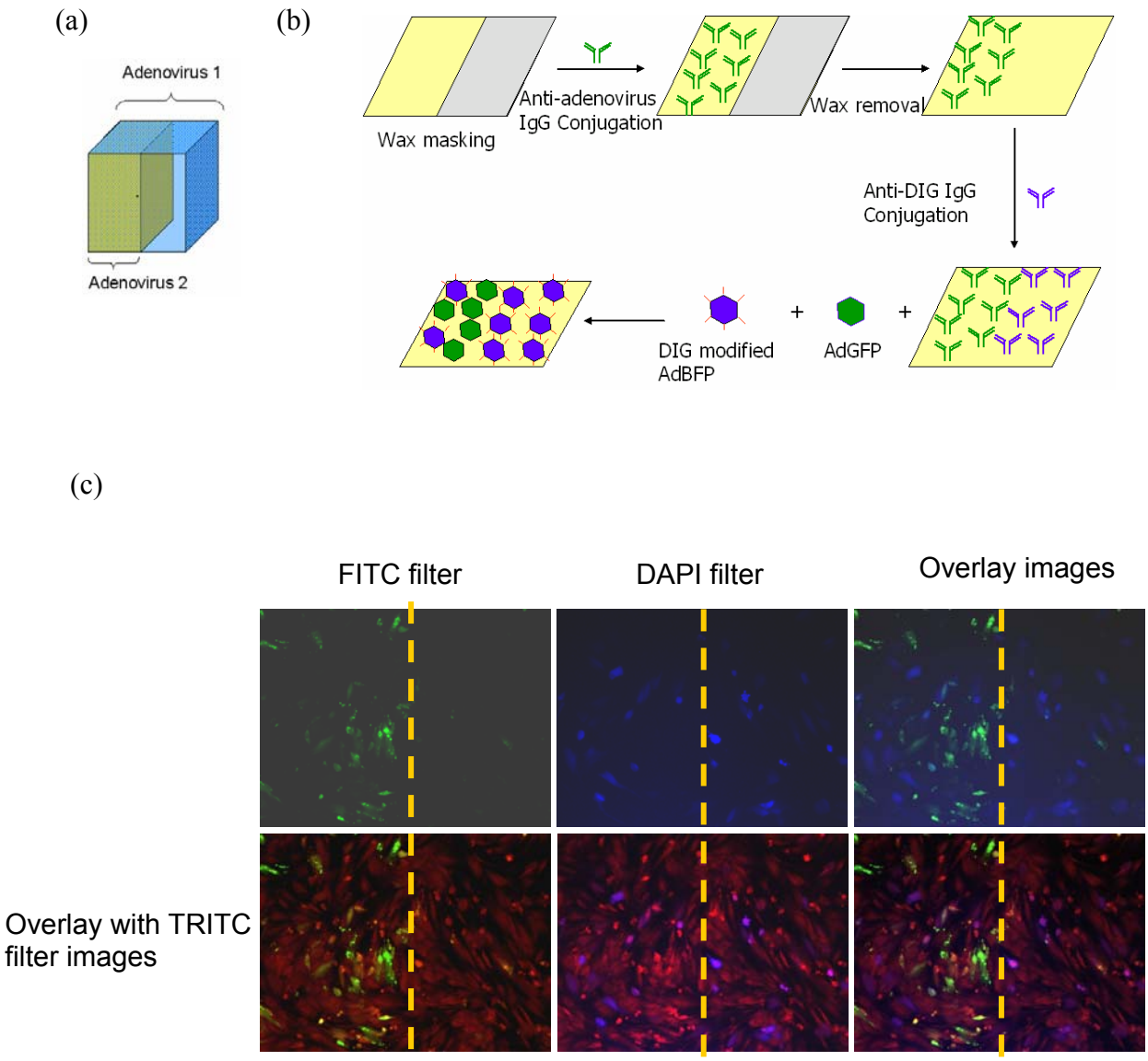

Figure 4.14. Dual adenoviral vector immobilization was performed to demonstrate the spatial control of *in situ* transduction. (a) Schematic of the viral delivery model. By conjugating two different antibodies against DIG and adenovirus using the wax masking technique, one viral vector is tethered on the entire scaffold, whereas the other virus is restricted to specific regions. (b) The scheme of the dual viral vector immobilization method to control two antibody conjugations on biomaterial surfaces. (c) The transduced cell distribution visualized under fluorescent microscopy. Red fluorescent staining demonstrated that cells grew to confluence on material surfaces (TRITC filter). Cells expressing BFP were distributed over the entire surface, whereas GFP expression was restricted to the left side, where AdGFP was bound by anti-adenovirus IgG

4.6 References

1. W.W. Hu, Z. Wang, S.J. Hollister, P.H. Krebsbach, Localized viral vector delivery to enhance in situ regenerative gene therapy, Gene Ther 14 (11) (2007); 891-901.

2. B.D. Klugherz, C. Song, S. DeFelice, X. Cui, Z. Lu, J. Connolly, J.T. Hinson, R.L. Wilensky, R.J. Levy, Gene delivery to pig coronary arteries from stents carrying antibody-tethered adenovirus, Hum Gene Ther 13 (3) (2002); 443-454.

3. R.J. Levy, C. Song, S. Tallapragada, S. DeFelice, J.T. Hinson, N. Vyavahare, J. Connolly, K. Ryan, Q. Li, Localized adenovirus gene delivery using antiviral IgG complexation, Gene Ther 8 (9) (2001); 659-667.

4. J.M. Abrahams, C. Song, S. DeFelice, M.S. Grady, S.L. Diamond, R.J. Levy, Endovascular microcoil gene delivery using immobilized anti-adenovirus antibody for vector tethering, Stroke 33 (5) (2002); 1376-1382.

5. H. Onishi, Y. Machida, Biodegradation and distribution of water-soluble chitosan in mice, Biomaterials 20 (2) (1999); 175-182.

6. S.B. Rao, C.P. Sharma, Use of chitosan as a biomaterial: studies on its safety and hemostatic potential, J Biomed Mater Res 34 (1) (1997); 21-28.

7. T.J. Aspden, J.D. Mason, N.S. Jones, J. Lowe, O. Skaugrud, L. Illum, Chitosan as a nasal delivery system: the effect of chitosan solutions on in vitro and in vivo mucociliary transport rates in human turbinates and volunteers, J Pharm Sci 86 (4) (1997); 509-513.

8. J.K. Suh, H.W. Matthew, Application of chitosan-based polysaccharide biomaterials in cartilage tissue engineering: a review, Biomaterials 21 (24) (2000); 2589-2598.

9. Y. Zhang, M. Zhang, Calcium phosphate/chitosan composite scaffolds for controlled in vitro antibiotic drug release, J Biomed Mater Res 62 (3) (2002); 378-386.

10. Z. Li, H.R. Ramay, K.D. Hauch, D. Xiao, M. Zhang, Chitosan-alginate hybrid scaffolds for bone tissue engineering, Biomaterials 26 (18) (2005); 3919-3928.

11. N.M. Green, Avidin. 1. the Use of (14-C)Biotin for Kinetic Studies and for Assay, Biochem J 89 (1963); 585-591.

12. D. Yao, A.G. Vlessidis, N.P. Evmiridis, Microdialysis sampling and monitoring of uric acid in vivo by a chemiluminescence reaction and an enzyme on immobilized chitosan support membrane, Anal Chim Acta 478 (1) (2003); 23-30.

13. M.B. Parrott, K.E. Adams, G.T. Mercier, H. Mok, S.K. Campos, M.A. Barry, Metabolically biotinylated adenovirus for cell targeting, ligand screening, and vector purification, Mol Ther 8 (4) (2003); 688-700.

14. L. Mei, X. Jin, C. Song, M. Wang, R.J. Levy, Immobilization of gene vectors on polyurethane surfaces using a monoclonal antibody for localized gene delivery, J Gene Med 8 (6) (2006); 690-698.

15. I. Fishbein, I.S. Alferiev, O. Nyanguile, R. Gaster, J.M. Vohs, G.S. Wong, H. Felderman, I.W. Chen, H. Choi, R.L. Wilensky, R.J. Levy, Bisphosphonate-mediated gene vector delivery from the metal surfaces of stents, Proc Natl Acad Sci U S A 103 (1) (2006); 159-164.

16. I. Fishbein, S.J. Stachelek, J.M. Connolly, R.L. Wilensky, I. Alferiev, R.J. Levy, Site specific gene delivery in the cardiovascular system, J Control Release 109 (1-3) (2005); 37-48.

17. S.J. Stachelek, C. Song, I. Alferiev, S. Defelice, X. Cui, J.M. Connolly, R.W. Bianco, R.J. Levy, Localized gene delivery using antibody tethered adenovirus from polyurethane heart valve cusps and intra-aortic implants, Gene Ther 11 (1) (2004); 15-24.

18. T. Lion, O.A. Haas, Nonradioactive labeling of probe with digoxigenin by polymerase chain reaction, Anal Biochem 188 (2) (1990); 335-337.

19. S.C. Gifford, T. Yoshida, S.S. Shevkoplyas, M.W. Bitensky, A high-resolution, double-labeling method for the study of in vivo red blood cell aging, Transfusion 46 (4) (2006); 578-588.

20. R.A. Vijayendran, D.E. Leckband, A quantitative assessment of heterogeneity for surface-immobilized proteins, Anal Chem 73 (3) (2001); 471-480.

21. R. Sips, On the Structure of a Catalyst Surface, J Chem Phys 16 (5) (1948); 490-495.

22. N.J. Dimmock, S.B. Primrose (eds). *Introduction to Modern Virology*. Blackwell Press: London, 1994; 345.

23. S.J. Soldin, Digoxin--issues and controversies, Clin Chem 32 (1 Pt 1) (1986); 5-12.

24. T.W. Smith, E. Haber, Digitalis. I, N Engl J Med 289 (18) (1973); 945-952.

25. E.L. Chan, R. Swaminathan, A rapid assay for the measurement of Na+,K(+)-ATPase inhibitors, Clin Biochem 25 (1) (1992); 15-19.

26. B. Bajaj, P. Lei, S.T. Andreadis, High efficiencies of gene transfer with immobilized recombinant retrovirus: kinetics and optimization, Biotechnol Prog 17 (4) (2001); 587-596.

27. H. Hanenberg, X.L. Xiao, D. Dilloo, K. Hashino, I. Kato, D.A. Williams, Colocalization of retrovirus and target cells on specific fibronectin fragments increases genetic transduction of mammalian cells, Nat Med 2 (8) (1996); 876-882.

28. D.A. Hobson, M.W. Pandori, T. Sano, In situ transduction of target cells on solid surfaces by immobilized viral vectors, BMC Biotechnol 3 (2003); 4.

29. B. Lu, M.R. Smyth, R. O'Kennedy, Oriented immobilization of antibodies and its applications in immunoassays and immunosensors, Analyst 121 (3) (1996); 29R-32R.

30. C. Yeung, D. Leckband, Molecular level characterization of microenvironmental influences on the properties of immobilized proteins, Langmuir 13 (25) (1997); 6746-6754.

31. C. Yeung, T. Purves, A.A. Kloss, T.L. Kuhl, S. Sligar, D. Leckband, Cytochrome c recognition of immobilized, orientational variants of cytochrome b(5): Direct force and equilibrium binding measurements, Langmuir 15 (20) (1999); 6829-6836.

32. M.A. Firestone, M.L. Shank, S.G. Sligar, P.W. Bohn, Film architecture in biomolecular assemblies. Effect of linker on the orientation of genetically engineered surface-bound proteins, J Am Chem Soc 118 (38) (1996); 9033-9041.

33. G.P. Anderson, M.A. Jacoby, F.S. Ligler, K.D. King, Effectiveness of protein A for antibody immobilization for a fiber optic biosensor, Biosens Bioelectron 12 (4) (1997); 329-336.

34. L.C. Shriver-Lake, B. Donner, R. Edelstein, K. Breslin, S.K. Bhatia, F.S. Ligler, Antibody immobilization using heterobifunctional crosslinkers, Biosens Bioelectron 12 (11) (1997); 1101-1106.

35. B. Lu, M.R. Smyth, R. Okennedy, Immunological activities of IgG antibody on pre-coated Fc receptor surfaces, Anal Chim Acta 331 (1-2) (1996); 97-102.

36. S.R. Ahmed, A.B. Kelly, T.A. Barbari, Controlling the orientation of immobilized proteins on an affinity membrane through chelation of a histidine tag to a chitosan-Ni++ surface, J Memb Sci 280 (1-2) (2006); 553-559.

37. W.W. Hu, M.W. Lang, P.H. Krebsbach, Development of adenovirus immobilization strategies for in situ gene therapy, J Gene Med 10 (10) (2008); 1102-1112.

CHAPTER 5

CHEMICAL VAPOR DEPOSITION TO FUNCTIONALIZE BIOMATERIALS FOR CONTROLLING GENE DELIVERY

5.1 Introduction

In our previous study, we demonstrated two different virus delivery systems, VBABM and DIG-AntiDIG IgG. In the VBABM system, material surfaces were conjugated with a layer of biotin molecules for avidin immobilization. These tethered avidin molecules were able to bind biotinylated adenovirus, and thus spatially control gene delivery. In the DIG-AntiDIG IgG method, DIG was applied to tag viral surfaces as antigenic determinants. Modified and non-modified viruses could then be distinguished and immobilized on specific sites on biomaterial scaffolds. In these studies, chitosan was used to develop both strategies due to its intrinsic amine groups; however, these two strategies are limited in application to biomaterials with reactive functional groups. Consequently, we sought to use an effective functionalization method to broaden the utilization of these virus immobilization deliveries to different biomaterials.

High energy radiation such as plasma, laser, and ion beam are frequently used to generate functional groups on non-reactive material surfaces [1-3]. However, these treatments may only be applied to 2-D films or very thin 3-D scaffolds due to limitation in penetration [4]. Chemical vapor deposition (CVD) polymerization is an alternative

modification, in which monomers are sublimated, activated, and then deposited on material surfaces. CVD polymerization of [2.2]paracyclophanes (PCP) into poly(*p*-xylylenes) (PPX) follows a well-established protocol. The PCP dimer can be modified with different reactive groups, including amines, alcohols, alkynes, carbonyls, and anhydrides [5, 6]. Functionalized PCPs are then polymerized into reactive PPX coatings, which present the functional groups on the substrate surfaces. In addition, many of the PPX coatings exhibit excellent biocompatibility properties compared to other polymer coatings, and thus are appropriate for scaffold modification [7]. Amino-[2.2]paracyclophane has been developed for deposition on implant materials surfaces and may be applied to conjugate biomolecules such as proteins, antigens or cell receptors [8]. Due to its reactive properties, it should be a potential CVD treatment to allow control of the interactions between biomaterials and living tissues.

To investigate the extent to which CVD-modified scaffold surfaces may be functionalized for bioconjugation, the virus-biotin-avidin-biotin-materials (VBABM) method was used as a model system [9]. Poly (ε-caprolactone) (PCL) is a frequently used scaffold material because of its biocompatibility and biodegradability, but it lacks active functional groups for covalent linkage [10]. Therefore, we sought to apply CVD modification to PCL surfaces to present a layer of amine groups. We hypothesized that biotin conjugation could be performed on these aminated surfaces for avidin immobilization, and thus biotinylated adenovirus could be bound in specific regions of scaffolds to spatially control cell transduction.

5.2 Materials and Methods

5.2.1 Polycaprolactone film preparation

Polycaprolactone (PCL) (Mn=42500, Mw=65000, Sigma-Aldrich) was dissolved in glacial acetic acid at 0.5% (w:v). After melting the polymer at 60 ˚C overnight, the PCL solution was filtered through a 0.22 μm membrane (Nalgene). The PCL solution (0.5 ml/well) was placed into 24-well culture plates (Corning) which were then incubated at 50 ˚C overnight to evaporate the solvent. Each well was neutralized with 2 M NaOH and then was washed with PBS.

5.2.2 Chemical vapor deposition

The PCL surfaces were modified using chemical vapor deposition (CVD) polymerization as documented in previous studies [5, 8, 11]. Four-Amino[2.2]-paracyclophane **(1)** was synthesized from [2.2] paracyclophane according to previously established protocols [12] (Fig 5.1 a). Approximately 30-40 mg of dimer **(1)** was loaded into the CVD system, and the working pressure was adjusted to 0.28 mbar. Dimer **(1)** sublimated at 90-100 ^{o}C and was transported through a pyrolysis zone (670 ^{o}C) and into the deposition chamber via argon carrier gas (20 sccm). The PCL coated multi-well plates were placed on the sample holder that was cooled to 15 ˚C. Sample holder rotation ensured uniform Poly [(4-amino-*p*-xylylene)-*co*-(*p*-xylylene)] (PPX-NH_2) **(2)** deposition of the polymer. The deposition time lasted 15-20 minutes. The surfaces before and after PPX-NH_2 **(2)** modification were qualified by Fourier transform infrared spectroscopy (FT-IR, Nicolet 6700 Spectrometer, Thermo Fisher, Waltham, MA, USA) utilizing the grazing angle accessory (Smart SAGA, Thermo) at an angle of 85˚.

5.2.3 The biocompatibility of CVD modified surface

To investigate the extent to which CVD modification affected the physiological status of cells, 3-(4,5-dimethylthiazol-2-yl)-5-(3-carboxymethoxyphenyl)-2-(4-sulfophenyl)-2H-tetrazolium (MTS) and lactate dehydrogenase (LDH) assays were performed to determine cell proliferation and cytotoxicity. Fibroblasts were seeded at a concentration of 5,000 cells/cm^2 on PCL surfaces before and after amination. In the MTS assay, 120 µl of CellTiter 96 AQ_{ueous} one solution (Promega, Madison, WI, USA) was added per well and incubated at 37^oC for 1 hr. The supernatants were sampled in volumes of 150µl in 96-well plates and were read spectrophotometrically at OD_{490nm}. Additionally, a standard curve of MTS assay with different numbers of fibroblasts was established, and the MTS time-course results were fitted to determine the cell numbers on material surfaces.

The cytotoxicity was determined using an LDH kit (CytoTox 96 Non-radioactive Cytotoxicity assay, Promega). Fibroblasts were cultured in 24-well plates before and after CVD modification, in the same way as the MTS assay. At different time points, 50 µl of the medium was transferred to a 96-well plate. The reconstituted substrate mix was then added (50 µl/well), and the reaction was incubated at room temperature in darkness for 30 minutes. Finally, 50 µl of stop solution was added to each well, and the samples analyzed spectrophotometrically at a wavelength of 490 nm. Furthermore, a calibration curve of the LDH assay was determined by lysing different numbers of fibroblasts. This was used to estimate the number of dead cells at different time points. The survival rates were then

calculated by comparing the cell death numbers to the total cell numbers determined by the MTS assay.

5.2.4 Adenovirus immobilization on CVD treated PCL surfaces

The CVD-modified plates were washed with water before the conjugation experiments. To immobilize biotinylated adenovirus for *in situ* transduction, aminated PCL surfaces were conjugated to Amine-PEO_3-Biotin (Pierce, Rockford, IL, USA) by glutaraldehyde crosslinking. Avidin was then indirectly docked on biotinylated PCL surfaces to tether biotinylated adenovirus (virus-biotin-avidin-biotin-material, VBABM), as described in our previous study [9]. The same procedure was also performed in 3-D PCL scaffolds which were fabricated by selective laser sintering (SLS) [13].

5.2.5 Wax masking to spatially control CVD treatment for virus immobilization in discrete locations on biomaterial surfaces

To spatially control CVD treatment to specific sites, low-melting polyester wax (EMS, Hatfield, PA) was applied to partially mask defined areas of scaffolds. Wax was melted at 40 ^{o}C and then added (200 µl/well) to the right side of PCL coated wells. The same process was performed in 3-D PCL scaffolds. 300 µl wax was added to the wells of 24-well plates to mask the lower portion of scaffolds (Fig 5.7 a). After the wax solidified, PPX-NH_2 was deposited via CVD onto exposed surfaces. The modified surfaces were biotinylated to immobilize avidin and the wax was removed by incubation in ethanol at 37 ^{o}C for 1 hour.

After avidin immobilization on biotinylated PCL surfaces, Biotin-fluorescein was used to stain the bound avidin. The labeled region was observed under a fluorescent microscope. To determine the distribution and activity of immobilized virus, *in vitro* cell culture was performed. For PCL films, fibroblasts were seeded at a concentration of $2.5x10^4$ cells/cm^2 for 2 days. The distribution of cells transduced by the immobilized virus was illustrated by X-gal staining followed by crystal violet counter staining. This experiment was also performed for 3-D scaffolds in which 1 million fibroblasts were seeded per scaffold. After 2 days in culture, the scaffolds were dissected at their midpoints and stained with X-gal and crystal violet.

5.3 Results

5.3.1 PCL surfaces are functionalized by CVD treatment

Because PCL lacks reactive functional groups, the CVD technique was used to create a layer of amines on PCL surfaces (Fig 5.1 a). After PPX-NH_2 deposition, the treated PCL surfaces were examined by attenuated total reflection FTIR (ATR-FTIR). When comparing the IR spectrum before and after modification, several specific absorption peaks characterized the newly formed amine groups (Fig 5.1 b). The absorption peaks at 1576 and 1632 cm^{-1} were due to the scissoring bending of primary amines. Additionally, the stretching of amines led to a specific absorption peak at 3361 cm^{-1}. These characterizations demonstrated that amine groups were presented on PCL surfaces after CVD surface modification.

5.3.2 The PPX-NH_2 deposition maintains similar biocompatibility to PCL films

Because safety is an extremely important issue for the use of biomaterials in humans, it is necessary to determine if a CVD treated surface is appropriate for cell adhesion and growth without cytotoxicity. Consequently, fibroblasts were cultured on PPX-NH_2 deposited PCL surfaces for 1 week, and cell proliferation rates and survival rates were determined by MTS and LDH assays, respectively (Fig 5.2 a-c).

In the MTS assay, the fibroblast numbers steadily increased from 10,000 to approximately 100,000 in 7 days of culture, suggesting that these surfaces supported cell proliferation (Fig 5.2 a). To investigate potential cytotoxicity of the modified surface, the numbers of dead cells were determined by an LDH assay. Cell death was not significant until day 5. This observation may have been caused by high concentrations of waste and toxic protein release from dead cells (Fig 5.2 b). However, a survival rate of grater than 90% was maintained, indicating that PPX-NH_2 treated surfaces did not lead to significant cell death (Fig 5.2 c). In both the MTS and LDH assays, there were no significant differences between the PPX-NH_2 deposited and non-deposited PCL groups.

5.3.3 Biotinylated adenovirus are specifically immobilized on modified PCL surfaces using the VBABM method

Aminated PCL surfaces were conjugated to Biotin-PEO_3-NH_2 to form a layer of biotin for avidin immobilization. To investigate if this surface modification specifically tethered biotinylated adenovirus, an ELISA assay was performed. Different concentrations of biotinylated adenoviral vectors were individually incubated on PCL surfaces with or without immobilized avidin. Unbound virus was removed and the surface immobilized adenovirus was detected by an indirect ELISA assay (Fig 5.3). The

binding of biotinylated adenovirus increased with increasing virus concentrations on avidin immobilized surfaces. In contrast, the untreated PCL surfaces had almost no virus adsorption. These results suggested that biotinylated adenovirus could be specifically bound to PPX-NH_2 treated PCL surfaces by avidin immobilization using the VBABM method.

5.3.4 Adenoviral particles are evenly immobilized on 2-D and PCL films treated with PPX-NH_2 deposition

Using the VBABM method, biotinylated adenovirus was bound to modified PCL films. To investigate the distribution of virus, immobilized viral particles were illustrated by SEM examination (Fig 5.4). Unique spheres with diameters ranging between 70-80 nm were observed on PCL films, suggesting adenovirus (typical size=70-90 nm) was able to be immobilized on modified PCL surfaces. These adenoviral particles were evenly distributed on material surfaces, indicating well-oriented avidin immobilization.

5.3.5 Adenoviruses are spatially immobilized on biomaterials controlled by the wax masking technique

Adenovirus was only tethered on PPX-NH_2 treated PCL surfaces by the VBABM method (Fig 5.3). Therefore, spatial control of virus immobilization to target sites of biomaterials should be possible. To determine the extent to which adenovirus could be bound on distinct regions of biomaterials by controlling the CVD modification, a wax masking technique was used to regulate PPX-NH_2 deposition on defined regions of PCL films. After avidin immobilization, the masking wax was removed and biotinylated AdLacZ was bound on materials surfaces.

The coated PCL films on 24-well plates were translucent. Using a phase contrast microscope, the crystals of PCL molecules led to a roughness in the films (Fig 5.5 a). By masking the right site of PCL films during CVD treatments, the non-masked area was functionalized by PPX-NH_2 deposition for biotinylation and avidin immobilization. The avidin distribution was examined by Biotin-fluorescein imaging (Fig 5.5 b). Only exposed PCL surfaces were identified by green fluorescence, suggesting that avidin immobilization was spatially controlled and that only unprotected regions were able to be conjugated.

In vitro cell culture was also performed to determine if this spatially controlled avidin could be applied to transduce cells that adhere and proliferate on biomaterial surfaces. After incubating for 2 days, the transduced cells were identified by X-gal staining and non-infected cells were identified by crystal violet counter staining (Fig 5.5 c). The distribution of cell transduction was consistent with the immobilized avidin, resulting in blue stained cells only being present on side of the PCL film that was functionalized. This suggests that cell transduction can be controlled by CVD modification and virus immobilization on specific sites of biomaterials.

5.3.6 The CVD treated 3-D scaffolds are functionalized for adenovirus immobilization

Because adenovirus was successfully immobilized on 2-D PCL films, we considered it important to investigate the feasibility of this technique in 3-D scaffolds. Cylindrical PCL scaffolds 12 mm in diameter and 5mm in height were treated by PPX-

NH_2 deposition and adenovirus was bound by the VBABM method. After adenovirus immobilization, the scaffolds were cross-sectioned at the mid-line of their heights before SEM examination.

Immobilized adenovirus was observed on the inner surfaces of the scaffolds (Fig 5.6). We observed five different regions of scaffolds and all of them demonstrated that viral particles were successfully bound on modified PCL surfaces. This indicated that CVD treatment was able to modify a complex 3-D structure and that functionalized surfaces could be applied for virus immobilization. These results demonstrated that CVD modification was not only feasible for functionalizing 2-D surfaces, but also 3-D structures for bioconjugation.

Using wax masking, PPX-NH_2 deposition was spatially controlled to functionalize half of a 3-D scaffold surface. Low-melting wax penetrated into complicate 3-D scaffolds and unwanted regions were physically protected from surface modification. The scaffolds were sectioned to examine the inner regions for evidence of bioconjugation. Biotin-fluorescein binding illustrated that avidin was only immobilized in non-masked regions of the scaffolds (Fig 5.7 a). Fibroblast culture in PCL scaffolds also demonstrated that AdLacZ distribution was consistently bound only to avidin in the 3-D structures (Fig 5.7 b,c). Counter staining with crystal violet illustrated that fibroblasts proliferated to confluence with the scaffolds. Transduced and non-transduced cells were restricted to two different regions with a distinct interface (Fig 5.7 d,e). These results were consistent

with 2-D experiments, suggesting that conjugation can be controlled by CVD treatment combined with wax masking, and can be applied to complex 3-D structures.

5.4 Discussion

Surface modification is an emerging technique used to functionalize materials for many useful applications due to the tunability of their properties by variation in chemical composition. Biomaterials with appropriate mechanical properties, but lacking a desired chemical reactivity, are capable of being custom-tailored by introducing a range of functional groups. Thus, these reactive moieties expand the function of biomaterials, especially in the application of bioconjugation [14].

In our previous studies, adenovirus was successfully immobilized on chitosan surfaces to transduce cells *in situ* using the biotin-avidin interaction [9]. Using the VBABM method, immobilized viral particles were evenly distributed on biomaterials, and the transduction efficiency was significantly improved. Although these results promisingly suggested that bioconjugation maintained virus binding on biomaterial surfaces to control gene delivery within scaffolds, the strategy was limited to the availability of reactive functional groups on biomaterials. Therefore, in this study, we utilized surface modification to generalize our established viral delivery methods to an inert biomaterial such as PCL. PPX-NH_2 was deposited on PCL surfaces to present a layer of amines on the surface. CVD coatings were characterized by FT-IR analysis, suggesting that this modification could be performed on polymeric materials (Fig 5.1 b).

Biocompatibility is an important issue for biomaterials, so a safety evaluation of surface modification is necessary before human studies. The assessments of MTS and LDH indicated that cells proliferated on PPX-NH_2 modified surfaces with extremely low death rates, suggesting that modified surfaces maintained cell proliferation without causing cytotoxicity (Fig 5.2 a-c). Prior studies also indicated that other PPX derivatives do not induce cell lysis [5]. These results support the findings that surface modification by PPX deposition is a feasible strategy for biological applications. In addition, we found that the hydrophobicity of CVD treated surfaces was reduced because the contact angle of modified surfaces was increased (data not shown). This may be due to the polar amine groups formed by PPX-NH_2 deposition. However, the cell survival performances were similar on PCL surface with and without modification, suggesting that hydrophobicity does not affect biocompatibility.

High energy radiation is broadly applied to generate reactive surfaces for bioconjugation. For example, allylamine plasma has been developed to modify polydimethylsiloxane (PDMS) substrates [15]. Epidermal growth factor with a homobifunctional N-hydroxysuccinimide (NHS) ester of PEG-butanoic acid (SBA2-PEG) was thus covalently conjugated on modified surfaces to investigate the nature of this bound growth factor and to optimize the conditions for the reaction. PLA films have been modified using the same process to conjugate poly (L-lysine) and RGD peptide [16]. Although these treatments create amines for functionalizing flat substrates, the application to non-planar structures are still not possible due to penetration limitations. Chemical vapor deposition is an improved strategy in which monomers are delivered to a

reaction chamber and then polymerized on biomaterial surfaces. Intrinsically, sublimated monomers conformally deposit over complex microgeometries, and can be evenly distributed in 3-D structures. This CVD treatment has been used to functionalize different materials, such as metal [5, 17-19], gold [6, 19], silicon [20], glass [5, 6, 19], poly(dimethylsiloxane) (PDMS) [19, 21-23], poly(methyl methacrylate) (PMMA) [24], poly(tetrafluoroethylene) (PTFE) [19, 24], poly(ethylene glycol) methyl ether methacrylate (PEGMA)and polystyrene [5, 24]. Therefore, we sought to apply this surface modification to the immobilization of adenovirus in 3-D inert PCL scaffolds. We found that viral particles were evenly distributed on the surfaces of the central regions of the scaffolds, suggesting that reactive amines were successfully created by the CVD treatment and the bioconjugation was capable of immobilizing virus on the surfaces of entire scaffolds (Fig 5.6).

Because inert biomaterials lack reactive groups for conjugation, bioconjugation may be controlled through CVD on specific sites in scaffolds. The specificity of biotinylated adenovirus on modified PCL surfaces suggested that biotinylated adenovirus was only immobilized on PPX-NH_2 modified biomaterials (Fig 5.3). Therefore, we further investigated the feasibility of spatially controlling virus delivery to specific sites of scaffolds. Using wax masking, avidin was specifically immobilized on non-masked regions (Fig 5.5 b and 5.7 a). Adenoviral vectors were thus bound on the desired surfaces to infect cells *in situ* (Fig 5.5 c and Fig 5.7 b-e). These results demonstrated that the surface modification could be tailored through physical protection, and that bioconjugation could be controlled on target sites.

For tissue engineering of complex tissues, regeneration of tissue interfaces is a challenge because the surrounding environment complicates the healing process. However, this may be improved by precise biofactor induction [25]. In this study, scaffolds were applied as gene carriers to investigate the feasibility of guiding appropriate tissue growth in implants. Using wax masking, the CVD technique was shown to spatially control *in situ* transduction, by which transduced and non-transduced cells were distributed in different regions of scaffolds with a distinct interface. This controllable gene delivery system should be beneficial in manipulating tissue regeneration. Using this strategy, surface modification may be used to regulate appropriate bioactive factor expression through the pattern of immobilized viral vectors and to engineer specific tissue formation in target sites of scaffolds.

5.5 Conclusions

In this study, surface modification was developed to functionalize biomaterial surfaces, by which viral particles were bound on materials and that gene expression was spatially controlled with a distinct interface. Although our novel strategy can effectively tether viral vectors on material surfaces to control gene delivery, this technique should not be restricted to this application only. Because PPX derivatives are capable of distributing not only on 2-D substrates but also in complex 3-D structures, this surface functionalization has been broadly applied to different biomaterial devices [17, 18, 21-23]. Using this CVD technique, some proteins such as extracellular matrix (ECM), inductive growth factors, or plasmid DNA could also potentially be bound in 3-D

biomaterials scaffolds to facilitate tissue regeneration. Consequently, we project that this surface modification may customize biomaterial surface properties to tailor bioconjugation to expand the possibility of material application in different fields.

(a)

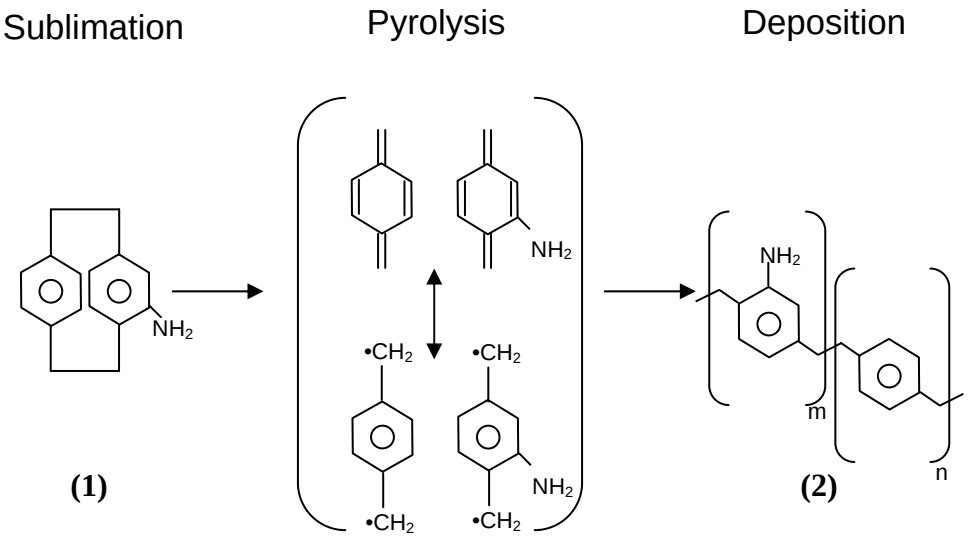

(b)

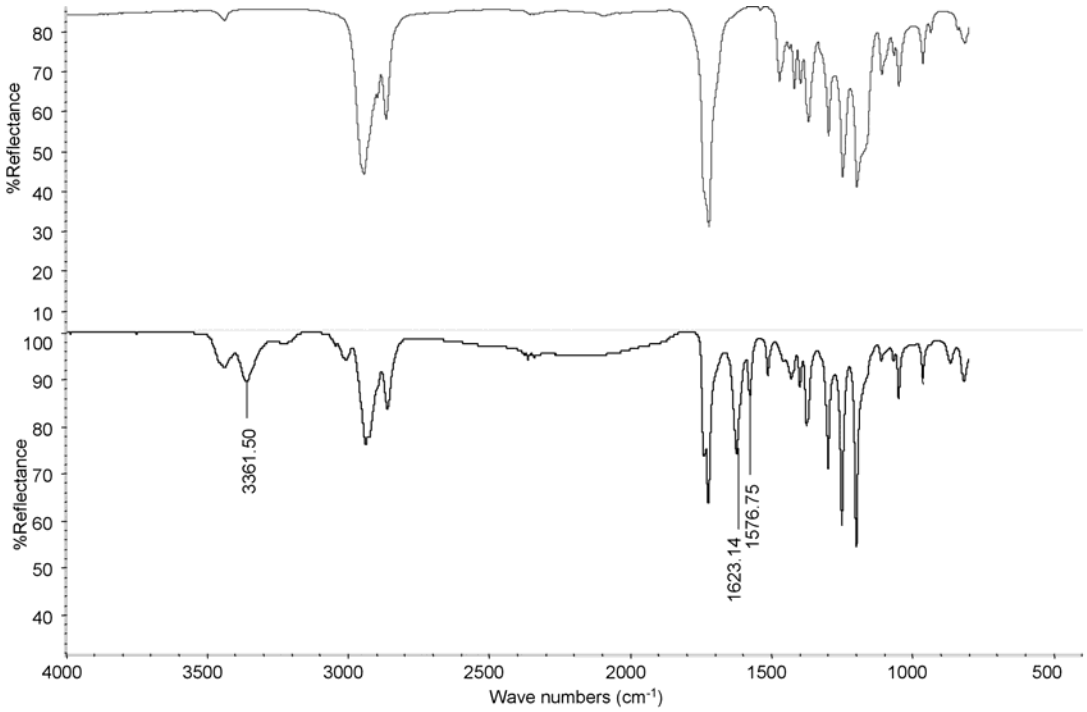

Figure 5.1. Surface modification by chemical vapor deposition (CVD) on polycaprolactone (PCL) (a) Scheme of Poly [(4-amino-*p*-xylylene)-*co*-(*p*-xylylene)] (PPX-NH_2) deposition on PCL surfaces (b) FT-IR spectrums of PCL before (top) and after (bottom) CVD treatment

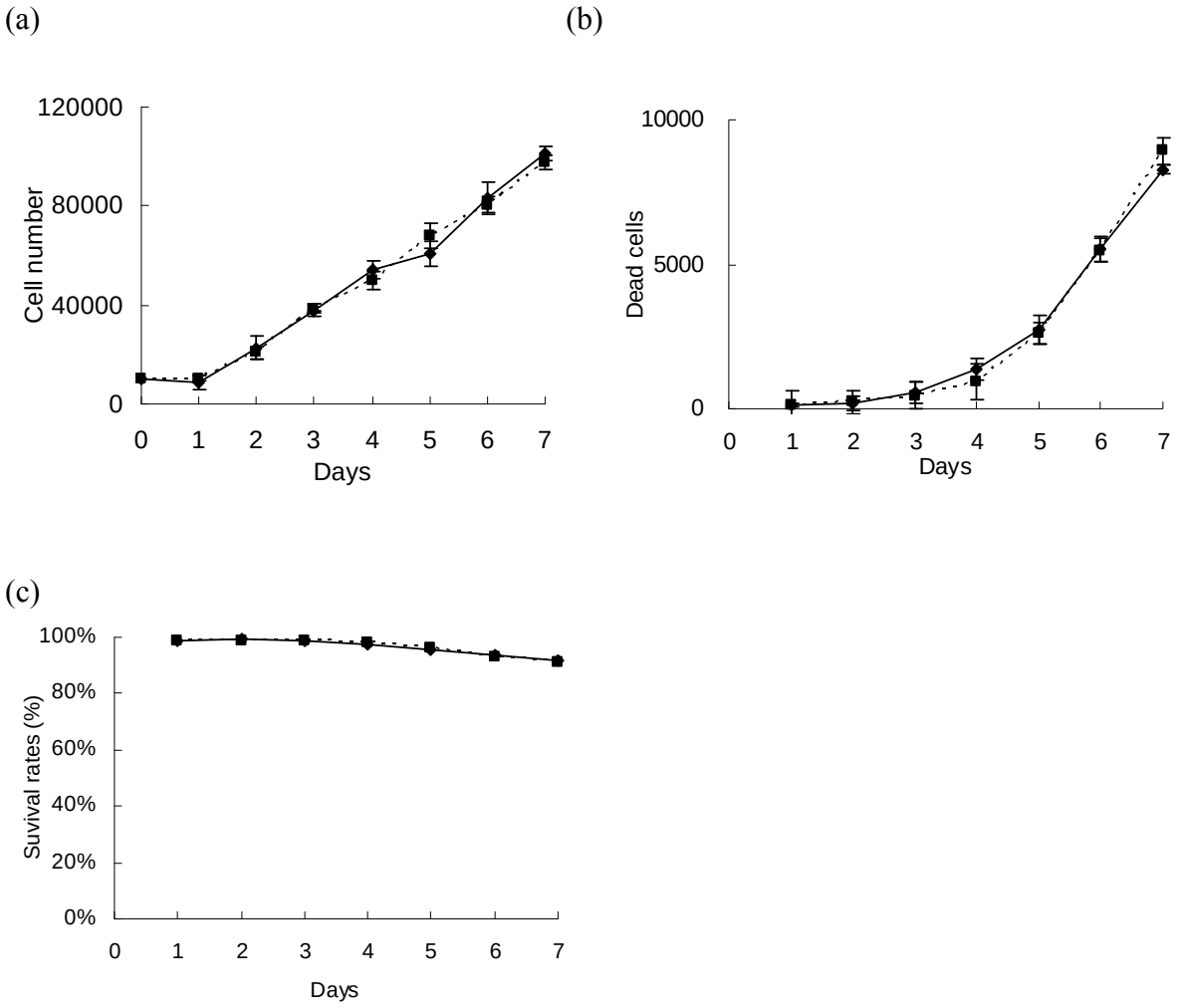

Figure 5.2. The biocompatibility of PCL with PPX-NH_2 treatment. To evaluate the biocompatibility of CVD treatment on PCL surfaces, fibroblasts were seeded on PCL films with (dashed line) and without (solid line) PPX-NH_2 deposition. (a) MTS and (b) LDH assay were performed to investigate the cell proliferation and cell death in 1 week, respectively. (c) The survival rates of surface cells were normalized by comparing the ratio of lysis cells to the total cell numbers at different time points. The data were compared by Student *t* test and there were no significant differences between these two groups. (n=3)

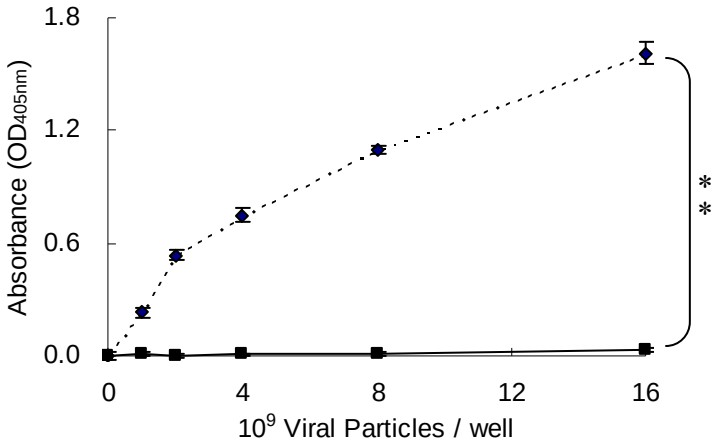

Figure 5.3. The specificity of adenovirus immobilization on PPX-NH_2 treated surfaces using the VBABM method. Biotin was conjugated on PPX-NH_2 deposited PCL surfaces to immobilize avidin, and then biotinylated adenoviral vectors in different concentrations were placed on the surfaces (dashed line). The same biotinylated virus solutions were placed on non-modified PCL surfaces as the control group (solid line). The bound adenovirus was determined by ELISA assay to investigate if these modified surfaces may specifically immobilize virus. The data were compared by Student *t* test. (n=3, **: $p<0.01$)

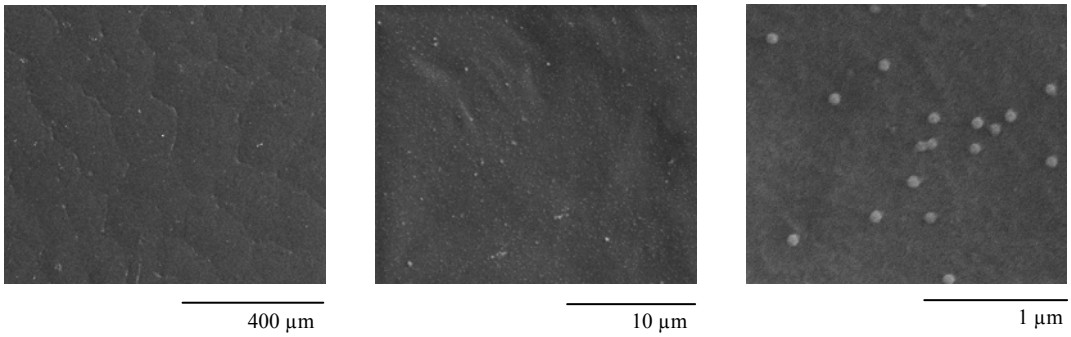

Figure 5.4. Adenovirus immobilization on 2-D PCL films. Biotinylated adenovirus was immobilized on the modified PCL surfaces by the VBABM method. The bound adenoviral particles were illustrated using SEM examination in different magnitudes.

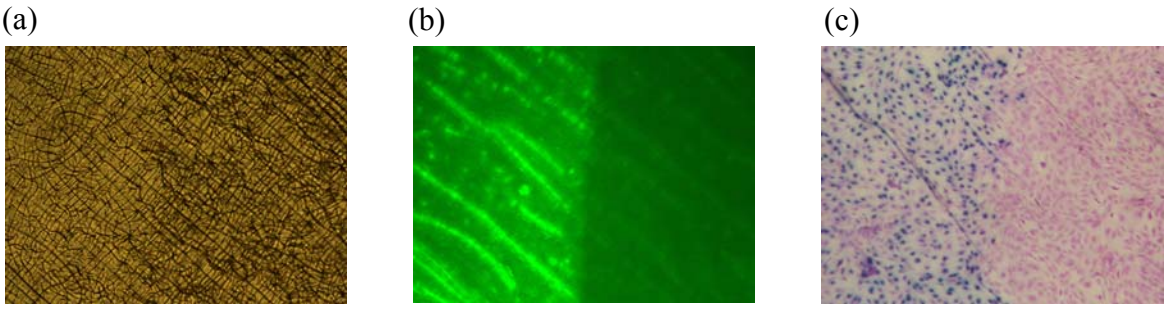

Figure 5.5. Spatial control of adenovirus immobilization to restrict cell transduction on specific sites. (a) The image of coated PCL surfaces by phase contrast microscope observation. The wax masking technique was utilized to control the CVD treatment only on the left of PCL surfaces, on which Amine-PEO_3-Biotin was conjugated to immobilize avidin. (b) Biotin-fluorescein was used to label the surface avidin. Only the exposed area without wax protection expressed green fluorescence. (c) Fibroblasts were cultured on PCL surfaces for 2 days. The transduced cells were turned blue after X-gal staining. Cells grew confluently on the material surfaces; however, cell transduction was restricted to the non-masked area, which was consistent with the avidin distribution.

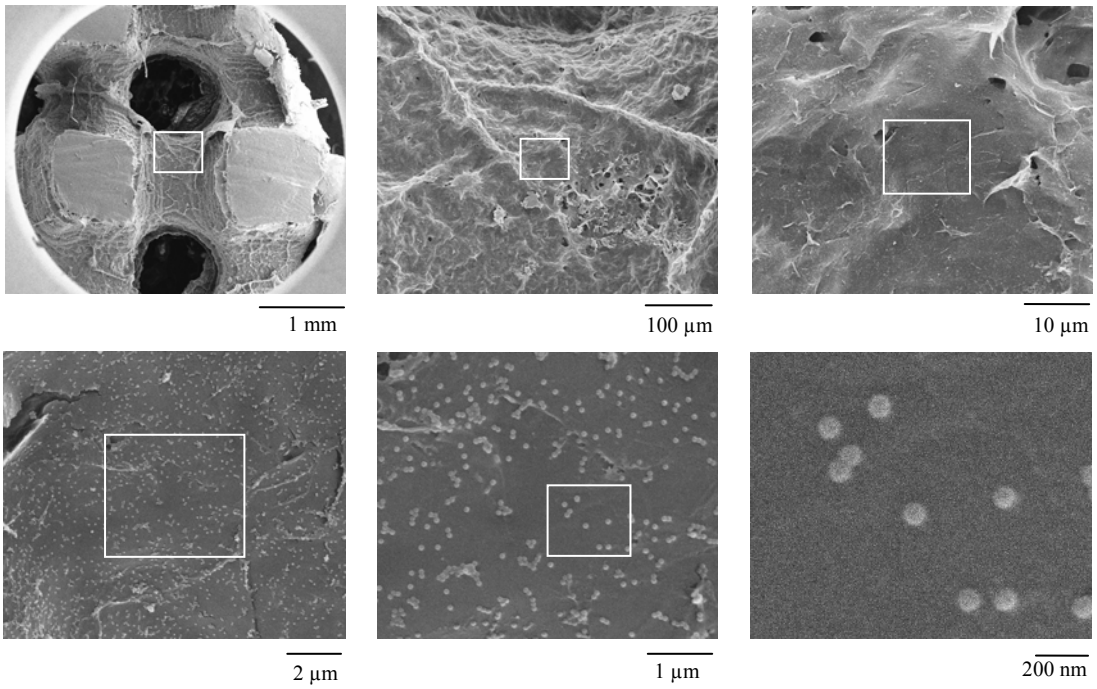

Figure 5.6. Adenovirus immobilization on CVD modified PCL scaffolds. To determine if CVD may functionalize on 3-D complex structures, the PPX-NH_2 was deposited on PCL scaffolds and biotinylated adenovirus was immobilized using the VBABM method. The scaffolds were cut halfway down their height and examined by SEM. Images in different magnitudes were captured, and the blocks were used to indicate the zoom-in regions in high magnitudes.

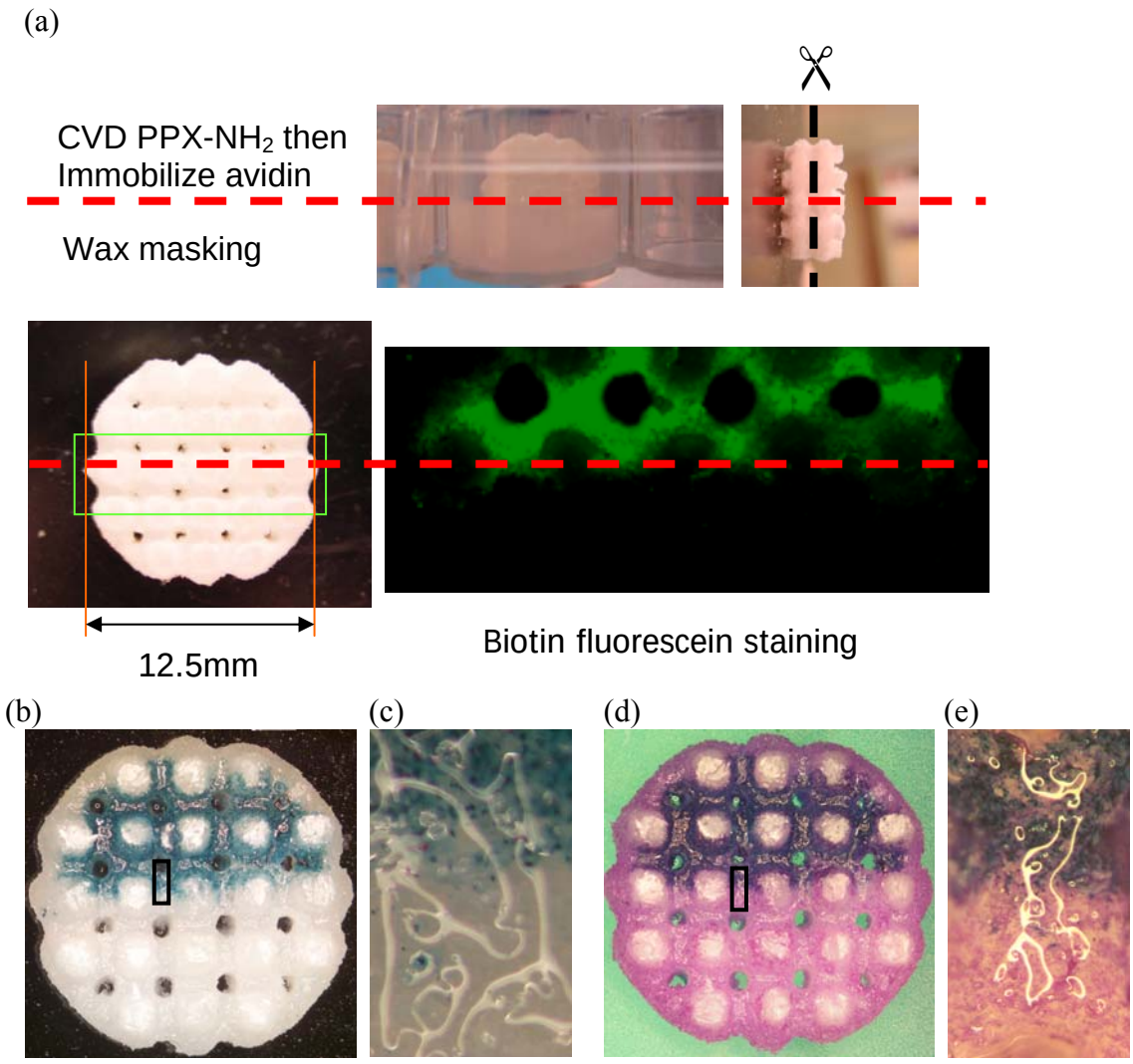

Figure 5.7. Spatial control of adenovirus immobilization in 3-D scaffolds. (a) Half of each scaffold was imbedded in low-melting wax to control the CVD treatment to only occur on non-masking regions for avidin immobilization. After wax removal, scaffolds were cut halfway down their heights and stained by biotin-fluorescein. The bound avidin was distributed on non-masking regions inside the scaffolds. (b) Biotinylated AdLacZ was immobilized in 3-D scaffolds before seeded fibroblasts. After 2 days' culture, scaffolds were cut halfway down their height and stained by X-gal. Transduced cells were distributed in the same regions as the bound avidin. (d) Counter staining by crystal violet illustrated that fibroblasts were grown confluently in the scaffolds. Transduced and non-transduced cells were controlled to distribute in two different regions with distinct interfaces. (c) and (e) are high magnitude images of block regions in (b) and (d), respectively.

5.6 References

1. J. Yang, J. Bei, S. Wang, Enhanced cell affinity of poly (D,L-lactide) by combining plasma treatment with collagen anchorage, Biomaterials 23 (12) (2002); 2607-2614.

2. J. Heitz, H. Niino, A. Yabe, Chemical surface modification on polytetrafluoroethylene films by vacuum ultraviolet excimer lamp irradiation in ammonia gas atmosphere, Applied Physics Letters 68 (19) (1996); 2648-2650.

3. M. Celina, H. Kudoh, T.J. Renk, K.T. Gillen, R.L. Clough, Surface modification of polymeric materials by pulsed ion beam irradiation, Radiation Physics and Chemistry 51 (2) (1998); 191-194.

4. X. Liu, P.X. Ma, Polymeric scaffolds for bone tissue engineering, Ann Biomed Eng 32 (3) (2004); 477-486.

5. Y. Elkasabi, M. Yoshida, H. Nandivada, H.Y. Chen, J. Lahann, Towards multipotent coatings: Chemical vapor deposition and biofunctionalization of carbonyl-substituted copolymers, Macromolecular Rapid Communications 29 (11) (2008); 855-870.

6. J. Lahann, R. Langer, Novel poly(p-xylylenes): Thin films with tailored chemical and optical properties, Macromolecules 35 (11) (2002); 4380-4386.

7. K. Schurmann, J. Lahann, P. Niggemann, B. Klosterhalfen, J. Meyer, A. Kulisch, D. Klee, R.W. Gunther, D. Vorwerk, Biologic response to polymer-coated stents: In vitro analysis and results in an iliac artery sheep model, Radiology 230 (1) (2004); 151-162.

8. J. Lahann, H. Hocker, R. Langer, Synthesis of Amino[2.2]paracyclophanes-Beneficial Monomers for Bioactive Coating of Medical Implant Materials, Angew Chem Int Ed Engl 40 (4) (2001); 726-728.

9. W.W. Hu, M.W. Lang, P.H. Krebsbach, Development of adenovirus immobilization strategies for in situ gene therapy, J Gene Med 10 (10) (2008); 1102-1112.

10. A. Kurella, N.B. Dahotre, Review paper: surface modification for bioimplants: the role of laser surface engineering, J Biomater Appl 20 (1) (2005); 5-50.

11. J. Lahann, D. Klee, H. Hocker, Chemical vapour deposition polymerization of substituted [2.2]paracyclophanes, Macromolecular Rapid Communications 19 (9) (1998); 441-444.

12. J.F. Waters, J.K. Sutter, M.A.B. Meador, L.J. Baldwin, M.A. Meador, Addition Curing Thermosets Endcapped with 4-Amino [2.2] Paracyclophane, Journal of Polymer Science Part a-Polymer Chemistry 29 (13) (1991); 1917-1924.

13. J.M. Williams, A. Adewunmi, R.M. Schek, C.L. Flanagan, P.H. Krebsbach, S.E. Feinberg, S.J. Hollister, S. Das, Bone tissue engineering using polycaprolactone scaffolds fabricated via selective laser sintering, Biomaterials 26 (23) (2005); 4817-4827.

14. J.M. Goddard, J.H. Hotchkiss, Polymer surface modification for the attachment of bioactive compounds, Progress in Polymer Science 32 (7) (2007); 698-725.

15. B.J. Klenkler, H. Sheardown, Characterization of EGF coupling to aminated silicone rubber surfaces, Biotechnol Bioeng 95 (6) (2006); 1158-1166.

16. Y. Hu, S.R. Winn, I. Krajbich, J.O. Hollinger, Porous polymer scaffolds surface-modified with arginine-glycine-aspartic acid enhance bone cell attachment and differentiation in vitro, J Biomed Mater Res A 64 (3) (2003); 583-590.

17. J. Lahann, D. Klee, H. Thelen, H. Bienert, D. Vorwerk, H. Hocker, Improvement of haemocompatibility of metallic stents by polymer coating, J Mater Sci Mater Med 10 (7) (1999); 443-448.

18. J. Lahann, D. Klee, W. Pluester, H. Hoecker, Bioactive immobilization of r-hirudin on CVD-coated metallic implant devices, Biomaterials 22 (8) (2001); 817-826.

19. H.Y. Chen, A.A. McClelland, Z. Chen, J. Lahann, Solventless adhesive bonding using reactive polymer coatings, Analytical Chemistry 80 (11) (2008); 4119-4124.

20. J. Lahann, I.S. Choi, J. Lee, K.F. Jenson, R. Langer, A new method toward microengineered surfaces based on reactive coating, Angewandte Chemie-International Edition 40 (17) (2001); 3166-+.

21. J. Lahann, M. Balcells, H. Lu, T. Rodon, K.F. Jensen, R. Langer, Reactive polymer coatings: a first step toward surface engineering of microfluidic devices, Anal Chem 75 (9) (2003); 2117-2122.

22. H.Y. Chen, J. Lahann, Fabrication of discontinuous surface patterns within microfluidic channels using photodefinable vapor-based polymer coatings, Anal Chem 77 (21) (2005); 6909-6914.

23. H.Y. Chen, Y. Elkasabi, J. Lahann, Surface modification of confined microgeometries via vapor-deposited polymer coatings, J Am Chem Soc 128 (1) (2006); 374-380.

24. X.W. Jiang, H.Y. Chen, G. Galvan, M. Yoshida, J. Lahann, Vapor-based initiator coatings for atom transfer radical polymerization, Advanced Functional Materials 18 (1) (2008); 27-35.

25. J.E. Phillips, K.L. Burns, J.M. Le Doux, R.E. Guldberg, A.J. Garcia, Engineering graded tissue interfaces, Proc Natl Acad Sci U S A 105 (34) (2008); 12170-12175.

CHAPTER 6

CONCLUSIONS AND PROSPECTUS

Regenerative gene therapy is a promising strategy to guide new tissue formation [1]. Viral vectors are powerful vehicles for gene delivery; however, how to restrict the distribution of transgenes remains a challenge. The goal of this thesis has been focused on developing different viral delivery models to spatially control cell transduction in biomaterial scaffolds. Using physical adhesion or chemical bioconjugation, adenoviral vectors have been localized or immobilized on material surfaces. These strategies demonstrated that gene delivery was controlled to transduce cells *in situ* after adhesion and growth on scaffolds. A wax masking method was also performed to spatially control cell transduction on specific sites of scaffolds. Furthermore, we introduced CVD techniques to functionalize the surface of inert biomaterials to gain further flexibility in spatially controlling gene delivery *in vitro* and *in vivo*.

6.1 Major Conclusions

Because the spatial control of cell transduction in target sites is extremely important for manipulating appropriate bioactive factor expression in wounds, we began our research using physical adhesion to locally deliver adenoviral vectors in scaffolds. Using a sucrose solution, adenovirus was controllably localized on substrates. These *in vitro*

studies also demonstrated that adenoviruses were concentrated on material surfaces, leading to the improvement of transduction efficiency. We further applied this gene delivery method to repair critical-sized calvarial defects in rats. Compared to freely suspended virus, lyophilized AdBMP-2 significantly enhanced bone regeneration in these clinically relevant wounds. This treatment has also been utilized to regenerate bone in the typically difficult scenario of osteoradionecrosis caused by preoperative radiotherapy. Furthermore, the lyophilized virus-scaffolds complexes were able to be stored long-term at -80 ^{0}C and maintained their stability and effectiveness, suggesting that these constructs have potential to be packaged as premade constructs that would be available at the time of surgery.

Although physical adhesion through lyophylization in sucrose effectively concentrates virus within scaffolds, the viral vectors were readily released from biomaterial scaffolds in the near aqueous *in vivo* environments. Therefore, we developed a new platform based on bioconjugation via covalent bonding of virus to the scaffolds. Because direct virus binding is too strong to allow for the efficient release of virus for cell internalization, indirect tethering of virus through specific interactions was investigated. Antibody-antigen interaction is the most well-known specific interaction, and also has been utilized to immobilize virus with implants [2-5]. To enhance the control of this antibody immobilization for the delivery of multiple genes, we developed a novel viral modification method to tag small chemicals such as Digoxigenin (DIG) on virus surfaces as antigenic determinants. In this case, modified virus could be reproducibly distinguished and specifically immobilized on biomaterials. The immobilized viral

vectors may stably and effectively be bound on material surfaces. Furthermore, a dual gene delivery method was developed based on antibody specificity. By combining anti-adenovirus and anti-DIG IgG conjugation, DIG-modified and non-modified viruses were capable of being bound on different regions of scaffolds to generate a distinct biological interface.

While antibody can effectively bind viral vectors, the titer of antibody is highly affected by the host animal, and maintaining a stable source of antibody may be problematic. In addition, immunization is expensive and time consuming. These drawbacks make antibody immobilization difficult to apply as a universal viral delivery method for clinical applications. Therefore, we established another virus immobilization method by taking advantage of the well-studied biotin-avidin interaction. By comparing two different immobilization strategies, we found that VBABM method enhanced avidin orientation, and thus provided more effective biotin-binding sites for biotinylated virus immobilization. This method not only evenly distributed viral particles on materials surfaces, but also improved cell transduction efficiency

Although virus immobilization via bioconjugation showed superior spatial control for gene delivery, such covalent binding is only possible on biomaterials with reactive functional groups. Therefore, surface modification using the CVD technique was developed to functionalize inert biomaterial scaffolds and thus allow conjugation of cell-signaling viruses. Due to the penetrability of sublimated monomers, the functional polymer can conformably be deposited over complex micro-geometries. Using this

method, we successfully presented a layer of amine groups on inert PCL surfaces. These modified surfaces were capable of being biotinylated to immobilize virus by our established VBABM methods. The SEM, immunologic staining, and cell culture assays all demonstrated that this method worked well not only on 2-D films, but also within complex 3-D structures. These results strongly suggest that surface modification may be used to regulate appropriate bioactive factor expression through the pattern of immobilized viral vectors, and to engineer specific tissue formation in defined sites of biomaterial scaffolds.

6.2 Significances and Implications

Natural tissue development follows a coordinated and sequential transformation process with individual stages involving time-dependent expression of several bioactive signals in the context of a 3-D environment [6]. Advanced tissue engineering approaches are based on the concept of controlling the spatiotemporal patterning of these cell-signal interactions to direct appropriate tissue formation [7]. Therefore, the combined application of gene therapy and tissue engineering has received much attention by scientists in the field of regenerative medicine [8]. In this thesis, we focused on the control of gene delivery and hypothesized that the controlled transduction of cells could lead to the development of tissue interfaces.

In this study, genes were delivered to specific sites for *in situ* transduciton. This *in vivo* gene delivery directly infects cells as they adhere to scaffolds to express bioactive factors. Compared to *ex vivo* studies in which cells are transduced and cultured *in vitro*

prior to implantation, *in vivo* gene therapy simplifies the gene administration and also reduces the need for cell harvest and multiple surgeries [1]. Furthermore, the risks of contamination and pathogen transmission are also reduced. However, because transduced cells for *ex vivo* gene delivery are harvested from patients or donors, virus concentrations can be controlled to avoid transgene overexpression. The strain of cell vehicles and the screening of transduced cells are all controllable in *ex vivo* methods. Consequently, how to decrease viral vector administration for reducing unwanted systemic infection is always a challenge for *in vivo* gene delivery.

Lyophilization was the first strategy tested in this thesis. Our hypothesis was that physically adhered viral vectors may be localized to biomaterial scaffolds. The *in vitro* release experiments indicated that lyophilized adenoviral particles adhered to the material surfaces. In an aqueous environment, adenovirus was locally released over time and approximate 35% of total virus was maintained on the surface after 16 hr. Because only a small fraction of virus particles remained on the material surface, this suggests that the binding force generated by lyophilization in sucrose was not strong. We deduce that the distribution of the virus lyophilized on biomaterials should be at a level between that of polymer release and substrate-mediated delivery.

The healing effect of lyophilized virus delivery was compared to freely suspended virus administration. Conceptually, the free delivery method is similar to gene activated matrices (GAM) which directly deliver genes through biomaterials carrier [9]. This combination of genes and carrier have been broadly used to facilitate different tissue

regeneration, including bone [9, 10], cartilage [11, 12], nerve [13], blood vessels [14], and skin wound healing [15, 16]. These matrix-based deliveries of viral or non-viral genes demonstrate therapeutic effects for tissue regeneration. In addition, the local delivery results in a gradient of transgene distributed from the scaffolds to surrounding tissue, which leads to a recruiting effects to attract cells due to the concentration profile of the expressed bioactive factors, which is especially useful in some clinical situations. For example, angiogenesis is always necessary during wound repair to provide sufficient nutrition and oxygen as well as to remove metabolic waste. Vascular endothelial growth factor (VEGF) has been delivered as a gradient profile which significantly enhanced blood vessel formation, perfusion and recovery [17]. In our study, bone regeneration in calvarial defects demonstrated that the GAM method (free virus in scaffold) induced modest bone formation, whereas the lyophilized virus significantly improved bone formation. This result is likely due the fact that more viral vectors are retained in scaffolds with lyophilized virus after implantation. This limited gradient distribution of expressed BMPs was thus more concentrated in lypohylized implants, and thus its therapeutic effect was improved.

To recreate complex tissue architectures, the spatially patterned delivery of genes encoding inductive factors may be used to direct tissue formation. Several gene delivery systems have been developed to spatially control gene delivery [18]. Vectors have been directly deposited on biomaterials using spotting, printing, microfluid, or pinning techniques [19-23]. Although these methods demonstrate the potential of patterned gene delivery to specific regions of a material, extending these techniques to 3-D scaffolds

remains a significant challenge. In this thesis, we introduced wax masking to control bioconjugation on desired regions of biomaterials. Due to the chemically-inert and low-melting point properties of the wax, this physical protection method is suitable to manipulate the pattern of virus immobilization. Our results suggest that gene delivery can be controlled to specific sites of scaffolds, by which bioactive signals may be regulated with precise spatial control.

Plasmid DNA is a non-viral vector that is frequently delivered by non-specific binding, such as van der Waals, hydrophobic/hydrophilic and electrostatic forces due to its negative charges [20, 24-27], whereas this strategy is inefficient to perform to viral vectors. Compared to DNA, virus is large and thus the interactions of physical adhesion are too weak to be stably maintained on implants. Therefore, to precisely control different viral vector immobilizations, specific binding was utilized in this study. Biotin-avidin and antibody-antigen complexes are highly specific and commonly used specific interactions to study biologic systems. Compared to non-specific binding, specific binding immobilizes a higher density of vector for a longer duration [18]. It is also more stable to maintain a vector in scaffolds in an *in vivo* environment [28]. In addition, tunable surface modification may facilitate fine control of vector immobilization [29]. In our study, we demonstrate that virus immobilization can be controlled in different concentrations with good stability in liquid environment. This suggests that this specific binding strategy is appropriate to apply to different clinical situation for *in vivo* administration.

Some studies indicate that ligand immobilization on solid phase substrates is highly

affected by the receptor orientation [30-33]. To increase the virus binding efficiency on biomaterials, the binding site alignment was also investigated in this study. For biotin-avidin interactions, direct avidin conjugation to biomaterials (VBAM) demonstrated a modest biotinylated virus binding effect, which is likely due to high heterogeneity and steric hindrance of the binding sites. However, this difficulty was significantly reduced by indirectly docking of avidin on biotinylated surfaces (VBABM) because the biotin binding sites were oriented by the grafted biotin on material surfaces. An oriented antibody conjugation was also developed in the DIG-modification study by linking sulfhydryls groups derived from the reduction of IgG hinge region to biomaterials. Due to the formation of covalent bonds between Fc and amines on chitosan surfaces, the active sites of IgG, Fab, were faced out from substrate surfaces to reduce steric hindrance. This Fab alignment strategy has also been studied in antibody conjugation on solid substrate [34-36]. Therefore, high binding efficiency of virus immobilization may be achieved through oriented binding sites strategies.

To spatially control bioactive factor expression on materials, we modified virus by conjugating the small chemicals, biotin and DIG, on viral capsids proteins as antigenic determinants. Because modified viruses can be specifically bound to avidin or anti-DIG antibody conjugated surfaces, the combination of these modified viral vectors may increase the controllability of multiple gene delivery. Through the CVD and wax masking techniques, different functional groups may be deposited to defined regions of scaffolds for antibody and avidin conjugation to control biotin- and DIG-modified virus immobilization. This should be extremely useful for the regeneration of biological

interfaces because patterned biologic cues are required to direct appropriate cell recruitment, proliferation, and differentiation. We project that these controllable virus immobilization strategies expand the feasibility of tissue engineering complex tissues and rescue patients from suffering.

Although this study focused on spatially controlled viral vector distribution, the effects of biomaterial scaffolds are undoubtedly critical to effective gene delivery and tissue regeneration. Because *in vivo* regenerative gene therapy is based on host cell transduction in wound sites, this strategy is greatly dependent on the respondent cell adhesion and transduction in scaffolds. To successfully transfer genes to target sites, host cells with appropriate types and numbers need to not only contact the genes loaded within vectors, but also must remain in the scaffolds without migration. Therefore, an appropriate scaffold is necessary for the success of the substrate-mediated gene delivery method. Sufficient numbers of target cells may be attracted to transplanted scaffolds and the bioconductive scaffold surfaces provide a suitable environment for cell adhesion [39]. Many materials used for drug delivery have also been applied to control virus delivery and cell transduction [18]. In addition, effective scaffold design should stably maintain cells in scaffold during the therapeutic period [40]. If enough host respondent cells for target gene expression were not available in some poor *in vivo* environments, such as compromised defects, seeding cells to virus-loaded scaffolds could be an alternative strategy to enhance the chance of appropriate cell population maintaining in biomaterial scaffolds.

The CVD method was studied to generalize our methods to a range of different biomaterials. We demonstrated that bioconjugation can be performed on functionalized scaffold surfaces to immobilize viral vectors on specific sites. Although the deposited polymer was stable on substrate surfaces [37, 38], the degradability of biomaterials probably lead to different the virus distributions. In this study, PCL was used as scaffold biomaterials which degrades extremely slowly in *in vivo* environments. Consequently, the conjugated proteins could be stably maintained on CVD deposited polymer on material surfaces. However, for some biomaterials which degrade quickly during implantation, the immobilized viral vectors may thus be released from degraded substrate with time. This may lead to a gradient of gene delivery as lyophilization and the delivery profile depends on material degradation rates.

6.3 Future Directions

The combination of gene therapy, drug delivery technology, and biomaterials scaffolds provides a promising strategy to generate new tissue for therapeutic purposes [41]. However, several challenges remain in developing a controllable delivery system to mimic the physiologic patterns that function during normal tissue development. Our work mainly addresses methods to improve spatial control of bioactive factor expression. While our results demonstrate the potential to direct appropriate tissue growth, their application should not be limited to our current study. For future work in this area, there are at least four important directions that may be explored.

6.3.1 Spatial and temporal control of gene delivery

In this thesis we demonstrated that immobilized virus on specific sites can spatially control gene delivery in target sites. However, in the gene therapy paradigm an ideal gene delivery should be controlled not only spatially but also temporally. For example, proliferation, matrix deposition, and mineralization are three phases of bone formation, in which different genes are expressed at different stages during bone formation [42]. An appropriate sequence of biologic cues is likely to reliably regulate bone regeneration. In the future, we may expand our established methods to develop controllable gene delivery for further regulating the temporal profile of *in situ* cell transduction. This could be achieved using two strategies. After virus is conjugated to scaffolds, a layer-by-layer biodegradable polymer may be applied to cover the scaffold surfaces. Because the degradation rates are controlled by the amounts of polymer layers coated on the scaffolds, the immobilized virus should be exposed to infect host cells at different time points. Another strategy is to immobilize viral vectors on biomaterial surfaces using degradable crosslinkers with ester or disulfide bonds in the spacer regions. These cleavable bonds are able to be broken in an *in vivo* environment. Viral vector released from conjugated sites would result in a gradient distribution of the expressed growth factors, which may recruit appropriate progenitor cells to the wound sites to recapitulate tissue differentiation. Therefore, the establishment of these strategies would enhance the adjustability of viral vector delivery to fit specific biological requirements.

6.3.2 Multiple gene deliveries to regenerate tissue interfaces

Tissue engineering has been successfully applied to repair different tissues, however, the healing of tissue interfaces is still a challenge due to the complexities inherent to

different tissues [43]. For example, in some complex clinical situations, such as orthopedic interfaces, the functional integration of subchondral bone with cartilage still poses a significant challenge because uncontrolled BMPs may lead to unwanted hard tissue formation outside the defects [44]. In this thesis, we preliminarily investigated the feasibility of controlled gene delivery on specific sites of scaffolds. Using bioconjugation and wax masking, virus was immobilized on different sites of a material to generate a biologic interface. These promising results suggest that spatially controlled virus patterns has the potential to direct appropriate tissue formation on desired regions of a scaffold. This is extremely important to regenerating tissue interfaces where controllable gene delivery may not only effectively restrict transgene expression in target sites of a scaffold, but also avoid unwanted interference of biologic signals.

To direct regeneration at interfaces, numerous bioactive factors may be required to mimic physiological tissue development. Multiple viral vector administration is a promising strategy to express different bioactive factors; however, how to precisely deliver specific genes to target sites is still a challenge. In this thesis, we have developed two different virus modifications which may be used as antigenic determinants to tag viral surfaces. Additionally, the CVD studies demonstrated that virus immobilization is controlled by deposited polymer on materials surfaces. Therefore, the combination of these established methods should be able to regulate target bioactive factors deliveries for interface tissue regeneration such as the bone-cartilage interface at articular joints. Chondrogenic cues differentiate mesenchymal stem cells to chondrcytes, and BMPs also facilitate mineralized tissue formation. In the case of orthopaedic interfaces, one strategy

would be to immobilize viral vectors encoding osteogenic and chondrogenic factors, such as BMP-2 and SOX-9, at two regions of one scaffold with a distinct interface. These engineered scaffolds may be able to promote reconstruction of damage articular joints.

6.3.3 Non-viral vector immobilization to spatially control gene delivery

In current gene therapy research, more and more studies are focusing on gene delivery using plasmid DNA encapsulated in non-viral vectors due to their relative safety, low immunogenicity and toxicity, ease of administration and manufacture, and lack of DNA insert size limitation [45]. While our previous study was to develop adenoviral delivery methods from biomaterials, these strategies are not limited to viral vectors. In the future studies, plasmid DNA administration may be able to control delivery based on the same bioconjugation mechanism. For example, Lipofectamine is a cationic liposome with amine functional groups. After encapsulating target DNA, these amine-equipped lipoplexes are capable of conjugating to small chemicals, such as biotin and digoxigenin, and to be available for antibody immobilization. Therefore, it may be possible to specifically deliver plasmid DNA on target sites of scaffolds to develop a spatially controlled gene delivery method for therapeutic purpose.

6.3.4 Custom-tailored materials surfaces using CVD technique to conjugate ECM molecules

Tissue regeneration can also be regulated through appropriate extracellular matrix (ECM) signals. Several studies have demonstrated that cell adhesion can be controlled by short peptides, such as RGD sequences [46]. It is also known that ECM molecules can

guide cells to differentiate into different tissues [47]. For example, proteoglycans are extremely important for chondrogenesis for catilage regeneration [48]. Although most biomaterial scaffolds are compatible for implanting *in vivo* to provide mechanical support, they frequently lack appropriate functional groups to stably maintain ECM molecules on the surfaces. In our previous study, we utilized CVD to graft functional groups on biomaterials surfaces for bioconjugation. This technique could also be applied to functionalize biomaterials for covalnetly binding ECM molecules or growth factors, and eventually control appropriate tissue regeneration in defects.

Because cells, scaffolds, and biological cues form the triad of traditional tissue engineering approach, the coordination of these three essential elements is required to ensure the success of tissue regeneration. By combining inductive biological factors to conductive biomaterial scaffolds, the appropriate respondant cells may be recruited. In addition, the delivery of bioactive factors should be controlled in a not only spatial but also temporal manner, by which a microenvironment in defects may be custom-tailored to guide defined tissue formation. Such compresive tissue engineering strategy should benefit the progress of regenerative medicine and be broadly applied in different clinical situation.

6.4 References

1. M. Heyde, K.A. Partridge, R.O.C. Oreffo, S.M. Howdle, K.M. Shakesheff, M.C. Garnett, Gene therapy used for tissue engineering applications, Journal of Pharmacy and Pharmacology 59 (3) (2007); 329-350.

2. J.M. Abrahams, C. Song, S. DeFelice, M.S. Grady, S.L. Diamond, R.J. Levy, Endovascular microcoil gene delivery using immobilized anti-adenovirus antibody for vector tethering, Stroke 33 (5) (2002); 1376-1382.

3. I. Fishbein, I.S. Alferiev, O. Nyanguile, R. Gaster, J.M. Vohs, G.S. Wong, H. Felderman, I.W. Chen, H. Choi, R.L. Wilensky, R.J. Levy, Bisphosphonate-mediated gene vector delivery from the metal surfaces of stents, Proc Natl Acad Sci U S A 103 (1) (2006); 159-164.

4. I. Fishbein, S.J. Stachelek, J.M. Connolly, R.L. Wilensky, I. Alferiev, R.J. Levy, Site specific gene delivery in the cardiovascular system, J Control Release 109 (1-3) (2005); 37-48.

5. S.J. Stachelek, C. Song, I. Alferiev, S. Defelice, X. Cui, J.M. Connolly, R.W. Bianco, R.J. Levy, Localized gene delivery using antibody tethered adenovirus from polyurethane heart valve cusps and intra-aortic implants, Gene Ther 11 (1) (2004); 15-24.

6. I. Nishimura, R.L. Garrell, M. Hedrick, K. Iida, S. Osher, B. Wu, Precursor tissue analogs as a tissue-engineering strategy, Tissue Eng 9 Suppl 1 (2003); S77-89.

7. M. Biondi, F. Ungaro, F. Quaglia, P.A. Netti, Controlled drug delivery in tissue engineering, Advanced Drug Delivery Reviews 60 (2) (2008); 229-242.

8. O. Bleiziffer, E. Eriksson, F. Yao, R.E. Horch, U. Kneser, Gene transfer strategies in tissue engineering, J Cell Mol Med 11 (2) (2007); 206-223.

9. J. Fang, Y.Y. Zhu, E. Smiley, J. Bonadio, J.P. Rouleau, S.A. Goldstein, L.K. McCauley, B.L. Davidson, B.J. Roessler, Stimulation of new bone formation by direct transfer of osteogenic plasmid genes, Proc Natl Acad Sci U S A 93 (12) (1996); 5753-5758.

10. J. Bonadio, E. Smiley, P. Patil, S. Goldstein, Localized, direct plasmid gene delivery in vivo: prolonged therapy results in reproducible tissue regeneration, Nat Med 5 (7) (1999); 753-759.

11. T. Guo, X. Zeng, H. Hong, H. Diao, R. Wangrui, J. Zhao, J. Zhang, J. Li, Gene-activated matrices for cartilage defect reparation, Int J Artif Organs 29 (6) (2006); 612-621.

12. A. Pascher, G.D. Palmer, A. Steinert, T. Oligino, E. Gouze, J.N. Gouze, O. Betz, M. Spector, P.D. Robbins, C.H. Evans, S.C. Ghivizzani, Gene delivery to cartilage defects using coagulated bone marrow aspirate, Gene Ther 11 (2) (2004); 133-141.

13. M. Berry, A.M. Gonzalez, W. Clarke, L. Greenlees, L. Barrett, W. Tsang, L. Seymour, J. Bonadio, A. Logan, A. Baird, Sustained effects of gene-activated matrices after CNS injury, Mol Cell Neurosci 17 (4) (2001); 706-716.

14. L.D. Shea, E. Smiley, J. Bonadio, D.J. Mooney, DNA delivery from polymer matrices for tissue engineering, Nat Biotechnol 17 (6) (1999); 551-554.

15. D.L. Gu, T. Nguyen, A.M. Gonzalez, M.A. Printz, G.F. Pierce, B.A. Sosnowski, M.L. Phillips, L.A. Chandler, Adenovirus encoding human platelet-derived growth factor-B delivered in collagen exhibits safety, biodistribution, and immunogenicity profiles favorable for clinical use, Mol Ther 9 (5) (2004); 699-711.

16. L.A. Chandler, J. Doukas, A.M. Gonzalez, D.K. Hoganson, D.L. Gu, C. Ma, M. Nesbit, T.M. Crombleholme, M. Herlyn, B.A. Sosnowski, G.F. Pierce, FGF2-Targeted adenovirus encoding platelet-derived growth factor-B enhances de novo tissue formation, Mol Ther 2 (2) (2000); 153-160.

17. R.R. Chen, E.A. Silva, W.W. Yuen, A.A. Brock, C. Fischbach, A.S. Lin, R.E. Guldberg, D.J. Mooney, Integrated approach to designing growth factor delivery systems, Faseb Journal 21 (14) (2007); 3896-3903.

18. L. De Laporte, L.D. Shea, Matrices and scaffolds for DNA delivery in tissue engineering, Advanced Drug Delivery Reviews 59 (4-5) (2007); 292-307.

19. K. Honma, T. Ochiya, S. Nagahara, A. Sano, H. Yamamoto, K. Hirai, Y. Aso, M. Terada, Atelocollagen-based gene transfer in cells allows high-throughput screening of gene functions, Biochem Biophys Res Commun 289 (5) (2001); 1075-1081.

20. A.K. Pannier, B.C. Anderson, L.D. Shea, Substrate-mediated delivery from self-assembled monolayers: effect of surface ionization, hydrophilicity, and patterning, Acta Biomater 1 (5) (2005); 511-522.

21. F. Yamauchi, K. Kato, H. Iwata, Micropatterned, self-assembled monolayers for fabrication of transfected cell microarrays (vol 1672, pg 138, 2004), Biochimica Et Biophysica Acta-General Subjects 1674 (1) (2004); 109-110.

22. P.M. Heron, B.M. Sutton, G.M. Curinga, G.M. Smith, D.M. Snow, Localized gene expression of axon guidance molecules in neuronal co-cultures, J Neurosci Methods 159 (2) (2007); 203-214.

23. T. Houchin-Ray, K.J. Whittlesey, L.D. Shea, Spatially patterned gene delivery for localized neuron survival and neurite extension, Mol Ther 15 (4) (2007); 705-712.

24. Z. Bengali, A.K. Pannier, T. Segura, B.C. Anderson, J.H. Jang, T.A. Mustoe, L.D. Shea, Gene delivery through cell culture substrate adsorbed DNA complexes, Biotechnol Bioeng 90 (3) (2005); 290-302.

25. J.H. Jang, Z. Bengali, T.L. Houchin, L.D. Shea, Surface adsorption of DNA to tissue engineering scaffolds for efficient gene delivery, J Biomed Mater Res A 77 (1) (2006); 50-58.

26. M. Singh, J.H. Fang, J. Kazzaz, M. Ugozzoli, J. Chesko, P. Malyala, R. Dhaliwal, R. Wei, M. Hora, D. O'Hagan, A modified process for preparing cationic polylactide-co-glycolide microparticles with adsorbed DNA, Int J Pharm 327 (1-2) (2006); 1-5.

27. J. Zheng, W.S. Manuel, P.J. Hornsby, Transfection of cells mediated by biodegradable polymer materials with surface-bound polyethyleneimine, Biotechnol Prog 16 (2) (2000); 254-257.

28. R.J. Levy, C. Song, S. Tallapragada, S. DeFelice, J.T. Hinson, N. Vyavahare, J. Connolly, K. Ryan, Q. Li, Localized adenovirus gene delivery using antiviral IgG complexation, Gene Ther 8 (9) (2001); 659-667.

29. J. Lahann, Vapor-based polymer coatings for potential biomedical applications, Polymer International 55 (12) (2006); 1361-1370.

30. C. Yeung, T. Purves, A.A. Kloss, T.L. Kuhl, S. Sligar, D. Leckband, Cytochrome c recognition of immobilized, orientational variants of cytochrome b(5): Direct force and equilibrium binding measurements, Langmuir 15 (20) (1999); 6829-6836.

31. C. Yeung, D. Leckband, Molecular level characterization of microenvironmental influences on the properties of immobilized proteins, Langmuir 13 (25) (1997); 6746-6754.

32. B. Lu, M.R. Smyth, R. O'Kennedy, Oriented immobilization of antibodies and its applications in immunoassays and immunosensors, Analyst 121 (3) (1996); 29R-32R.

33. M.A. Firestone, M.L. Shank, S.G. Sligar, P.W. Bohn, Film architecture in biomolecular assemblies. Effect of linker on the orientation of genetically engineered surface-bound proteins, J Am Chem Soc 118 (38) (1996); 9033-9041.

34. L.C. Shriver-Lake, B. Donner, R. Edelstein, K. Breslin, S.K. Bhatia, F.S. Ligler,

Antibody immobilization using heterobifunctional crosslinkers, Biosens Bioelectron 12 (11) (1997); 1101-1106.

35. G.P. Anderson, M.A. Jacoby, F.S. Ligler, K.D. King, Effectiveness of protein A for antibody immobilization for a fiber optic biosensor, Biosens Bioelectron 12 (4) (1997); 329-336.

36. B. Lu, M.R. Smyth, R. Okennedy, Immunological activities of IgG antibody on pre-coated Fc receptor surfaces, Anal Chim Acta 331 (1-2) (1996); 97-102.

37. J. Lahann, D. Klee, H. Thelen, H. Bienert, D. Vorwerk, H. Hocker, Improvement of haemocompatibility of metallic stents by polymer coating, Journal of Materials Science-Materials in Medicine 10 (7) (1999); 443-448.

38. H.Y. Chen, Y. Elkasabi, J. Lahann, Surface modification of confined microgeometries via vapor-deposited polymer coatings, Journal of the American Chemical Society 128 (1) (2006); 374-380.

39. S. Segvich, H.C. Smith, L.N. Luong, D.H. Kohn, Uniform deposition of protein incorporated mineral layer on three-dimensional porous polymer scaffolds, J Biomed Mater Res B Appl Biomater 84 (2) (2008); 340-349.

40. S. Srouji, T. Kizhner, E. Livne, 3D scaffolds for bone marrow stem cell support in bone repair, Regenerative Medicine 1 (4) (2006); 519-528.

41. J. Bonadio, Tissue engineering via local gene delivery, J Mol Med 78 (6) (2000); 303-311.

42. L.D. Shea, D. Wang, R.T. Franceschi, D.J. Mooney, Engineered bone development from a pre-osteoblast cell line on three-dimensional scaffolds, Tissue Eng 6 (6) (2000); 605-617.

43. K.L. Moffat, I.N.E. Wang, S.A. Rodeo, H.H. Lu, Orthopedic Interface Tissue Engineering for the Biological Fixation of Soft Tissue Grafts, Clinics in Sports Medicine 28 (1) (2009); 157-+.

44. H. Peng, A. Usas, D. Hannallah, A. Olshanski, G.M. Cooper, J. Huard, Noggin improves bone healing elicited by muscle stem cells expressing inducible BMP4, Mol Ther 12 (2) (2005); 239-246.

45. D.A. Jackson, S. Juranek, H.J. Lipps, Designing nonviral vectors for efficient gene transfer and long-term gene expression, Molecular Therapy 14 (5) (2006); 613-626.

46. T. Reintjes, J. Tessmar, A. Gopferich, Biomimetic polymers to control cell adhesion, Journal of Drug Delivery Science and Technology 18 (1) (2008); 15-24.

47. H.J. Chung, T.G. Park, Surface engineered and drug releasing pre-fabricated scaffolds for tissue engineering, Advanced Drug Delivery Reviews 59 (4-5) (2007); 249-262.

48. C. Gaissmaier, J.L. Koh, K. Weise, Growth and differentiation factors for cartilage healing and repair, Injury-International Journal of the Care of the Injured 39 (2008); S88-S96.